

Aus der Chirurgischen Klinik und Poliklinik Großhadern
der Ludwig-Maximilians-Universität München
(Direktor: Prof. Dr. med. Dr. h.c. mult. Karl-Walter Jauch)

***Genetically Engineering Mesenchymal Stem Cells for Targeting Tumor
Stroma and Angiogenesis in Hepatocellular Carcinoma***

Dissertation

zum Erwerb des Doktorgrades der Humanbiologie

an der medizinischen Fakultät der

Ludwig-Maximilians-Universität zu München

vorgelegt von

Qi Bao

Aus Zhejiang, China

2012

Mit der Genehmigung der medizinischen Fakultät
der Universität München

Berichterstatterin: Prof. Dr. med. Christiane J. Bruns

Mitberichterstatter: Priv. Doz. Dr. med. Norbert Grüner
Prof. Dr. med. Simon Rothenfusser
Prof. Dr. med. Natascha C. Nüssler

Mitbetreuung durch den
promovierten Mitarbeiter: Dr. med. Hanno Niess

Dekan: Prof. Dr. med. Dr. h.c. Maximilian Reiser
FACR, FRCR

Tag der mündlichen Prüfung: 09.07.2012

*Enter to grow in wisdom
Depart to serve better thy country and thy kind*

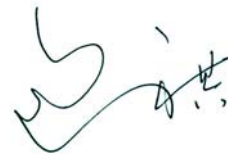
Declaration

I hereby declare that the thesis is my original work and I have not received outside assistance. All the work and results presented in the thesis were performed independently. Only MR image part of work was performed in collaboration with Dr. Mike Notohamiprodjo (Department of Clinical Radiology, University Hospitals Munich). Anything from the literature was cited and listed in the reference. Part of the results have been published in the paper Niess H, Bao Q, Conrad C, Zischek C, Notohamiprodjo M, Schwab F, Schwarz B, Huss R, Jauch KW, Nelson PJ, Bruns CJ. Selective targeting of genetically engineered mesenchymal stem cells to tumor stroma microenvironments using tissue-specific suicide gene expression suppresses growth of hepatocellular carcinoma. *Ann Surg.* 2011; 254(5):767-74. No unauthorized data was included.

All the data presented in the thesis will not be used in any other thesis for scientific degree application.

The work for the thesis began from Oct. 2009 with the supervision from Prof. Dr. med. Christiane J. Bruns in, Chirurgische Klinik und Poliklinik, Klinikum Großhadern, Ludwig-Maximilians University Munich, Germany.

Munich, on 24.07.12

A handwritten signature in black ink, appearing to be 'Qi Bao', written in a cursive style.

(Qi Bao)

I. CONTENTS

I.	CONTENTS	- 4 -
II.	ABSTRACT	- 7 -
III.	INTRODUCTION	- 9 -
	<i>3.1 Mesenchymal stem cells</i>	<i>- 9 -</i>
	3.1.1 Background.....	- 9 -
	3.1.2 Genetically engineering MSCs in non-gastrointestinal cancer therapy.....	- 10 -
	3.1.3 Dual effects of MSCs on gastrointestinal cancers.....	- 11 -
	3.1.4 Additional examples of genetically engineered MSCs in gastrointestinal cancer therapy	- 12 -
	<i>3.2. Hepatocellular carcinoma</i>	<i>- 16 -</i>
	3.2.1. Background.....	- 16 -
	3.2.2. Treatment of HCC	- 17 -
	3.2.2.1. Surgical resection	- 17 -
	3.2.2.2. Liver transplantation.....	- 17 -
	3.2.2.3. Trans-arterial embolisation therapy	- 17 -
	3.2.2.4. Non-surgical local ablative treatments.....	- 18 -
	3.2.2.5. Chemotherapy	- 18 -
	3.2.3. Summary for this part	- 19 -
	<i>3.3. Tumor microenvironment</i>	<i>- 19 -</i>
IV.	MATERIALS UND METHODS	- 21 -
	<i>4.1. Materials</i>	<i>- 21 -</i>
	4.1.1. Cell lines	- 21 -
	4.1.1.1. Human hepatocellular carcinoma cell Huh7	- 21 -
	4.1.1.2. Murine bone marrow-derived mesenchymal stem cell	- 21 -
	4.1.1.3. RFP or HSV-Tk engineered mesenchymal stem cell	- 21 -
	4.1.2. Technical equipments	- 22 -
	4.1.3. Cell culture materials	- 23 -
	4.1.4. Medium, buffer, solution for cell culture	- 23 -
	4.1.4.1. Cell culture medium.....	- 24 -
	4.1.4.2. Cell storage medium	- 24 -
	4.1.5. Materials for immunohistochemistry	- 24 -
	4.1.5.1. Tris-buffer.....	- 25 -
	4.1.5.2. Tris buffered saline (TBS) buffer, 10×	- 25 -
	4.1.5.3. PBS wash buffer, 1×	- 25 -
	4.1.6. Materials for animal experiment	- 25 -
	4.1.6.1. Animals.....	- 25 -
	4.1.6.2. Surgery instruments	- 26 -
	4.1.6.3. Medicine	- 26 -

4.1.6.4.	Other materials.....	- 26 -
4.1.7.	Materials for ELISA	- 26 -
4.1.8.	Materials for qRT-PCR.....	- 27 -
4.1.9.	Software.....	- 27 -
4.2.	<i>Methods</i>	- 28 -
4.2.1.	Cell culture conditions	- 28 -
4.2.2.	Passage of cells.....	- 28 -
4.2.3.	Determination of cell number	- 28 -
4.2.4.	Storage and recultivation of the cells	- 30 -
4.2.4.1.	Storage of the cells.....	- 30 -
4.2.4.2.	Recultivation of the cells	- 30 -
4.2.5.	Orthotopic hepatocellular carcinoma mouse model.....	- 30 -
4.2.5.1.	Animals.....	- 30 -
4.2.5.2.	Animal's living conditions.....	- 30 -
4.2.5.3.	Anesthesia.....	- 31 -
4.2.5.4.	Surgical techniques	- 31 -
4.2.5.4.1.	Intra-hepatic Huh7 cell injection.....	- 31 -
4.2.5.4.2.	Ear markers.....	- 31 -
4.2.5.4.3.	Injection of eMSCs	- 33 -
4.2.6.	Injection of SPIO-transfected MSC in tumor-bearing mice	- 33 -
4.2.6.1.	Labeling of MSC by transient supermagnetic iron oxide (SPIO) transfection.....	- 33 -
4.2.6.2.	In vivo MR-Imaging of SPIO-labeled MSC	- 34 -
4.2.7.	Experimental setting	- 35 -
4.2.8.	Histology	- 37 -
4.2.8.1.	Haematoxylin Eosin (HE) staining	- 37 -
4.2.8.2.	Immunohistochemistry	- 38 -
4.2.8.3.	Ki67 proliferation rate assay	- 38 -
4.2.8.4.	Microvascular density and vessel thickness analysis	- 39 -
4.2.9.	ELISA analysis of CCL5 secretion of Huh7 and p53 ^{-/-} MSCs co-culture in vitro	- 39 -
4.2.10.	qRT-PCR analysis of Tie2, CCL5 and CCR5 expression in patient liver samples	- 40 -
4.2.10.1.	Disruption and homogenization of the tissue.....	- 40 -
4.2.10.2.	RNA isolation.....	- 41 -
4.2.10.3.	Measurement of RNA concentration	- 41 -
4.2.10.4.	cDNA synthesis	- 41 -
4.2.10.5.	qRT-PCR TaqMan gene expression assay	- 41 -
4.2.11.	Statistical analysis.....	- 41 -
V.	RESULTS	- 43 -
5.1.	<i>eMSCs are actively recruited to the site of hepatocellular carcinoma</i>	- 43 -
5.1.1.	MSCs show tropism for recruitment to tumor sites	- 43 -
5.1.1.1.	SPIO-transfected MSCs recruit to tumor site	- 43 -
5.1.1.2.	Prussian blue staining confirmed the recruitment of SPIO-labeled MSCs.....	- 44 -
5.1.2.	Reporter gene engineered of MSCs promote: targeting tumor growth, and angiogenesis.	- 45 -
5.1.2.1.	Reporter gene engineered MSCs promote tumor growth.....	- 46 -
5.1.2.1.1.	Total liver weight and volume increased after eMSCs injection.....	- 46 -

5.1.2.1.2. HE staining of HCC tumors.....	- 48 -
5.1.2.2. Reporter gene engineered MSCs promote angiogenesis and proliferation.....	- 49 -
5.1.2.3. eMSCs promote cancerous ascites.....	- 51 -
5.2. <i>Stroma- or angiogenesis-related signal or receptor expression in MSC recruited to the tumor site..</i> -	52 -
5.2.1. Systemically injected MSCs can activate Tie2- or CCL5- promoter driven reporter genes (RFP) following their recruitment to the HCC microenvironment.....	- 52 -
5.2.2. Expression of CCL5 receptors in the tumor-stroma.....	- 54 -
5.3. <i>In vitro data showed that CCL5 is secreted by MSCs</i>	- 56 -
5.4. <i>Tie2, CCL5, CCR5 expression in human samples</i>	- 56 -
5.5. <i>Suicide gene engineering MSCs inhibit tumor growth</i>	- 59 -
5.5.1. Tumor volume decreased after suicide gene engineered MSCs injection.....	- 59 -
5.5.2. Effect on microvessel density.....	- 61 -
5.5.3. Effect on tumor proliferation.....	- 61 -
VI. DISCUSSION.....	- 63 -
VII. PERSPECTIVES.....	- 70 -
VIII. SUMMARY.....	- 71 -
IX. ZUSAMMENFASSUNG.....	- 72 -
X. ABBREVIATION.....	- 74 -
XI. REFERENCES.....	- 76 -
XII. CURRICULUM VITAE.....	- 85 -
XIII. ACKNOWLEDGEMENTS.....	- 89 -

II. ABSTRACT

Hepatocellular carcinoma (HCC) is a major life threatening cancer world wide. Radical resection and liver transplantation are the two curative treatment options. However, when patients are diagnosed with HCC, the majority are in advanced stages thus limiting surgical options. Although bridging therapies such as transcatheter arterial chemoembolization (TACE), radio frequency ablation (RFA), and percutaneous ethanol injection (PEI) offer therapeutic options, new targeted strategies with less side effects, better prognosis, and easier tolerance are urgently needed.

Targeted therapy of tumor cells is the future prespective for different types of cancer. Suicide gene therapy allows the transfer of genes responsible for converting nontoxic products to toxic drugs, finally inducing a cytotoxic bystander effect on tumor cells. Transfection of suicide genes into mesenchymal stem cells (MSCs) and using them as cellular vehicles is a novel and promising approach for gene therapy against cancer. MSCs are naturally recruited to the tumor sites, selectively proliferate there, and participate in the formation of tumor stroma and angiogenesis. Transfection of suicide genes into mesenchymal stem cells (MSCs) under the control of tissue-specific promoters has been proposed to allow a tissue-specific expression of genes.

The goal of this study was to analyze the efficacy of engineered mesenchymal stem cell as therapy directed towards tumor stroma and angiogenesis of hepatocellular carcinoma. MSCs are in general actively recruited to the stroma and angiogenic milieu of tumors where they enhance growth, angiogenesis, and metastasis. In this study murine MSCs were engineered to express reporter genes, or therapeutic genes, under the control of the CCL5 or Tie2 promoter, and adoptively transferred into mice with growing HCCs. The effect on tumor growth, proliferation, and angiogenesis was evaluated. MSCs isolated from bone marrow of C57BL/6 p53^{-/-} mice were stably transfected with red fluorescent protein (RFP) or herpes simplex virus – thymidine kinase (HSV-Tk) gene driven by the CCL5 or Tie2 promoter. MSCs were intravenously applied once per week over 3 weeks to nude mice bearing xenogeneic HCC tumors. RFP signals driven by the CCL5 or Tie2 promoter were detected accompanying stromal specific CCL5 and angiogenesis specific CD31 signals in MSC treated HCC samples. The MSC-HSV-Tk therapy groups treated intraperitoneal with the prodrug ganciclovir 5 to 7

days after stem cell application lead to 66% and 42% reduction of HCC tumor growth as well as tumor cell proliferation following either CCL5- or Tie2-promoter driven HSV-Tk expression (* $p=0.027$; $p=0.165$). The highly selective expression of the therapeutic gene driven by different tumor environment-specific promoters in engineered MSCs represents a new targeted approach in cancer therapy and needs clinical validation.

III. INTRODUCTION

3.1 Mesenchymal stem cells

3.1.1 Background

The cell populations referred as mesenchymal stem cells (MSCs) are usually isolated from the mononuclear fraction of bone marrow aspirates which are then depleted of CD45⁺ cells and subsequently isolated as a sub-population of cells that adhere to plastic tissue culture dishes. The term “mesenchymal” defines a progenitor cell with fusiform shape able to actively move - as compared to “epithelial” or “parenchymal”. A unique surface marker identifying MSCs has not yet been identified, necessitating the application of a panel of antigens for their characterization. These include the expression of CD105, CD73 and CD90 at higher than 95% in culture, and an absence of markers for CD14, CD34, CD19, HLA-DR and CD45¹. MSCs can proliferate for many passages in culture and have the ability to give rise to diverse cell types, including adipocytes, chondrocytes, osteoblasts², pericytes³ and endothelial cells⁴.

Researchers have recently made use of MSCs as delivery vehicles for gene therapy, in part due to their accessibility for genetic modification *in vitro* and their ability to be cultured and expanded *in vitro*. The cells are easily obtained from a simple bone marrow aspirate and can be readily expanded. Their extraordinary high proliferative capacity is thought to contribute to the *in vivo* maintenance of both tumor stroma and connective tissue in organs remote from the bone marrow. MSCs successfully engraft into tissues under conditions of increased cell turnover, for example, those triggered by tissue damage, or neoplastic growth. They have the ability to efficiently home to sites of tissue injury including tumor environments. The exact mechanism governing this recruitment is not well understood. MSCs are thought to show a strong tropism for tumors because the tumor environment can be considered as the equivalent of a chronic wound – e.g. “the wound that never heals”⁵⁻⁸. Furthermore, MSCs inhibit T-cell proliferation^{9, 10}, induce T-cell apoptosis¹¹, alter migratory property of T-cells¹², and are resistant to natural killer cell-mediated cytotoxicity due to non-expression of MHC-I¹³. These evidences provide a plausible explanation for the immunoprevalency of MSCs. Each of these attributes contributes to the potential application of MSCs for cell-based delivery of therapeutic genes to solid tumors.

3.1.2 Genetically engineering MSCs in non-gastrointestinal cancer therapy

Molecules that physiologically control cell proliferation are often produced locally in tissues, and are rapidly turned over when they enter the peripheral circulation (e.g. TGF- β , TNF- α , IL-2, INF- β). The application of these biologic agents for cancer therapy is limited by their short biologic half-life or excessive toxicity. For effective anti-proliferative therapy the biologic concentration of these or other therapeutic agents required to achieve a therapeutic effect can often be substantially higher than serum levels achievable after systemic administration at the maximally tolerated dose. Similar issues arise when one considers general questions of regional *vs.* systemic therapy using more focused biologic approaches, for example, the use of suicide gene therapy.

An early application of MSCs as vehicles for cancer therapy was described by Studeny et al.¹⁴. The authors transfected hMSC with IFN- β which were then used to treat melanoma xenografts in mice. Injection of the transfected MSCs into the peripheral circulation lead to reduced tumor growth and prolonged survival of tumor-bearing mice. Subsequently, MSCs from different sources, including human bone marrow-derived MSCs (hBM-MSCs)¹⁵⁻¹⁸, human adipose tissue-derived MSCs (hAT-MSC)¹⁹, mouse bone marrow-derived MSCs (mMSC)²⁰⁻²³, and rat MSCs (rMSC)²⁴⁻²⁷, have been evaluated as vehicles for tumor therapy. The expression of diverse therapeutic genes including IFN- β ^{14, 15, 17}, TRAIL^{16, 19}, IL-12²⁰, CX3CL1²¹, VEGFR-1²³, iNOS²⁷, HSV-Tk^{22, 24-26} have been engineered into MSCs to allow a targeted release of the agents in models of melanoma^{14, 15}, breast cancer^{16, 20}, Lewis lung carcinoma²¹, glioma^{17, 22, 24}, glioblastoma^{25, 26}, cervical cancer¹⁹, and fibrosarcoma²⁷. In each of these tumor models, treatment showed efficacy in the inhibition of local tumor growth, suppression of metastasis, or prolongation of animal survival (Table 3.1).

Table 3.1. Transfected MSCs for non-gastrointestinal anti-cancer therapy

MSC	Transfected products	Tumor	Effect
hBM-MSC*	IFN- β	Melanoma ^{14, 15} Breast cancer ¹⁵ Glioma ¹⁷	inhibit tumor growth, suppress pulmonary metastasis and prolong survival
	TRAIL	Breast cancer ¹⁶	reduce tumor growth and metastasis
hAT-MSC [#]	TRAIL	Cervical cancer ¹⁹	inhibit tumor growth
mMSC [§]	IL-12	Creast cancer ²⁰	significantly interfere with cancer

			growth
	CX3CL1	Lewis lung carcinoma ²¹	inhibit growth of lung metastasis and prolong survival
	VEGFR-1	Lewis lung carcinoma ²³	decrease lung metastases and prolong lifespan
	HSV-Tk	Leptomeningeal glioma ²²	reduce tumor size and prolong survival
rMSC [†]	HSV-Tk	Glioma ²⁴ Glioblastoma ^{25, 26}	tumor growth suppression, survival prolongation
	iNOS	Fibrosarcoma ²⁷	inhibit tumor growth

*: hBM-MSCs, human bone marrow-derived mesenchymal stem cells; #: hAT-MSCs, human adipose tissue-derived mesenchymal stem cells; §: mMSCs, mouse bone marrow-derived mesenchymal stem cells; †: rat bone marrow-derived mesenchymal stem cells.

3.1.3 Dual effects of MSCs on gastrointestinal cancers

As shown in Table 3.1, in non-gastrointestinal cancers, MSCs have demonstrated comparable effects regarding tumor growth, metastasis, and animal survival. Control, or non therapeutic MSCs, are also recruited to the tumor site where they can function as stroma cells to support tumor development. However, in gastrointestinal cancers the biology appears more complicated as conflicting data exists regarding the biology of MSC in these tumor settings.

Following subcutaneous co-injection of liver cancer cells and hMSCs transfected with the human telomerase reverse transcriptase (hTERT) gene, Qiao²⁸ showed that the engineered hMSCs inhibited tumor growth through down-regulation of NF- κ B or Wnt signalling pathways²⁹. In contrast, our group has shown that systemically applied MSCs can strongly promote tumor growth in orthotopic pancreatic^{30, 31} or in hepatocellular carcinoma (HCC) models³².

Similar experimental settings have shown apparently disparent results concerning the biologic effects of MSCs. Li et al.³³ reported that hMSCs can enhance tumor growth *in vivo* in a s.c. HCC model, whereas MSCs were found to inhibit the invasion and metastasis of the same cell type *in vitro*. Interestingly, expression levels of TGF β 1 by the MSCs were decreased in both *in vitro* and *in vivo* experiments.

MSCs appear to have a complex biology in other gastrointestinal cancers, including esophageal cancer, gastric cancer, and pancreatic carcinoma. Li et al.³⁴ applied hMSCs

together with esophageal cancer cells subcutaneously in nude mice. The authors showed that hMSCs could promote tumor growth with increased tumor vessel formation *in vivo*. Interestingly, the MSCs were found to inhibit the proliferation and invasion of tumor cell *in vitro*. These effects were associated with a general down-regulation of canonical Wnt signaling^{28, 35}. In a gastric cancer xenograft mouse model, You et al.³⁶ injected hMSC transfected with the suicide gene cytosine deaminase (CD), which was followed by treatment with the prodrug 5-fluorouracil (5-FU). This resulted in a pronounced inhibition of tumor growth. In a chronic *Helicobacter felis* induced gastric dysplasia mouse model, Wang³⁷ applied murine bone marrow-derived Lin-CD44^{hi}Sca1-cKit⁺CD34⁻ MSCs via tail vein injection. Surprisingly, these MSCs were found to reduce tumor progression to low-grade gastric dysplasia, and correlated with reduced gastric IL-17F, IL-22, and ROR- γ t gene expression. Kidd et al.³⁸ showed that hMSCs with or without transfected IFN- β were both found to suppress tumor growth in the same orthotopic pancreatic cancer mouse model. This is in contrast to the results of our studies in an orthotopic pancreatic cancer model³¹, where control MSCs were found to strongly promote primary tumor growth and to increase metastases, whereas suicide gene (HSV-Tk) transfected MSCs substantially inhibited local pancreatic tumor growth and the incidence of metastases.

3.1.4 Additional examples of genetically engineered MSCs in gastrointestinal cancer therapy

Apparently contradictory reports of the biology of MSCs have been described in gastrointestinal cancers (summarized in Table 3.2). There are additional examples demonstrating MSCs in general promoting tumor growth and therapeutic gene engineered MSCs inhibiting tumor growth. Shinagawa³⁹ intravenously injected hMSCs in an orthotopic colon cancer model which resulted in an enhancement of tumor growth and metastases. Using CD-transfected hAT-MSCs in a colon adenocarcinoma xenograft model, Kucerova et al.⁶ could show tumor growth inhibition. Moreover, Chen⁴⁰ and Hu²³ transfected mMSC with IL-12 and VEGF-1 and then successfully demonstrated prevention of colon cancer carcinogenesis in a mouse model, reduction of lung metastasis, and a prolongation of lifespan.

Studený published the first two reports describing hMSC-based gene therapy in tumor models^{14, 15}. Wolf⁴¹ argued that the selective homing of systemically injected human MSCs in this model might be too artificial to be relevant to the clinical situation. To address this, the

authors used a complete syngenic murine model as their experimental system where in addition to MSC engraftment into syngenic tumors they observed exogenously applied MSCs in additional tissue sites, including spleen, liver, and normal lung⁴¹. The authors suggested that human tumors may selectively attract human MSCs by secretion of human-specific chemoattractants.

Our group has previously shown³¹ that GFP transfected mMSCs in an orthotopic murine pancreatic cancer model are effectively recruited to the tumor, but some signals were also found in spleen, lymph nodes, thymus, skin, and gut. More recent studies using imaging in xenogenic tumor models further support the effect of solid tumors in recruiting adoptively engineered MSC whether they are syngenic or xenogenic to the tumor cells³².

The potential recruitment of adoptively transferred MSC to non-tumor tissue environments with associated side effects is a potential concern for the general adaption of this technology for the treatment of cancer.

One approach is to specifically direct the expression of the transgene only in a tissue specific environment by using tissue specific promoters. Studeny¹⁵ made an early referral to the use of specific promoters. The authors transfected IFN- β into hMSCs using an adenoviral vector and as expected found that the inhibition of tumor cell growth by MSC-IFN- β cells was not permanent. Adenoviral vectors generally lack a sustained effect as adenoviral transgenes do not integrate into the genomes of transduced cells, and that the transgene copy number per cell declines as the virally engineering MSC cells proliferate in tumors. To this end a more sustained inhibition of tumor cell proliferation may be achievable through by using MSCs that are stably transfected with a plasmid that expresses IFN- β under the control of a conditional promoter. Loebinger¹⁶ made use of the inducible tetracycline-on system to activate MSCs transfected with TRAIL to treat different cancers. The Tet-on system allowed the TRAIL effector and the GFP reporter gene expression to be induced under the control of a tetracycline promoter following MSC engineering by a lentiviral vector. It allowed researchers to control the expression of the transgene through of the use of doxycycline.

Our group has approached this question from a different perspective through the use of tissue specific promoters. The general concept makes use of the differentiative capacity of MSCs following their recruitment into tumor microenvironments to drive a more restrictive expression of a therapeutic transgene only in a specific tissue context (e.g. by activation of the transgene by tissue specific signals) thus potentially sparing non-tumor tissues from

“therapeutic” damage.

In one example, we made use of the observations of Karnoub et al.⁴² who studied the role of MSCs in a xenograft model of breast cancer. The authors demonstrated that MSCs are actively recruited into tumor associated stroma. Once there, the MSCs actively secrete the chemokine CCL5. We tested the use of the CCL5 promoter to drive the expression of the suicide transgene HSV-Tk (accompanied with GCV) by engineering MSCs in a syngeneic model of pancreatic cancer³¹. After verifying the induction of CCL5 by MSCs in the context of pancreatic cancer, the promoter was used to drive the expression of the thymidine kinase suicide gene (HSV-Tk). In the context of treatment with ganciclovir, strong inhibition of tumor growth was seen with this selective targeting of the tumor stroma approach. Importantly, treatment also significantly reduced metastases in this model.

In a second set of experiments, expression of HSV-Tk was driven by the Tie2 enhancer/promoter. The idea was to drive transgene expression in engineered MSCs only when a subgroup of tumor infiltrating MSCs differentiate to endothelial related cells in the context of tumor angiogenesis. The Tie2 targeting strategy also effectively inhibited growth of experimental pancreatic cancer³⁰.

In each of these settings, a refined targeting was achieved such that only when the engineered MSCs infiltrate the tumor and undergo activation/differentiation the promoters are driving the transgene activation. We refer to this as a “Trojan Horse” approach. With this approach, even if engineered MSCs reach other organs, the effect of the transgenes will be limited as they are under the control of promoters that are not active in these other tissue settings (schematic view in Figure 3.1).

Table 3.2. Opposite effects of MSCs on gastrointestinal cancers

Gastrointestinal cancer	Author	MSC	effects	Opposite effects	MSC	Transfected reagent	Author
Gastric cancer	Wang ³⁷	mMSC [#]	reduced the progression to low-grade gastric dysplasia	↔ inhibit tumor growth in vivo with 5-FC	hMSC	CD [†]	You ³⁶
Pancreatic cancer	Kidd, Cousin ^{38, 43}	hMSC [§] , hAT- MSC	suppress tumor growth	↔ suppress tumor growth in vivo	hMSC	IFN-β	Kidd ³⁸ Zischek, Conrad ^{30, 31}
				↘ promote tumor growth in vivo	mMSC	GFP / RFP	
				↘ inhibit tumor growth in vivo accompanied with GCV	mMSC	HSV-Tk	
Hepatocellular carcinoma	Qiao ²⁸	hMSC [*]	inhibit tumor growth in vivo	↔ promote tumor growth in vivo	mMSC	RFP	Niess ³²
	Li ³³	hMSC	enhance tumor growth in vivo	↔ inhibit tumor cell invasiveness and metastasis in vitro	mMSC	HSV-Tk	
Esophageal cancer	Li ³⁴	hMSC	promote tumor growth and increase tumor vessel in vivo	↔ inhibit proliferation and invasion of tumor cell in vitro			

#: Lin-CD44hiSca1-cKit+CD34- MSC; §: transfected without IFN-β; *: immortalized by hTERT; †: CD, cytosine deaminase.

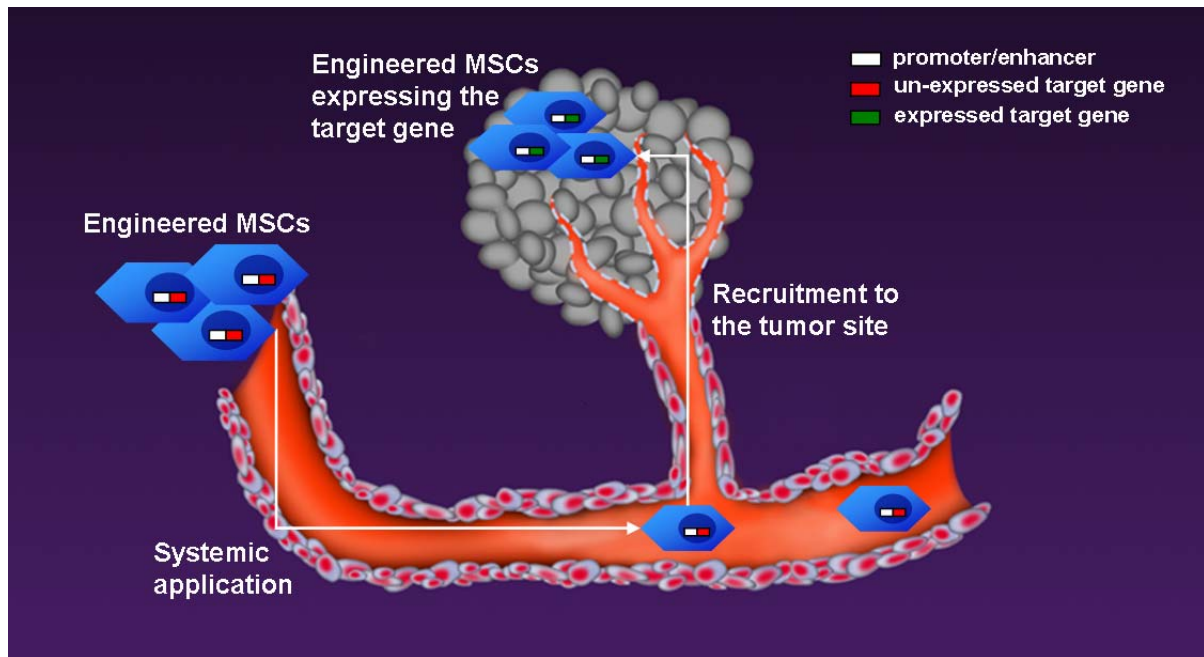


Figure 3.1. Schematic view of target-expressed MSCs recruit to tumor. The genes under the control of promoter/enhancer were transfected into MSCs, and these MSCs applied through peripheral circulation. The genes only expressed when the vehicle cell reached the tumor site, because of the promoter/enhancer started to induce tissue-specific transcription of target genes. If the MSCs reached other organs, the target genes cannot be expressed.

3.2. Hepatocellular carcinoma

3.2.1. Background

Hepatocellular carcinoma (HCC) is a major health problem with over 660,000 new cancer cases per year, making it the sixth most common malignancy and the third most common cause of cancer-related death worldwide^{44, 45}. In unresectable but yet curable patients, who constitute a major portion of patients, orthotopic liver transplantation remains the only curative option. The long transplant waiting list involved high dropout rates due to tumor progression and deaths⁴⁶. Bridging therapies, such as TACE, RFA, and PEI have been applied but have only limited capability of prolonging survival in unresectable patients⁴⁷. Thus, additional therapeutic strategies need to be evaluated to improve survival in HCC patients on the transplant waiting list.

3.2.2. Treatment of HCC

3.2.2.1. Surgical resection

Within selected patient populations, radical surgical resection is the primary treatment for HCC providing the highest chance of long-term survival. In recent years, the perioperative mortality has been reduced to less than 5% depending on the extent of resection and hepatic reserve⁴⁸. Because of advances in surgical and radiologic techniques, advanced perioperative care, and more accurate indication determination, the outcome of HCC surgical resection is improving. However, when patients are diagnosed with HCC, they are generally in an advanced stage or with significant liver cirrhosis. In this regard, only 5% of diagnosed cases of HCC in the West, and 40% in Asia are within the established criteria for resection treatment. New treatment strategies are clearly need to address those patients that fall outside the surgical resection option⁴⁴.

3.2.2.2. Liver transplantation

Liver transplantation has been used to tackle the problems of liver dysfunction and HCC simultaneously. It is considered to be the best treatment option for patients with one tumor and decompensated cirrhosis or multicentric small tumors⁴⁹. The best candidates for transplantation generally have one HCC smaller than 5 cm or up to three nodules smaller than 3 cm who, in tertiary referral centres, achieve 70% survival at 5 years, with a recurrence rate lower than 15%⁵⁰⁻⁵⁴. Although liver transplantation has completely changed the treatment for HCC, the shortage of donors has clearly reduced the potential benefits of this approach. During the long waiting time seen in some Western countries, there is a drop-out rate of 20-50% of cases. Adjuvant treatments, such as chemotherapy, chemoembolisation and percutaneous ablation, can be used to slow some tumor progression.

3.2.2.3. Trans-arterial embolisation therapy

Trans-arterial embolisation is the most widely applied treatment for unresectable HCC. This therapy is based on the fact that most of the tumor's blood supply is derived from the hepatic artery. Obstruction of hepatic artery causes extensive necrosis in the large vascularised HCC⁵⁵.⁵⁶ Trans-arterial embolization can induce ischemic necrosis in HCC, achieves partial response in 15-55% patients, and substantially delays tumor progression and vascular invasion⁵⁷⁻⁶⁰. In

order to improve the efficacy of trans-arterial embolisation, chemotherapeutic agents (chemoembolisation) have been administered together with the embolisation particles, and oils such as lipiodol that are selectively taken up by HCC. This treatment is limited to patients with preserved liver function and asymptomatic multinodular tumors without vascular invasion. Otherwise, it will cause higher incidence of treatment-induced liver failure, overturn the potential benefits.

3.2.2.4. Non-surgical local ablative treatments

Destruction of cancer cells by percutaneous treatment is achieved by chemical substances (alcohol, acetic acid) or by modifying the temperature of cancer cells (radiofrequency, microwave, laser, and cryoablation)⁶¹. Percutaneous ethanol injection (PEI), which kill the tumor by a combination of cellular dehydration, coagulative necrosis, and vascular thrombosis, achieves responses of 90-100% in HCC smaller than 2 cm, to 70% in those of 3 cm, and 50% in HCC of 5 cm in diameter^{62, 63}. Compared with PEI, percutaneous injection of acetic acid has stronger necrotizing abilities, making it more useful in septated tumors⁶⁴. The radiofrequency ablation (RFA) uses high-frequency alternating current to create heat around an inserted probe, resulting in temperatures greater than 60°C and immediate cell death. It can be applied percutaneously, laparoscopically, or during laparotomy, and it may provide better anti-tumor benefits than PEI in tumor larger than 3 cm. The 5-year survival estimates for RFA are 33-40%^{65, 66}. In a review of 3670 patients treated by RFA, mortality was 0.5% and the complication rate 8.9%⁶⁷. Cryoablation therapy, which uses a specialized cryoprobe to freeze and thaw tumor and surrounding liver tissue with resulting necrosis, has as disadvantage the so-called heat-sink effect, limiting the utility of freezing near major blood vessels and is associated to a relatively high complication rate from 8% to 41%⁶⁴.

3.2.2.5. Chemotherapy

To prolong the survival of patients with unresectable HCC, systemic chemotherapy is also conducted. Albeit anthracyclines are considered the most effective agents and single-agent doxorubicin regimens have been widely used, the response rates of chemotherapy are low (<20%) with no survival advantage. Because of toxicity, especially in patients with underlying liver disease, systemic chemotherapy is neither recommended as first-line therapy nor as control treatment within clinical trials⁶⁸⁻⁷⁰.

3.2.3. Summary for this part

The curative treatments for HCC are radical resection of tumor and liver transplantation. However, both have strict criteria for candidate selection. Meanwhile, liver transplantation is limited by availability of organ donors. Although the new bridging therapies, such as PEI, RFA, and TACE, facilitate to improve the prognosis of HCC patient recent years, they all have disadvantages, such as narrow range of patient's selection, relative high complication rate, unspecific tumor killing, or influence of remnant liver function. To this end, new strategies, which are designed to be easily applicable and specifically targeting tumor tissue with low influence on normal liver, are urgently needed.

3.3. Tumor microenvironment

Malignant cells exist in a complex cellular and extracellular microenvironment referred to as the tumor stroma, which significantly influences the initiation and maintenance of the malignant phenotype⁷¹⁻⁷³. Solid tumors are comprised of malignant cells and the supporting "normal" cells that comprise the stroma including fibroblasts, endothelium, pericytes, lymphatics, and generally, mononuclear infiltrates. These stromal cells are required for tumor survival and represent an important target for chemotherapeutic intervention⁷⁴⁻⁷⁶. The tumor stroma surrounding is of crucial importance for tumor growth, progression, recurrence, and metastases.

Tumor stroma and tumor angiogenesis are the two important aspects of tumor progression. Karnoub and colleagues showed that in breast cancer MSCs are recruited to the tumor environment where they induce the expression of the chemokine CCL5⁴². CCL5 (chemokine (C-C motif) ligand 5, also called RANTES, regulated upon activation of normal T cell) is a chemokine or chemotatic cytokine that has been shown to play diverse roles in immunoregulatory and inflammatory processes⁷⁷. Further studies have shown that it is also a critical signal in tumor stroma and tumor neovascularization^{42, 78-81}. CCL5 functions as a chemoattractant for blood monocytes, memory T helper cells and eosinophils. It causes the release of histamine from basophils and activates eosinophils. In addition, CCL5 is thought to contribute to tumor growth and metastasis by autocrine activation of tumor cells as well as through the recruitment of a number of stromal cell types to sites of primary tumor growth⁷⁹⁻⁸¹.

Neoangiogenesis is a crucial step in the transition of a tumor from a small group of malignant cells to a macroscopic tumor lesion^{82, 83}. Tumor growth is promoted when the proliferation of vascular endothelial cells is increased, and tumor growth is inhibited when the proliferation of vascular endothelial cells is targeted or suppressed. Therefore, angiogenic tumor vessels represent promising targets for the selective delivery of cancer therapeutics. Tie2 is an endothelial cell surface tyrosine kinase receptor, which binds Ang-1 or Ang-2, and has wide-ranging effects on tumor malignancy that includes angiogenesis, inflammation, and vascular extravasation. Tie2 expression is increased in angiogenic “hot spots” during tumor growth and progression.

IV. MATERIALS UND METHODS

4.1. Materials

4.1.1. Cell lines

4.1.1.1. Human hepatocellular carcinoma cell Huh7

Huh-7 is a well differentiated hepatocyte derived cellular carcinoma cell line originally isolated from a liver tumor in a 57-year-old Japanese male in 1982. The line was established by Nakabayshi, H. and Sato, J.⁸⁴.

4.1.1.2. Murine bone marrow-derived mesenchymal stem cell

Mesenchymal stem cells were isolated from the bone marrow of C57BL/6 mice homozygous for the targeted deletion of *p53* as described⁸⁵. The *p53* knockout phenotype lead to the partial immortalization of the cells and allowed expansion, culture and subcloning of the resultant MSC cells. The cell line has retained significant pluripotency⁸⁶. The cells grew adherently and continuously in cell culture and retained significant pluripotency. After subcloning, single cell clones were selected and characterized. These CD34- MSCs express CD73 and CD105 and lack CD14, CD45 and MHC class II^{86, 87}.

4.1.1.3. *RFP* or *HSV-Tk* engineered mesenchymal stem cell

The cells were transfected with red fluorescent protein (*RFP*) or herpes simplex thymidine kinase (*HSV-TK*) under the control of *Tie2* promoter and enhancer or under the control of the *CCL5* promoter, respectively, to achieve tissue specific expression of the construct. Four MSC lines were produced: 1) C57BL/6 *Tie2/RFP*⁺, 2) C57BL/6 *CCL5/RFP*⁺, 3) C57BL/6 *Tie2/HSV-Tk*⁺ and 4) C57BL/6 *CCL5/HSV-Tk*⁺. All vectors included a *Bsr2* blasticidin resistance gene controlled by the *CMV* promoter used to select for transfected cells at a blasticidin concentration of 5 µg/mL. Schematic diagrams of these four vectors are shown in Figure 4.1.

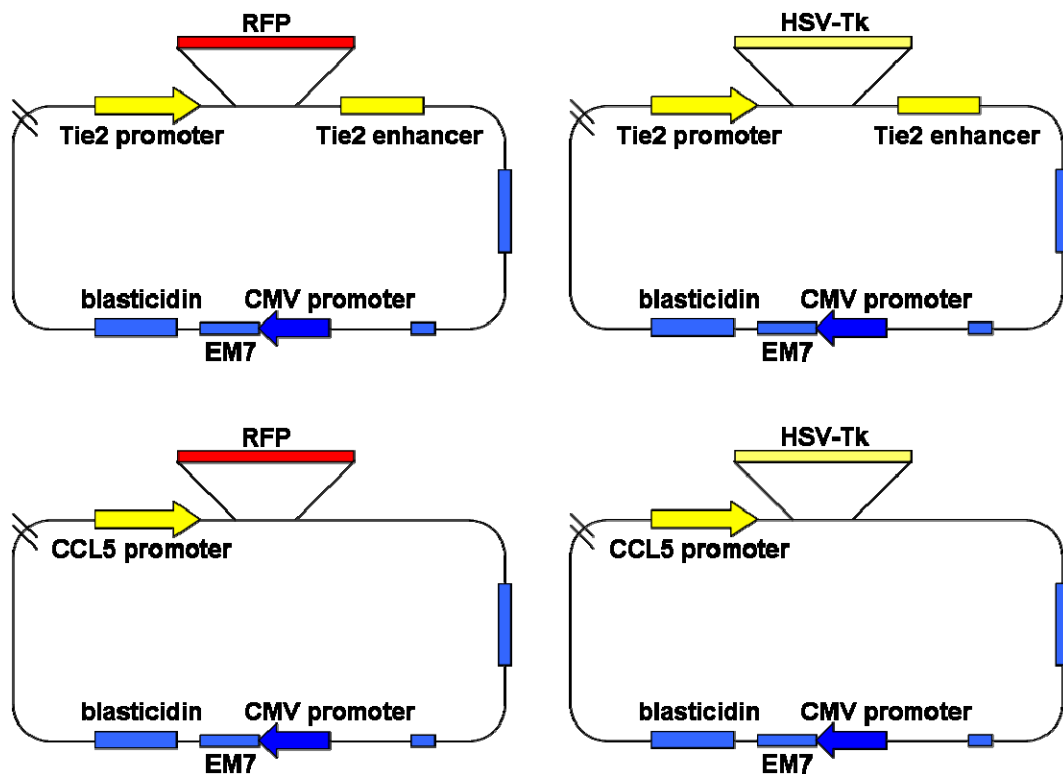


Figure 4.1. Schematic diagrams of the vectors of *Tie2/RFP*, *Tie2/HSV-Tk*, *CCL5/RFP*, and *CCL5/HSV-Tk*, which are stably transfected into C57BL/6 p53^{-/-} mesenchymal stem cell.

4.1.2. Technical equipments

Freezer -80°C	Heraeus, Hanau, Germany
Freezer -20°C	Siemens AG, Germany
Fridge 4°C	Siemens AG, Germany
Automatic pipettes	Gilson, Middleton, WI, USA
AxioCam MRc5 camera	Carl Zeiss GmbH, Germany
Microscopes	Carl Zeiss GmbH, Germany
Centrifuges	Eppendorf, Germany
CO ₂ Incubators	Heraeus, Rodenbach, Germany
Digital Precision Scale	KERN & Sohn GmbH, Germany
Microwave oven	Siemens, Germany
Hand tally counter	Carl Roth GmbH, Karlsruhe, Germany

Liquid nitrogen tank	MVE, New Prague, MN, USA
Vortex	IKA Works, Wilmington, NC, USA
Water bath	GFL, Burgwedel, Germany
Thermo Scientific Heraeus Incubator	Thermo Fisher Scientific Inc, Germany
Herasafe EN12469 2000 Class II Safety Cabinet	Thermo Fisher Scientific Inc, Germany
TECAN GENios Plus ELISA reader	TECAN, Salzburg, Austria
Leica RM2255, Fully Motorized Rotary Microtome	Leica Microsystems, Nussloch, Germany
RNA/DNA Calculator	GeneQuant Pro, GE Healthcare Life Sciences, USA
Applied Biosystems 7000 Real-Time PCR System	Applied Biosystems, USA
Automatic Tissue Processors Model 2065/2	MDS Group GmbH, Buseck, Germany
Philips Infrared Lamp	Philips Consumer Lifestyle, Drachten, Netherlands

4.1.3. Cell culture materials

Sterile tissue culture plastic flasks	NUNC, Roskilde, Denmark
Centrifuge tubes 15 mL	TPP, Switzerland
Falcon tubes 50 mL	BD, NJ, USA
Hemocytometer and cover-slip (Cell counting chambers)	Bürker-Türk, Germany
Cryotube (1.0 mL)	NUNC, Roskilde, Denmark
Eppendorf safe-lock tubes (1.5 mL, 2.0 mL)	Eppendorf AG, Hamburg, Germany
6-well culture plates	Nunc, Roskilde, Danmark

4.1.4. Medium, buffer, solution for cell culture

RPMI 1640 + Glutamax-1 500 mL	61870-044, Gibco Invitrogen, Germany
Fetal Bovine Serum 500 mL	Biochrom AG, Berlin, Germany
Penicillin/Streptomycin 100 mL (10.000 Units Penicillin/mL, 10 mg Streptomycin/ml)	PAN Biotech GmbH, Germany
Trypsin0.05%/EDTA0.02 % in PBS without Ca ²⁺ and Mg ²⁺ 100 mL	

PBS-buffer	PAN Biotech GmbH, Germany
DMSO (Dimethylsulphoxide)	Biochrom AG, Berlin, Germany
Trypan Blue (0.4%)	Sigma-Aldrich, Steinheim, Germany
	Sigma-Aldrich, Steinheim, Germany

4.1.4.1. Cell culture medium

RPMI 1640+ Glutamax-1 Medium	plus	10% FCS
		100 IU/mL Penicillin
		100 µg/mL Streptomycin

4.1.4.2. Cell storage medium

90% FCS	plus	10% DMSO
---------	------	----------

4.1.5. Materials for immunohistochemistry

Neo-Clear [®] (Xylene substitute)	Merck, Darmstadt, Germany
Ethanol 70%, 80%, 96%, 100%	CLN GmbH, Niederhummel, Germany
TRIZMA Base	Sigma-Aldrich, Steinheim, Germany
TRIZMA Hydrochloride	Sigma-Aldrich, Steinheim, Germany
Sodium chloride	Merck, Darmstadt, Germany
Hydrogen peroxide 30% (H ₂ O ₂)	Merck, Darmstadt, Germany
Albumin from bovine serum (BSA)	Sigma-Aldrich, Steinheim, Germany
Target retrieval solution 10×	Dako, CA, USA
Avidin/Biotin blocking kit	Vector Laboratories, CA, USA
Normal rabbit serum	Vector Laboratories, CA, USA
Normal goat serum	Vector Laboratories, CA, USA
Mayer's hemalum solution	Merck, Darmstadt, Germany
Kaiser's glycerol gelatine	Merck, Darmstadt, Germany
Triton [®] X-100	Sigma-Aldrich, Steinheim, Germany
Vectastain [®] ABC kit	Vector Laboratories, CA, USA
Liquid DAB+ substrate chromogen system	Dako, CA, USA
Monoclonal rabbit anti-Ki67 antibody	Abcam, UK

Polyclonal rabbit anti-CD31 antibody	Abcam, UK
Polyclonal goat anti-mouse CCL5/RANTES antibody	R&D systems, USA
Polyclonal goat anti-human CCR5 antibody	Novus, USA
Polyclonal rabbit anti-RFP antibody	MBL, Japan
CKR-1 (C-20) anti-CCR1 antibody	Santa Cruz, USA

4.1.5.1. Tris-buffer

1 L H ₂ O (dest.)	plus	0,9 g/L TRIZMA Base
		6,9 g/L TRIZMA Hydrochloride
		8,8 g/L Sodium chloride

Adjust pH to 7.5

4.1.5.2. Tris buffered saline (TBS) buffer, 10×

1 M	Tris-HCl, pH7.4
1.5 M	NaCl

4.1.5.3. PBS wash buffer, 1×

140 mM	NaCl
2.7 mM	KCl
10 mM	Na ₂ HPO ₄
1.8 mM	KH ₂ PO ₄

High purity dH₂O, adjust pH to 7.4

4.1.6. Materials for animal experiment

4.1.6.1. Animals

Bagg-albino/c(Balb/c) nu/nu male mice (8-10 week old, 20-22g)	Charles River, Sulzfeld, Germany
--	----------------------------------

4.1.6.2.Surgery instruments

Forceps	Dosch GmbH, Heidelberg, Germany
Disposable scalpels	Feather Safety Razor Co., Japan
Scissors, sharp / blunt	Dosch GmbH, Heidelberg, Germany
Needle holder	Dosch GmbH, Heidelberg, Germany

4.1.6.3.Medicine

Growth Factor Reduced (GFR) BD Matrigel™ Matrix10mL	354230, BD Biosciences, USA
Ketaminhydrochlorid (Ketavet®) 100mg/mL	Pfizer Pharmacia GmbH, Berlin Germany
Xylazinhydrochlorid, Xylazin (Rompun®) 2% 25mL	Bayer Healthcare, Leverkusen, Germany
Ganciclovir (Cymeven®) 500mg	Roche, Grenzach-Wyhlen, Germany

4.1.6.4.Other materials

Normal saline	Braun AG, Germany
BODE Cutasept® F	Bode Chemie, Hamburg, Germany
Syringe (1mL, 5 mL)	BD Plastipak™, Madrid, Spain
Hypodermic needle(30G)	B-Braun, Melsungen, Germany
Injection needle (20G)	BD Microlance™, Spain
Thread with needle USP 4/0 Seralon®,	Serag-Wiessner AG, Naila, Germany
Rotilabo®-embedding cassettes	Carl Roth GmbH, Karlsruhe, Germany
4% Formalin	Pathology LMU, Germany
Q-tips (cotton applicator)	NOBA, Wetter, Germany

4.1.7. Materials for ELISA

Mouse CCL5/RANTES DuoSet ELISA Development kit	R&D Systems, Minneapolis, USA
Wash buffer	PBS wash buffer plus 0.05% Tween-20
Reagent Diluent	1% BSA in PBS
Substrate Solution	BD optEIA TMB Substrate Reagent Set

Stop Solution	H ₂ SO ₄
Streptavidin-HRP	BD Pharmingen, Germany

4.1.8. Materials for qRT-PCR

RNeasy Mini Kit (250)	QIAGEN, Hilden, Germany
High-capacity cDNA reverse transcription kit	Applied Biosystems, USA
Platinum Quantitative PCR SuerMix-UDG with ROX	Invitrogen, USA

TaqMan Gene Expression Assays:

CCL5, Hs00174575_m1

CCR5, Hs99999149_s1

TEK (Tie2), Hs00945146_m1 Applied Biosystems, USA

Eukaryotic 18S rRNA Endogenous Control (VIC/TAMRA Probe, Primer Limited)

Applied Biosystems, USA

β-Mercaptoethanol Sigma-Aldrich, Steinheim, Germany

Liquid nitrogen Klinikum Grosshadern, LMU, Germany

Dry ice Klinikum Grosshadern, LMU, Germany

Mortar and Pestle Carl Roth GmbH, Karlsruhe, Germany

RNase-free filter tips Starlab GmbH, Ahrensburg, Germany

4.1.9. Software

Adobe Acrobat 7.0 Professional Adobe Systems Inc., USA

Axio Vision 4.4 Carl Zeiss GmbH, Germany

Microsoft Office 2003 (Word, Excel, Powerpoint) Microsoft Corporation, USA

EndNote X3 (Windows Version X3) Thomson Reuter

IBM SPSS Statistics 19 SPSS STATISTICS Inc., USA

Windows XP Professional Microsoft Corporation, USA

SoftMax[®] Pro Molecular Devices Corp., USA

Image-Pro Plus 5.0 Media Cybernetics, Inc., USA

4.2. Methods

4.2.1. Cell culture conditions

All kinds of cell lines used in this experiment were incubated at 37°C under 5% CO₂. The humidity of the incubator was 98%. Cells were kept cultured in 75 cm² or 175 cm² flasks, and the medium was changed every 3 days.

4.2.2. Passage of cells

The cells grew until 80-90% confluent, and then were washed once by 1× PBS. Cells were passaged by brief trypsinization with 0.025% trypsin (Trypsin/EDTA, PAN biotech GmbH, Aidenbach, Germany).

4.2.3. Determination of cell number

The dye Trypan Blue stains dead cells with membrane defects. Thus, living and dead cells can be distinguished by their ability to exclude the blue dye.

100µL of the cell resuspension was aspirated into 1.5mL Eppendorf tube, then added an equal volume of 0.4% Trypan Blue and gently mixed. The hemacytometer was prepared by first cleaning the chamber surface with 70% ethanol, then covered with cover-slip (Figure 4.2 a). 10µL of the stained cells was added into the space between the cover-slip and hemacytometer chamber. Using a hand tally counter, the number of viable (unstained) cells was counted in an area of 16 squares. As shown in Figure 4.2 b, the cell number was counted using the microscope, and was determined in four 16-corner-square regions (blue, Figure 4.2 b). The counting rule is schematically shown in Figure 4.2 c, which means that cells riding on the lines of the lower and left quarter are included, whereas cells on the lines of the upper and right quarter are excluded (red ones are included, and white ones are excluded, Figure 4.2 c).

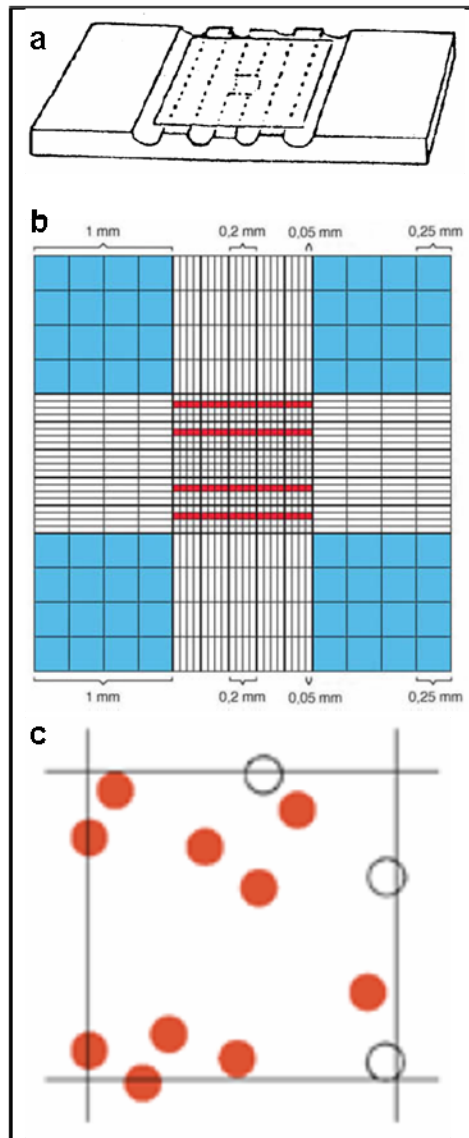


Figure 4.2. Determine the cell number. a) Hemacytometer and cover-slip; b) A sketch of the grid seen on a hemacytometer, cells are counted in four sets of 16 squares at each corner of the grid (in blue); c) Schematic picture of cell-counting rule in one small square.

The cell count was summed up from all 4 sets of 16 corner squares. This total number was divided by 4 to find the average number, and then multiplied by 2 (to adjust for the 1:2 dilution factor with trypan blue). Finally, the concentration of cells per mL was obtained as multiplying by 1×10^4 (the formula listed below).

$$\text{Cell number / mL} = (4 \text{ blue-region total cell number} / 4) \times 2 \times 10000$$

4.2.4. Storage and recultivation of the cells

4.2.4.1.Storage of the cells

The cell resuspension number was determined by the method mentioned above. Normally, the cells were stored in 1 to 4 million per cryotube (1.0 mL). Then 1 to 4 million cells were centrifuged at 350g (rph) for 5 minutes, and the supernatant was aspirated. The remaining cell pellet was then suspended with 1mL Fetal Bovine Serum and 10% DMSO. The dimethylsulphoxide (DMSO) is a cryoprotective agent which can minimize the cellular injury by freezing and thawing procedures, such as intracellular ice crystals and osmotic effects. The tubes are moved to a gradually temperature-decreasing tank and then kept in a -80°C freezer. After 72 hours, the tubes were moved to a liquid nitrogen tank for long-time storage.

4.2.4.2.Recultivation of the cells

The culture medium was first aspirated into the cell culture flask. The frozen tubes were taken out of the liquid nitrogen tank, and were immediately put into the 37°C water bath for 1-2 minutes. After almost complete thawing of the cells, the tubes were taken out of the bath. The cells were then added into the cell culture flask. After one day of culturing in the incubator, the medium was changed to avoid toxic effect of the remaining DMSO.

4.2.5. Orthotopic hepatocellular carcinoma mouse model

4.2.5.1.Animals

The 6- to 8-week old, 18-20g weight of Balb/c (Baggalbino/c) nu/nu mice were obtained from Charles River, Inc (Sulzfeld, Germany). All animal experiments were conducted according to German legislation for the protection of animals.

4.2.5.2.Animal's living conditions

Animals were housed and maintained in laminar flow cabinets under specific pathogen-free conditions with free access to food and water.

4.2.5.3. Anesthesia

The mice were anesthetized using 100mg/kg Ketaminhydrochlorid (Ketavet[®]) and 5mg/kg Xylazinhydrochlorid (Rompun[®]). The mixed anesthesia reagent was injected intraperitoneally. Normal saline, Ketavet and Rompun were mixed in a ratio of 1:1:1 (1 mL of each). The intraperitoneal injection volume for each mouse was 50 uL of this solution.

4.2.5.4. Surgical techniques

4.2.5.4.1. Intra-hepatic Huh7 cell injection

The operation site was prepared in a sterile manner. A 1 cm incision in the midline of the upper abdomen was performed and the lateral lobe of liver was exposed. A 1 ml syringe and 30G needle were used to inject 1×10^6 Huh7 human hepatocellular carcinoma cells in 40 μ l PBS mixed with 40 μ l Matrigel (BD Biosciences, USA) into the left lobe of the liver. To avoid spilling into the peritoneal cavity, a Q-tip was pressed lightly on the injection site for one minute after the needle was pulled out of the liver. After injection of the tumor cells, the peritoneum and skin were closed with interrupted sutures of USP 4/0 Seralon (Serag-Wiessner AG, Naila, Germany). The procedure is shown in Figure 4.3.



Figure 4.3. Intra-hepatic Huh7 cells injection. a) The median incision of the mouse abdomen was conducted to expose the left lateral liver lobe; b) Q-tips were used to better expose the liver lobe; c) Injection of Huh7 cells into the liver lobe.

4.2.5.4.2. Ear markers

In order to distinguish the mice in the whole process of the experiment, the mice were marked using ear markers. The ears were marked with ear staples (Figure 4.4) right after the surgery and still during the anesthesia.



Figure 4.4. The mouse ear marker and the hole on the mouse ear

The ear markers were conducted as shown in Table 4.1.:

Table 4.1. Schematic pictures of mouse ear markers

Mouse number	Ear Marker	Mouse number	Ear Marker	Mouse number	Ear Marker
1		6		11	
2		7		12	
3		8		13	
4		9		20	
5		10		30	

4.2.5.4.3. Injection of eMSCs

The Philips Infrared Lamp (Philips Consumer Lifestyle B.V., Drachten, Netherlands) was used to warm up the tails of the mice for vein dilation, so that the eMSCs can be easily injected into the tiny tail veins.

Tail vein injections were conducted without anesthesia to better observe pulmonary embolism which is the most critical problem in this procedure. In order to better observe the mice breathing during and after the peripheral injection, we kept the mice awake and adjust our procedure according to their respiration (e.g., slow down the injection rate, oxygen inhalation, etc.)

For intravenous tail vein injection the animals were kept in cylindric chambers to limit their activity and completely expose their tail. The cells were then slowly injected as shown in Figure 4.5.

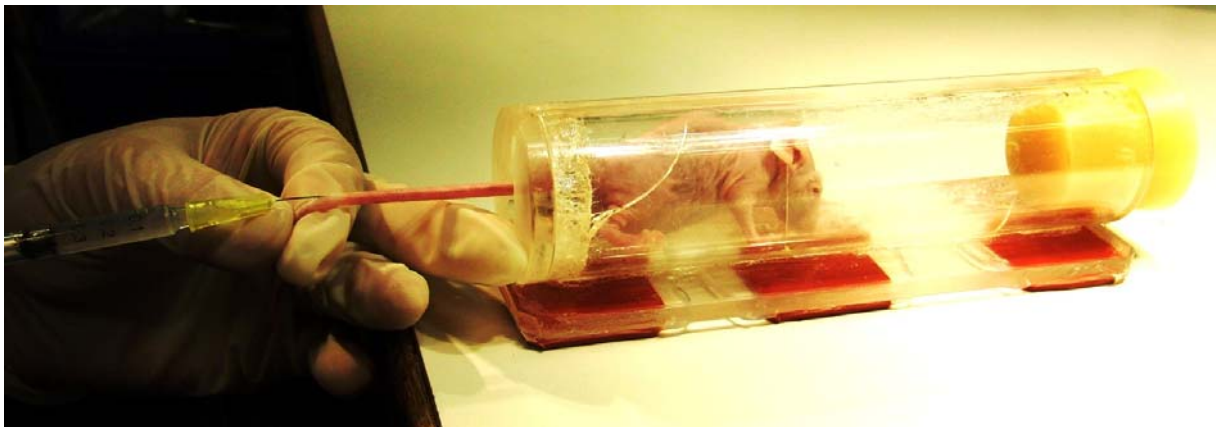


Figure 4.5. Nude mouse tail vein injection

4.2.6. Injection of SPIO-transfected MSC in tumor-bearing mice

4.2.6.1. Labeling of MSC by transient supermagnetic iron oxide (SPIO) transfection

The SPIO-containing contrast agent Resovist (Bayer Schering Pharma AG, Berlin, Germany) was used for labelling of MSCs. Resovist is a clinically approved carboxydextran-coated SPIO with an average hydrodynamic diameter of 60 nm. Its iron oxide particles have an R1 relaxivity of $4.6 \text{ mM}^{-1} \text{ s}^{-1}$ and an R2 relaxivity of $143 \text{ mM}^{-1} \text{ s}^{-1}$ at 37°C and 3T^{88} .

The liposomal agent Lipofectamine (Invitrogen, Berlin, Germany) was applied for labelling. Contrast agents at a dose of $50 \mu\text{g Fe}$ were pre-mixed with $20 \mu\text{L}$ Lipofectamine in a total

volume of 100 μL DMEM and incubated for 30 min at 37°C. Then the volume was increased to 0.8 mL of contrast medium. The SPIO – Lipofectamine complexes were added to the cells. Afterwards the cells were incubated for 4h under standard cell culture conditions (37°C, 5% CO_2). To eliminate residual contrast agent particles, cell samples were washed at least three times with DMEM after the incubation. Afterwards, cells were resuspended in 0.3 mL DMEM and filtered through a 30- μm Filcon filter (BD Immunocytometry Systems, Erembodegem, Belgium) to avoid cell agglutination. To determine the effectiveness of the labelling procedure, the intracellular SPIO-particles were stained with Prussian Blue. The presence of extracellular, membrane-associated SPIO–Lipofectamine complexes was microscopically excluded. The iron oxide-labelled cells were counted in a Neubauer counting chamber. For MR imaging, unlabelled and labelled cells (1×10^6) were centrifuged in Eppendorf tubes and resuspended in PBS.

4.2.6.2. *In vivo* MR-Imaging of SPIO-labeled MSC

Mice carrying hepatocellular carcinoma four weeks after tumor cell inoculation received intravenous injections of sterile normal saline, 1×10^6 unlabeled C57BL/6 MSCs, or 1×10^6 supermagnetic iron oxide (SPIO) labeled C57BL/6 MSCs (MSC^{iron}) (as shown in Figure 4.6). Thirty-six hours after the respective injections mice were sacrificed directly before evaluation with MR imaging. As control, mice without prior tumor cell inoculation also received normal saline or MSC^{iron} injections and were scanned by MRI as well (n=2 animals in each group).

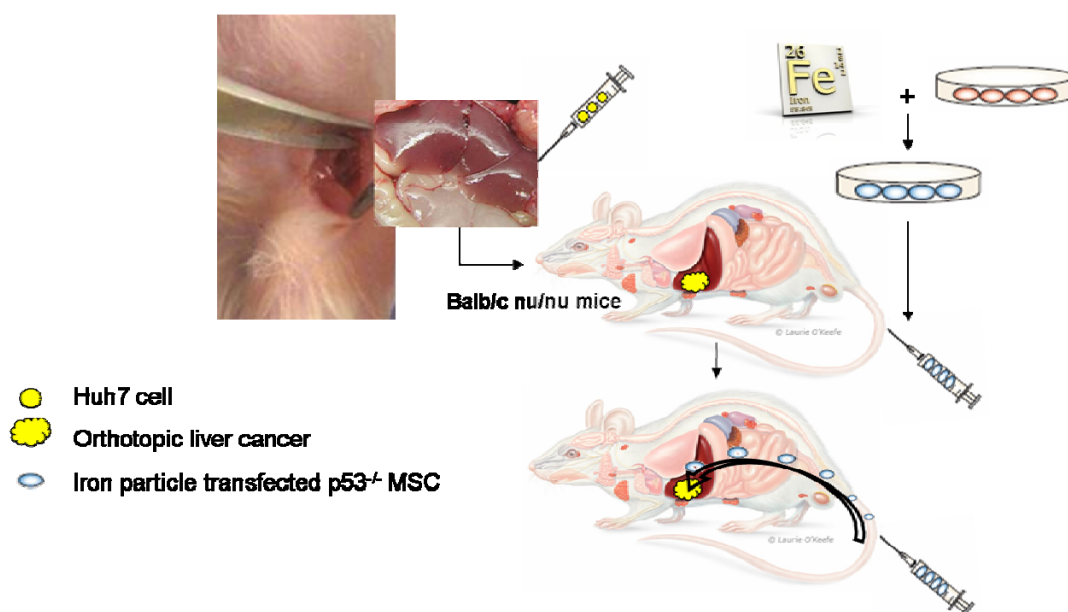


Figure 4.6. SPIO-transfected MSCs injected into HCC-bearing mice

The transfected SPIOs cause disturbances of the magnetic field, leading to a signal decay, which can be detected with T2- and T2*-weighted MR-sequences. Increasing iron concentrations lead to a decreasing T2* relaxation time of the surrounding tissue. The rate of spin dephasing, R2*, is therefore an index of the iron concentration in tissue ($R2^* = 1/T2^*$). However one must note, that other factors, e.g. hemosiderin or bowel air may cause a similar drop in signal, i.e. increasing R2*⁸⁹. Therefore, areas of increased R2* signals were correlated with areas of vital tumor in the T2-weighted MR images as well as by Prussian Blue staining in histology to confirm the SPIO-labeled MSCs as the origin of the iron particles.

Imaging was performed with a clinical 3T-Scanner (Magnetom Verio, Siemens Healthcare Sector, Erlangen, Germany) using a dedicated 8-channel-mouse-coil. The animals were placed in a head first - prone position. Coronal T2-weighted TSE sequences (repetition time (TR) 2930ms; echo time (TE) 89ms, matrix: 384x384, FoV: 79x70mm, slice thickness= 1mm, flip angle=150°) and coronal T2*- weighted-sequences (3D FLASH, Matrix=448x112, FoV=37x150mm, slice thickness=1mm, flip angle=15°) with increasing TEs were obtained (TR 50ms; TE6/8.5/10/15ms).

Postprocessing was performed with an in-house built MatLab-Software (7.2.0.529 (R2009B)). A pixel-based fit to the signal decay over the increasing echo times was computed, resulting in color-coded R2*-maps. This work was performed in collaboration with Dr. Mike Notohamirodjo, Department of Clinical Radiology, University Hospitals Munich.

4.2.7. Experimental setting

All mice were randomized into the respective experimental groups (as shown in Table 4.2).

Group A: no stem cells or GCV injections (n=10 mice)

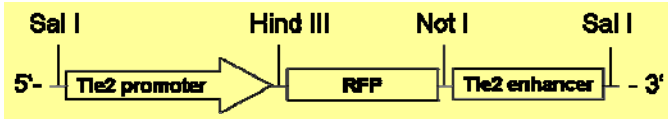
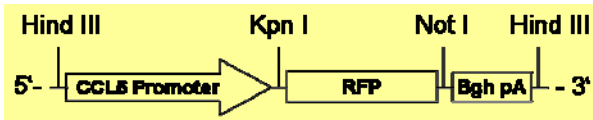
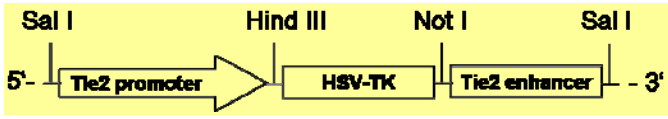
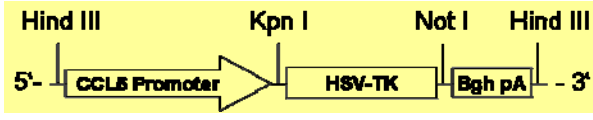
Group B: C57BL/6 *Tie2/RFP*⁺ MSCs injections (n=5 mice)

Group C: C57BL/6 *CCL5/RFP*⁺ MSCs injections (n=5 mice)

Group D: C57BL/6 *Tie2/HSV-TK*⁺ MSCs and GCV injections (n=10 mice)

Group E: C57BL/6 *CCL5/HSV-TK*⁺ MSCs and GCV injections (n=10 mice).

Table 4.2. Group design of the reporter gene engineered MSCs and suicide gene engineered MSCs in HCC-bearing mice

Groups	Transfected vector	GCV injection
Control	No MSCs	No GCV
Non-therapeutic MSC group		
P53 ^{-/-} Tie2/RFP ⁺ eMSC		No GCV
P53 ^{-/-} eMSC		No GCV
Therapeutic MSC group		
P53 ^{-/-} Tie2/HSV-Tk ⁺ eMSC		GCV
P53 ^{-/-} eMSC		GCV

All stem cell injections were dosed at 0.5×10^6 cells per week and administered via the tail vein. Ganciclovir (Cymeven[®], Roche, Germany) injections of group D and group E at a dose of 1.5 mg/mouse were applied intraperitoneally on days 4 to 6 after the stem cell injections (as shown in Figure 4.7). All mice were killed after three cycles of treatment (five weeks after tumor cell inoculation) and the liver specimen including tumors as well as other organs were harvested and weighed.

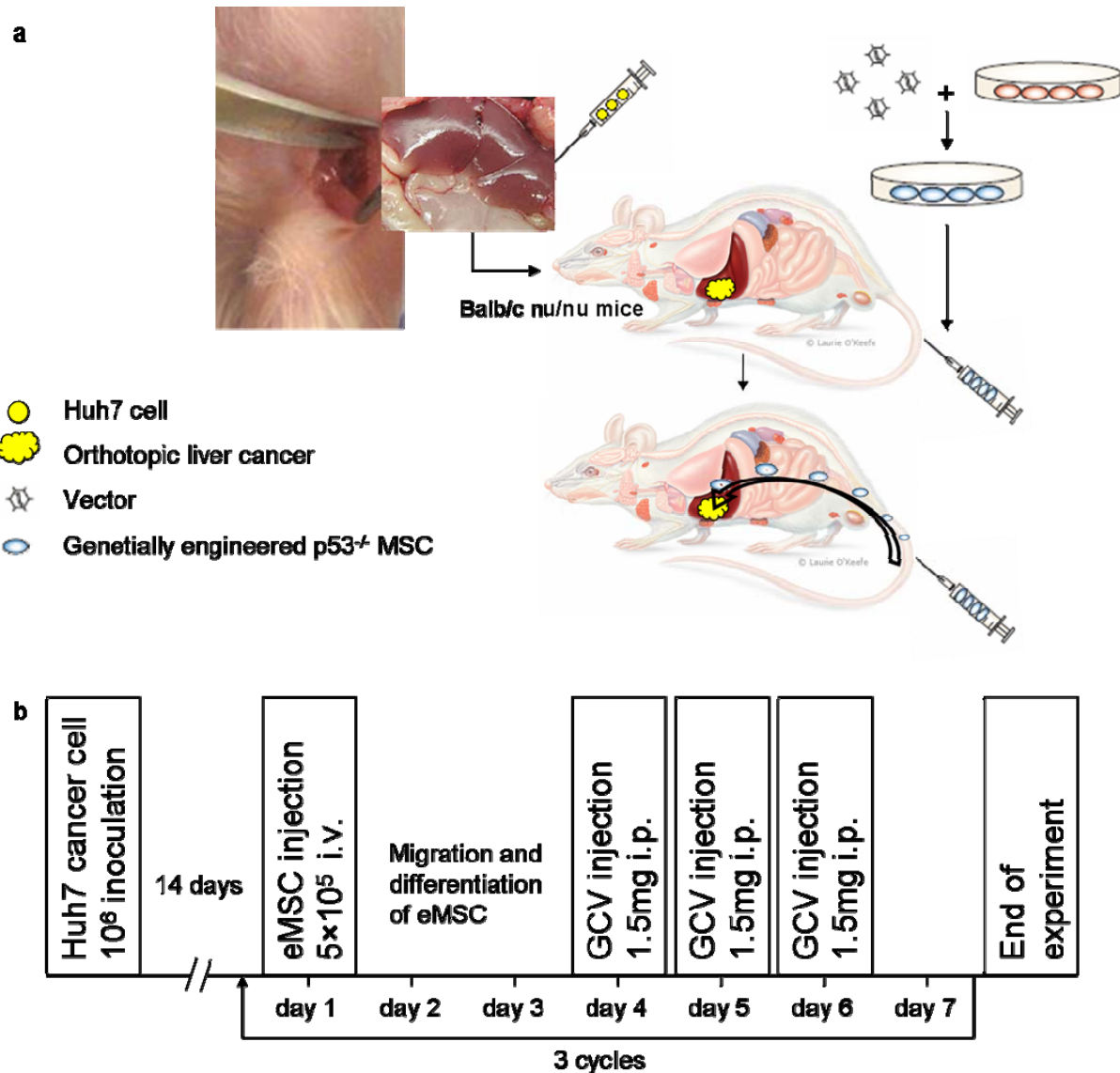


Figure 4.7. Genetically engineered MSCs injected into HCC-bearing mice. a) Schematic picture of genetically engineering MSCs injected into HCC-bearing mice; b) Timeline of the suicide gene engineering MSC combined with GCV injection in HCC-bearing mice.

4.2.8. Histology

4.2.8.1. Haematoxylin Eosin (HE) staining

All liver tumors were formaldehyde-fixed and embedded in paraffin wax. Then 2 μ m serial sections were generated. Tissues were deparaffinized in xylene, and rehydrated in a graded series of ethanol. After 8 minutes in Mayers Haematoxylin immersion, the sections were washed 8 minutes with warm running water. Then the sections were immersed several seconds in Millipore water and stained with 0.1% Eosin solution for 12 minutes. After

dehydration with graded series of ethanol, the sections were mounted with Kaiser's glycerol gelatine (Merck, Germany) and coverslips.

4.2.8.2. Immunohistochemistry

The sections were deparaffinized and rehydrated as mentioned above. Endogenous peroxidase was blocked by incubation with 3% hydrogen peroxide (H₂O₂). Antigen retrieval was performed in Antigen Retrieval Solution (Dako, USA) in a microwave at temperatures between 90-100°C for 20 minutes. Endogenous avidin and biotin was blocked using the Avidin/Biotin Blocking Kit (Vector, USA). The primary antibodies were diluted in phosphate-buffered saline (PBS) containing 3% bovine serum albumin (BSA). Additionally, the slides were treated for 20 minutes with blocking solution (8% goat serum or rabbit serum in PBS with 3% BSA, according to the host species of the secondary antibody) before the primary antibody was applied. The following antibodies were used: monoclonal rabbit anti-Ki67 antibody (ab16667, Abcam, UK), polyclonal rabbit anti-CD31 (ab28364, Abcam, UK), polyclonal goat anti-mouse CCL5/RANTES antibody (AF478, R&D systems, USA), polyclonal goat anti-human CCR5 antibody (NB100-714, Novus, USA), polyclonal goat anti-CCR1 antibody (CKR-1(C-20): sc-6125, Santa Cruz Biotechnology, USA), polyclonal rabbit anti-RFP antibody (PM005, MBL Medical & Biological Laboratories, Japan).

Overnight incubation with the primary antibodies in 4°C fridge was followed by incubation with the respective biotinylated secondary antibody (Goat anti-rabbit, BA-1000; Rabbit anti-goat, BA-5000, Vector, USA), and the ABC reagent for signal amplification at room temperature (Vectastain ABC-Peroxidase Kits, PK-4000, Vector, USA). Between the incubation steps the slides were washed in TBS. Further, 3,3'-diaminobenzidine (DAB, Dako, USA) was used to develop the color. Finally, the slides were counter-stained with hematoxylin and mounted in Kaiser's glycerol gelatine (Merck, Germany) and coverslips.

4.2.8.3. Ki67 proliferation assay

After immunohistochemical staining for *Ki67* slides were observed at 200× magnification using a microscope. Areas showing the highest *Ki67* density were chosen and photos were taken. These photos were analyzed by Image-Pro Plus 5.0 (Media Cybernetics, Inc., USA). For each slide at least three microscopic visual fields (200-fold magnification) were counted. The *Ki67* index was evaluated in a blinded manner and calculated as *Ki67* positive cells

divided by all tumor cells in one field⁹⁰.

4.2.8.4. Microvascular density and vessel thickness analysis

Staining against the endothelial marker CD31 by means of immunohistochemistry was followed by observation at 100× and 200× magnification under the microscope. Tumor slides were examined in a blinded manner and representative areas of vital tumor were selected for examination. As described by others, spots with the highest density concerning CD31 (“hot spots”) were chosen, vessel number per field was counted⁹¹, and the thickness of the perivascular layer was measured. Each slide was evaluated with 3 fields and the data analyzed as mean vessel number or mean vessel thickness of these three fields^{92, 93} (the measurement of vessel thickness is shown in Figure 4.8).

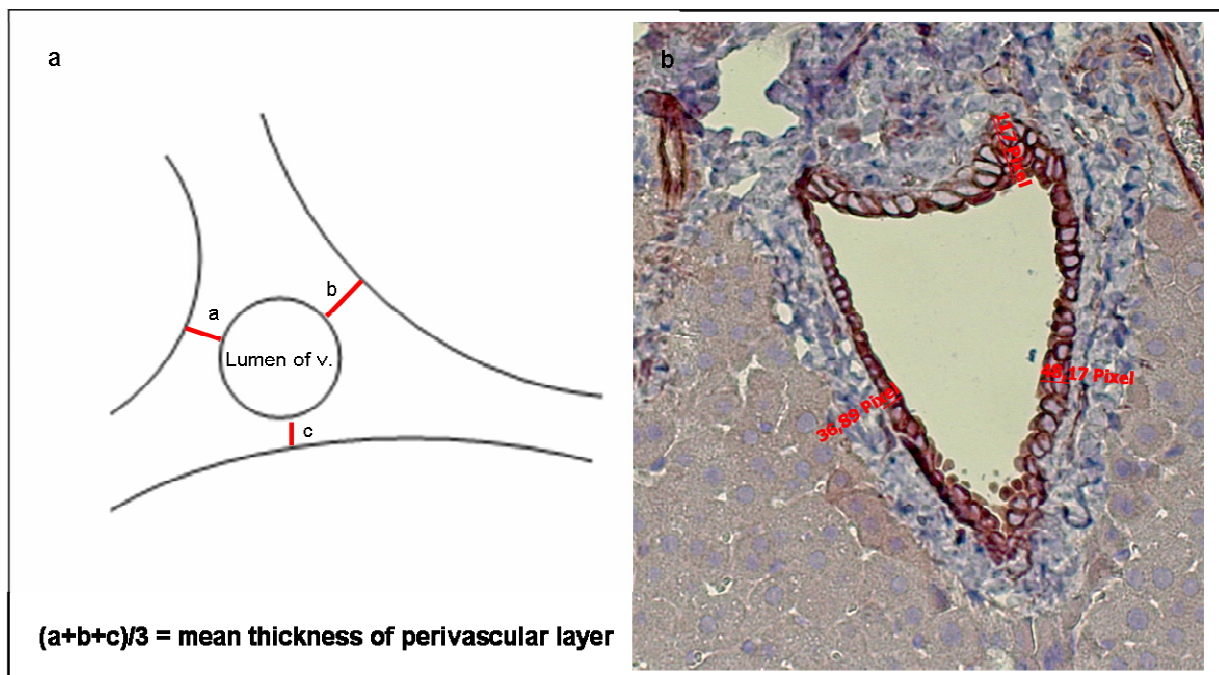


Figure 4.8. Measurement of the mean thickness of perivascular layer by anti-CD31 staining. a) Schematic figure shows how to measure the thickness of vessels; b) The example figure shows the measurement of the vessel thickness under the microscope at 200x magnification and valued the distances by pixel.

4.2.9. ELISA analysis of CCL5 secretion of Huh7 and p53^{-/-} MSCs co-culture *in vitro*

Murine C57BL/6 p53^{-/-} MSCs were co-cultured with human Huh7 hepatocellular carcinoma cells in 6-well culture plates (Nunc, Roskilde, Danmark) in RPMI1640. Cells were co-

cultured at the following MSC/Huh7 ratios: all MSCs, 4:1, 2:1, 1:1, 1:2, 1:4, all Huh7 at a total cell count 1×10^5 cells. The cell supernatant was collected from the wells after 48 and 72 hours, respectively. CCL5 levels were detected by ELISA kit according to the manufacturer's instructions (mouse CCL5/RANTES DuoSet ELISA Development kit, R&D Systems, Minneapolis, USA). Briefly, a 96-well microplate was coated with capture antibodies (2.0 $\mu\text{g/ml}$) overnight at 4°C. Plate contents were emptied and then washed 3 times with PBS/Tween-20 solution, and non-specific binding was blocked using 1% BSA in PBS for 1 hour at room temperature. The blocking buffer was removed and wells were washed for 3 times. 100 μl samples of the supernatants or standards were added to the coated plate and incubated at room temperature for 2 hours. A biotinylated goat anti-mouse CCL5 antibody was used as a detection antibody according to the manufacturer's guidelines. The plate was washed 3 times and 100 μl Streptavidin-HRP was added per well. Then the substrate and stop solution were added according to instructions. Finally, the plate was read at an optical density of 450 nm (GENios Plus, TECAN, Salzburg, Austria). The standard curve was generated from a serial dilution of a known-concentration solution of the standard. The concentration of the CCL5 was determined by the equation which was created by Excel (Microsoft, USA) according to the standard-curve linear regression line. The murine CCL5 concentrations were normalized to equal MSC count in each well.

4.2.10. qRT-PCR analysis of Tie2, CCL5 and CCR5 expression in patient liver samples

Angiogenesis- or stroma-related gene expression, like Tie2, CCL5 or CCR5, was assessed by qRT-PCR in human liver specimen obtained from HTCR (Human Tissue and Cell Research, Regensburg, Germany). 8 pairs of cancer and normal liver tissue from hepatocellular carcinoma patients and 9 other completely normal liver samples were analyzed. Commercial real time PCR probes were used for quantitation (see 4.2.10.5).

4.2.10.1. Disruption and homogenization of the tissue

The tissue samples were taken from the storage -80°C freezer and were brought in liquid nitrogen. One of the samples was put on the big dry-ice plate and scratched with a scalpel into extremely little pieces. The tissue powder was moved into the 2ml Eppendorf tube with lysis buffer (RNeasy Mini Kit, QIAGEN). The tube was vortexed and the content was homogenized by 20 gauge syringe for 10 times. Then the tube was centrifuged at full speed

for 3 minutes and 400µl supernatant was moved to a new Eppendorf tube.

4.2.10.2. RNA isolation

350-400µl of fresh or thawed sample was transferred to a new Eppendorf tube with the same volume of 50% ethanol. The following RNA isolation steps were performed according to the manufacturer's instructions using the RNeasy Mini Kit (74106, QIAGEN, Germany).

4.2.10.3. Measurement of RNA concentration

2µl sample was aspirated from the above step final product, and was mixed with 98µl RNA-free water. The RNA concentration was determined by RNA/DNA Calculator (GeneQuant Pro, GE Healthcare Life Sciences).

4.2.10.4. cDNA synthesis

2µg of total RNA per 20µl reaction system was conducted, and the cDNA synthesis steps were performed according to the manufacturer's protocol (High-Capacity cDNA Reverse Transcription Kit, Applied Biosystems)

4.2.10.5. qRT-PCR TaqMan gene expression assay

The Platinum Quantitative PCR SuperMix-UDG with ROX (Invitrogen) was used as mastermix in this assay. Tie2 (TEK, Hs00945146_m1), CCL5 (Hs00174575_m1) and CCR5 (Hs99999149_s1) were chosen as TaqMan Gene Expression Assays, and the Eukaryotic 18s rRNA (VIC/TAMRA Probe, Primer Limited, 4310893E) was chosen as endogenous control. 20µl system was applied as real-time PCR probe including 2µl cDNA sample and 18µl system mix. The probes were added into 96-well plate, and the plates were analyzed using the ABI system 7000 machine (Applied Biosystems, USA). The results were analyzed by Microsoft Office Excel 2003.

4.2.11. Statistical analysis

Statistical significance was assessed by comparing median values using the non-parametric Mann-Whitney-U test for independent samples and t-test for random samples (IBM SPSS

19.0 for Windows). *P* values <0.05 were considered significant. Continuous, non-parametric data is presented as median [range] values.

V. RESULTS

5.1. MSCs are actively recruited to the site of hepatocellular carcinoma

5.1.1. MSCs show tropism for recruitment to tumor sites

In the orthotopic tumor model, human Huh7 hepatocellular carcinoma cells were injected into the left lateral lobe of the liver of nude mice. This led to the formation of solid intrahepatic tumor xenograft. Using this animal model, the recruitment of systemically injected murine MSCs to the tumor site was evaluated.

5.1.1.1. SPIO-transfected MSCs recruit to tumor site

Superparamagnetic iron oxide nanoparticles (SPIO) have demonstrated their utility as an important tool for monitoring transiently labeled MSCs on magnetic resonance (MR) images. This work was performed in collaboration with Dr. Mike Notohamiprodjo (Department of Clinical Radiology, University Hospitals Munich). The SPIO labeled MSCs (MSCs^{iron}) were used to investigate the natural tropism of these cells to tumor site. The mice with 4-week old hepatic tumors received intravenous injections of either sterile normal saline, 1×10^6 unlabeled C57BL/6 p53^{-/-} MSCs, or 1×10^6 SPIO labeled C57BL/6 p53^{-/-} MSCs. After 36 hours of the respective injections, mice were sacrificed and evaluated by MR imaging. As control, mice without prior tumor cell inoculation also received normal saline or MSCs^{iron} injections and were scanned by MRI. Figure 5.1 demonstrates two exemplary cases of tumor bearing mice with and without iron-labeled MSCs. The mean size of the orthotopic hepatic tumors was 2cm.

In non-tumor bearing mice receiving MSCs^{iron} injections, the largest signal decay as compared to mice receiving normal saline injections was only detectable in the spleen. This effect was not seen in animals receiving unlabeled MSCs. This indicates homing of MSCs after intravenous injections to secondary lymphatic organs, such as the spleen which has been shown previously³⁰.

In tumors of animals following injection of SPIO-labeled stem cells, a distinct signal decay in T2- and T2*-weight-sequences could be detected. In the R2*-maps, elevation of R2* could be detected, indicating an accumulation of iron labeled stem cells, confirmed by histology of Prussian blue staining (Figure 5.2 c, d) Tumors of animals receiving either normal saline or unlabeled MSC injections did not show a significant signal decay. Injection of unlabeled MSCs did not lead to hypo-intense signals inside the spleen of the animals.

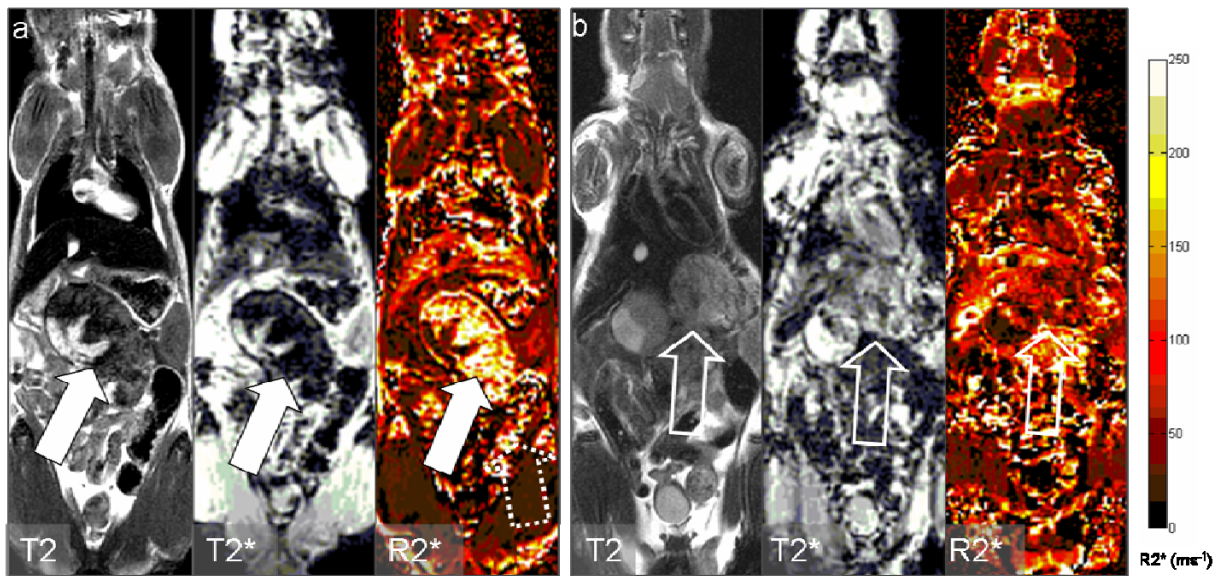


Figure 5.1. MRI of exemplary cases of tumor bearing mice with SPIO labeled and unlabeled MSC. a) Mice were injected with SPIO labeled MSC. The tumor (solid arrows) exhibited a hypointense appearance in T2- and T2* (TE=15ms)-weighted sequences. R2*-calculation reveals an increased spindephasing caused by disturbance of the magnetic field. The hyperintense portions of the tumor indicate necrosis. Note that other factors, such as bowel air also lead to an increase of R2* (dotted arrow); b) In tumors of mice with unlabeled stem cells (empty arrows), non-hemorrhagic tumors exhibited a relatively hyperintense appearance and low R2*. Qualitatively, the tumor is much less visible on the R2* maps, corresponding to considerably lower R2* values than in a). Both R2* maps are obtained by a pixel-based fit to all echo times.

5.1.1.2. Prussian blue staining confirmed the recruitment of SPIO-labeled MSCs

In order to confirm that the MSCs^{iron} are recruited to the tumor site, the Prussian blue staining was conducted. In tumor bearing mice injected with unlabeled MSCs, there was no iron particle in the lung (Figure 5.2 a). Figure 5.2 b demonstrates that only a few iron particles were shown in the lung of tumor bearing mice which were injected with MSCs^{iron}. This indicates that peripherally injected MSCs reach the pulmonary circulation before they are recruited to the tumor site, and after 36 hours, most of them leave the lung for the tumor or other organ sites. Moreover, as mentioned above, the Prussian blue positive signals at the liver tumor site of MSCs^{iron} injected group proved that the MSCs^{iron} home to the tumor site and cause the signal decay in T2- and T2*- weight sequences of MR image (Figure 5.2 c, d).

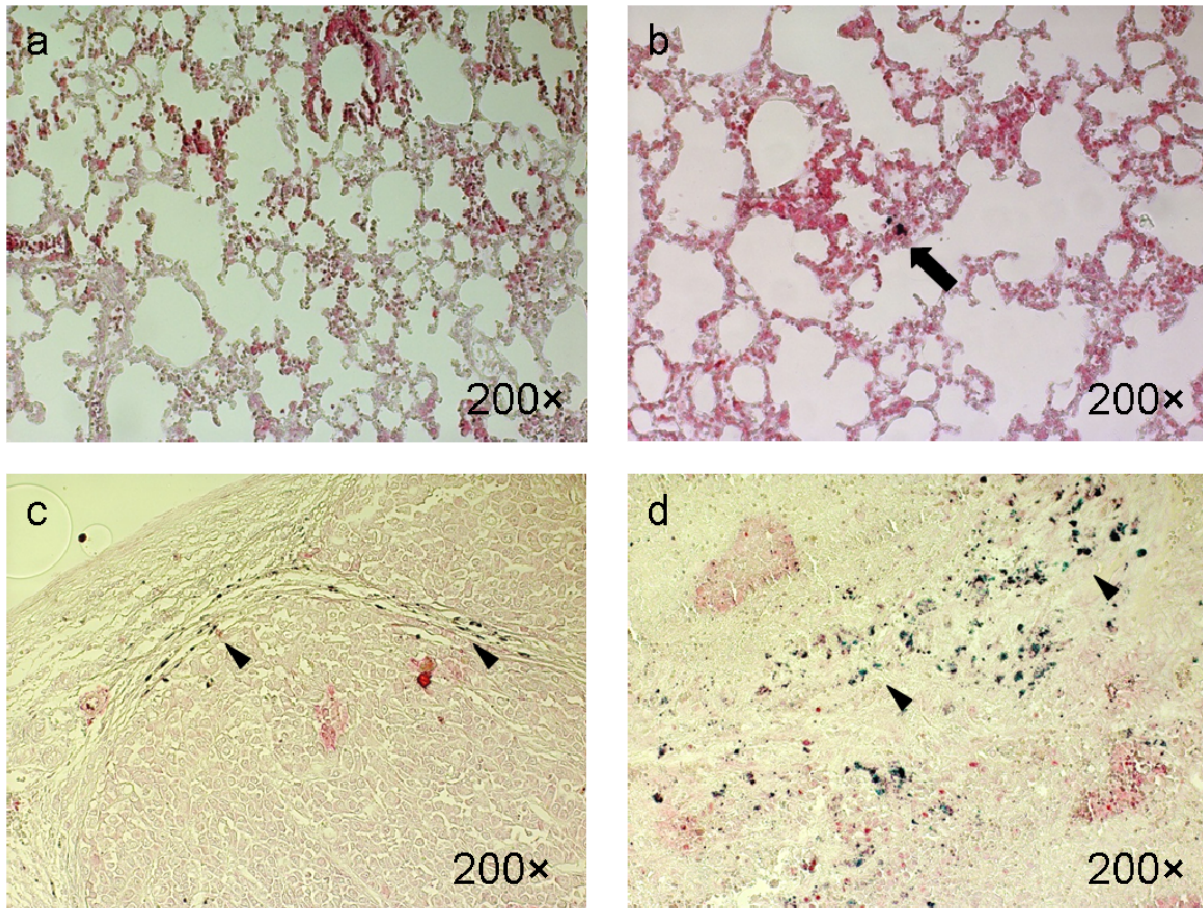


Figure 5.2. Prussian blue staining for detection SPIO labeled MSCs. a) Mice were injected with unlabeled MSCs. No iron particle was detected in lung tissue; b,c,d) Mice were injected with SPIO labeled MSCs. A few iron particles were seen in the lung (b, arrow). Many iron particles were seen at liver tumor site (c and d, arrowhead).

5.1.2. Reporter gene engineered MSCs promote tumor growth and angiogenesis.

The tropism of MSCs to the HCC tumor model was confirmed. C57BL/6 p53^{-/-} MSCs were engineered with plasmid vectors containing either the Tie2 or CCL5 promoters driving the expression of the Red Fluorescent Protein (RFP) reporter gene. These engineered MSCs were then injected at a dose of 0.5×10^6 in the tail vein of HCC bearing mice once per week for a period of three weeks. The general effect of the adoptively transferred MSCs on tumor growth as well as the expression of the RFP transgene was monitored.

5.1.2.1. Reporter gene engineered MSCs promote tumor growth

5.1.2.1.1. Total liver weight and volume increased after MSCs injection

All animals were sacrificed 5 weeks after tumor cell injection and 3 weeks after the first of three cycles of injection of MSCs. Total liver weight and volume was evaluated (Figure 4.7).

At the end of the experiment, there are 10 mice left in the control group, 3 mice in each reporter gene engineered MSC group, 5 mice in the *Tie2/HSV-TK*⁺ MSC group and 8 mice in the *CCL5/HSV-TK*⁺ MSC group, as is shown below:

Group A: no stem cells or GCV injections: 10 mice

Group B: C57BL/6 *Tie2/RFP*⁺ MSCs injections: 3 mice

Group C: C57BL/6 *CCL5/RFP*⁺ MSCs: 3 mice

Group D: C57BL/6 *Tie2/HSV-TK*⁺ MSCs and GCV injections: 5 mice

Group E: C57BL/6 *CCL5/HSV-TK*⁺ MSCs and GCV injections: 8 mice

The total liver weight, due to increased tumor growth, was increased in mice receiving injections of either *Tie2*- or *CCL5*- promoter MSCs as compared to mice receiving no stem cells. A 1.49-fold elevation between control and *Tie2/RFP*⁺ MSCs (median of 5.23 [1.50-7.20]g vs. median of 7.79 [6.29-9.88]g; *p=0.049), and a 1.58-fold elevation between control and *CCL5/RFP*⁺ MSCs (median of 5.23 [1.50-7.20]g vs. median of 8.25 [7.33-9.38]g; **p=0.007, Table 5.1, Figure 5.3 a) were demonstrated.

Due to larger tumors total liver volume also was increased in the *CCL5/RFP*⁺ MSCs group as compared to the control group. A 1.47-fold elevation between control and *CCL5/RFP*⁺ MSCs (median of 5.30 [1.50-7.50]cm³ vs. median of 7.80 [6.80-9.20]cm³; *p=0.014, Figure 5.3 b) were demonstrated.

Although there was no statistical significant elevation between the control group and the *Tie2/RFP*⁺ MSCs group (median of 5.30 [1.50-7.50]cm³ vs. median of 8.00 [5.70-9.80]cm³; p=0.077), a tendency of increased liver volume could be measured (Table 5.1, Figure 5.3 b). Exemplary images of tumors of 3 groups are shown in Figure 5.3 c.

Table 5.1. Total liver weight and volume increased after MSCs injection

	Control	<i>Tie2/RFP</i> ⁺	<i>CCL5/RFP</i> ⁺
Total liver weight (g)	5.23 [1.50-7.20]	7.79 [6.29-9.88]*	8.25 [7.33-9.38]**
Total liver volume (cm ³)	5.30 [1.50-7.50]	8.00 [5.70-9.80]	7.80 [6.80-9.20]*

Note: all data is shown as median [range] values. As compared with control group, *p<0.05, **p<0.01.

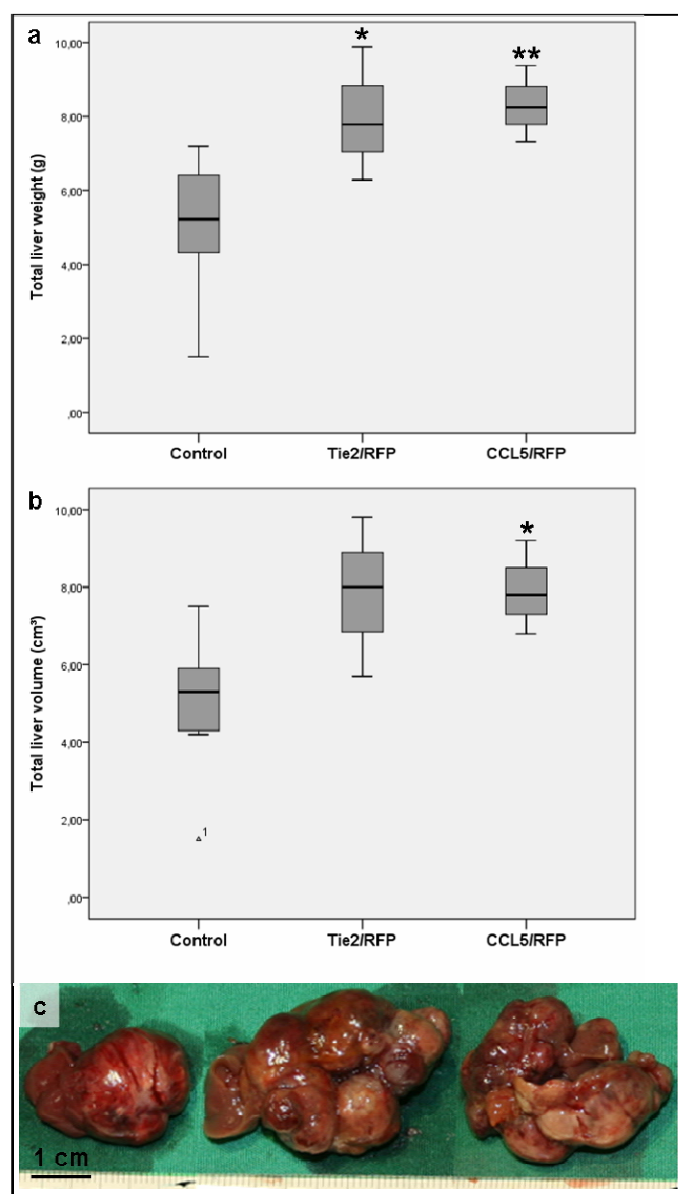


Figure 5.3. Total liver weight and volume increased after MSCs injection. MSC injections dosed at 0.5×10^6 cells per week were intravenously applied starting two weeks after tumor cell injection. Total liver weight was evaluated after sacrifice of animals five weeks after tumor cell inoculation. Medians were compared and p-values calculated by Mann-Whitney U-

test for independent samples. a) Box plots of total liver weight show an increase in tumor associated liver weight by MSC injections; b) Box plots of total liver volume show an increase in tumor volume associated with liver volume by MSC injections ($\Delta 1$ is an outlier, all * and ** compared with control group, $*p < 0.05$, $**p < 0.01$); c) Macroscopic images of three exemplary tumors of each group are shown (left to right: control, *Tie2/RFP*⁺ and *CCL5/RFP*⁺).

The body weight of the animals varied throughout the entire experiment. It showed no significant difference in total body weight of animals in the treatment groups (*Tie2/HSV-Tk*⁺, *CCL5/HSV-Tk*⁺) as compared to the control groups (control, *Tie2/RFP*⁺, *CCL5/RFP*⁺) (Figure 5.4).

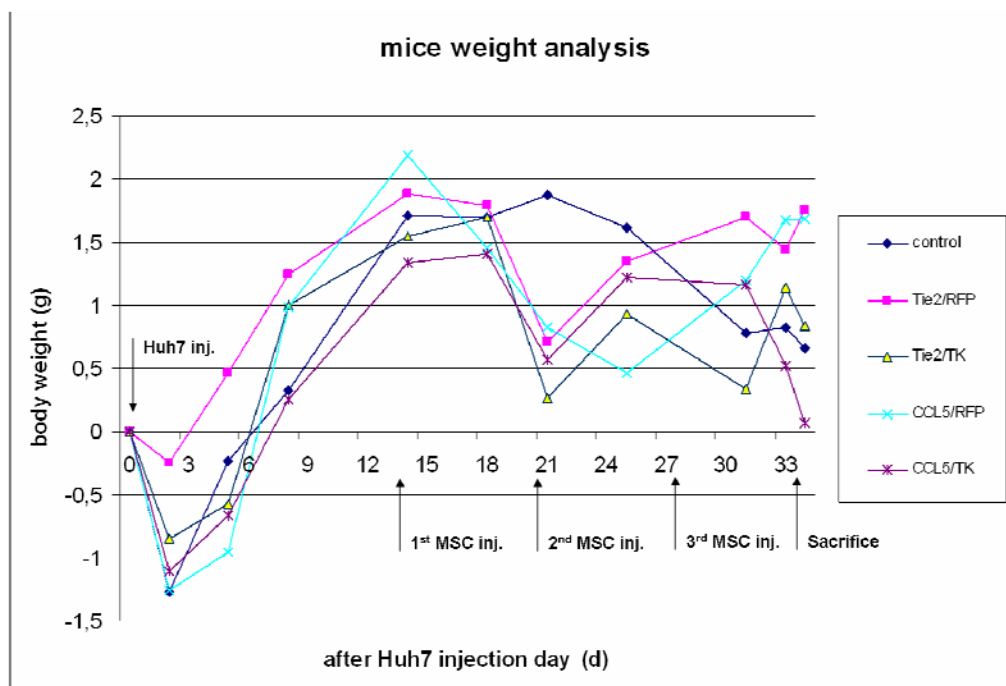


Figure 5.4. Mice total body weight curves. The weight curves show no significant difference in total body weight among the control, *Tie2/RFP*⁺, *Tie2/HSV-Tk*⁺, *CCL5/RFP*⁺, and *CCL5/HSV-Tk*⁺ engineered MSCs groups.

5.1.2.1.2. HE staining of HCC tumors

Tumor growth was further confirmed by HE staining. In C57BL/6 MSC groups, the dark brown/yellow pigmented material or bile pigments, were easily identified in the cytoplasm of

tumor cells and in the middle of tubular areas. This reflected extra bile secretion from liver cancer cell which may be influenced by the adoptively applied MSCs (Figure 5.5 a). Furthermore, hemorrhage and mitosis were detected in these tumors. This may be caused by aggressive angiogenesis and consecutive tumor cell proliferation enhanced by MSC recruitment (Figure 5.5 b, c). Aggressive tumor growth as reflected by invasion into neighbouring organs was also seen in these groups. Figure 5.5 d shows tumor invasion directly into proximate bowel.

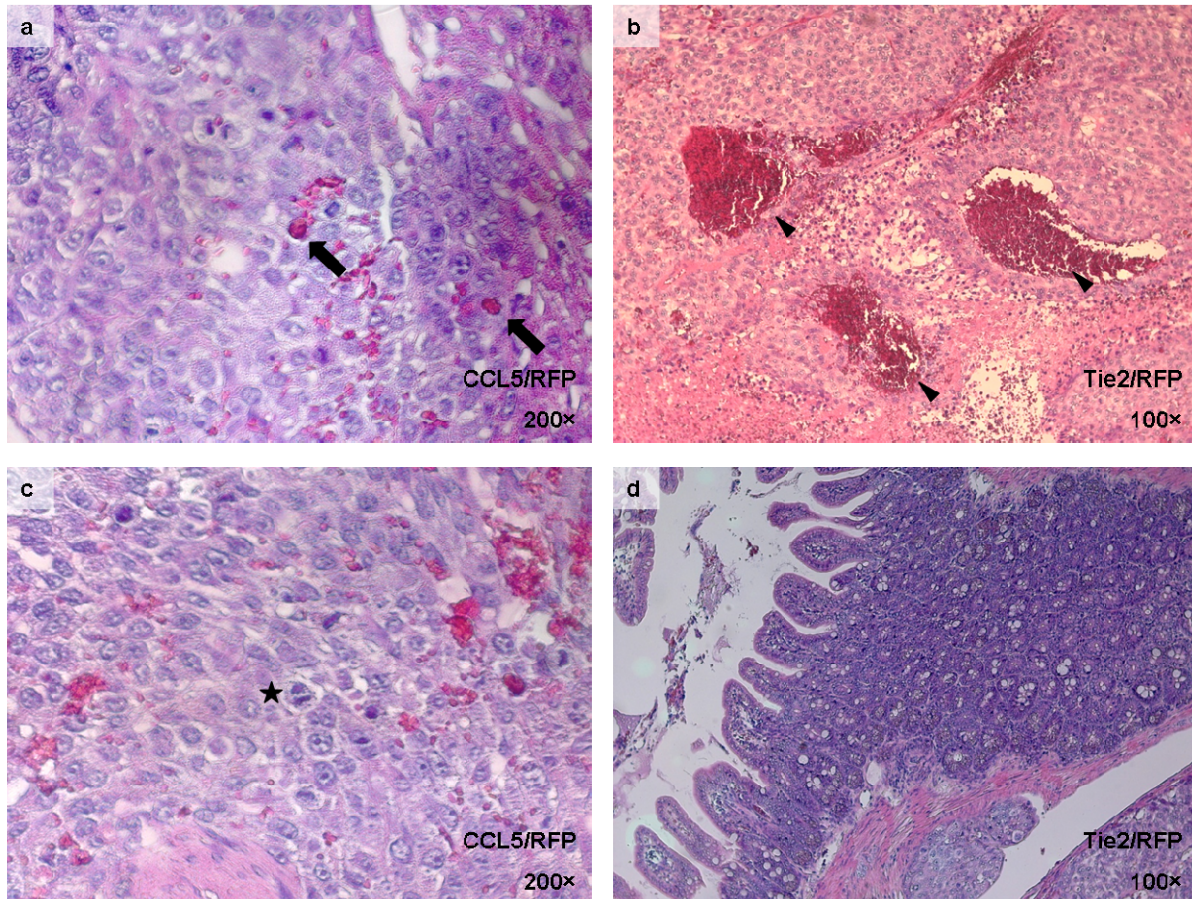


Figure 5.5. HE staining showed morphologic characteristics changes in C57BL/6 MSCs groups. a) Brownish droplets represent the ability of neoplastic hepatocytes to produce bile in excess, 200× magnification; b, c) The hemorrhage (arrowheads) and mitosis (star) could be detected in tumors indicating the aggressive tumor cell proliferation, 100×, 200× magnification; d) Liver cancer cells directly invading into the bowel, 100× magnification.

5.1.2.2. Reporter gene engineered MSCs promote angiogenesis and proliferation

Microvessel density as measured by immunohistochemical staining against CD31 revealed increased angiogenesis in tumors of mice following injection of *Tie2/RFP*⁺ MSCs (1.49-fold

increase as compared to control group: 9.17 [7.76-12.00] CD31⁺ vessels / 100× magnification field in the control group vs. 13.67 [13.33-17.67] in the *Tie2/RFP*⁺ MSC group, *p=0.012). Although there is no statistical significant between the *CCL5/RFP*⁺ and control group, a tendency of increased MVD still can be seen (Table 5.2). Exemplary images of anti-CD31 staining which are evaluated for MVD of each group are shown in Figure 5.6 first row.

Table 5.2. Effect of reporter gene engineered MSC on tumor angiogenesis and proliferation

	Control	<i>Tie2/RFP</i> ⁺	<i>CCL5/RFP</i> ⁺
MVD	9.17 [7.76-12.00]	13.67 [13.33-17.67]*	13.00 [10.00-17.33]
Thickness of vessel	17.72 [7.33-48.33]	42.89 [25.22-141.89]	86.87 [65.22-168.11]*
Ki67 index	0.68 [0.52-0.86]	0.98 [0.89-0.98]*	0.98 [0.98-0.99]*

Note: all data is shown as median [range] values. MVD, CD31⁺ vessels / 100× magnification field. As compared to control group, *p<0.05.

The vessels in the MSC treated tumors showed broader perivascular staining. As detailed in material and methods, the thickness of the perivascular layer was evaluated by CD31 staining. Compared to the control group, in the *CCL5/RFP*⁺ MSC treated group the thickness of the perivascular layer was significantly enlarged (4.89-fold increase compared to control group: 17.72 [7.33-48.33] pixels in the control group vs. 86.87 [65.22-168.11] in the *CCL5/RFP*⁺ MSC group, *p=0.012). Although there was no statistical significance between the *Tie2/RFP* and control group, a tendency of an increased thickness of the perivascular layer still can be seen (Table 5.2). Exemplary sample images of anti-CD31 staining, which are evaluated as perivascular thickness, are shown in Figure 5.6 second row.

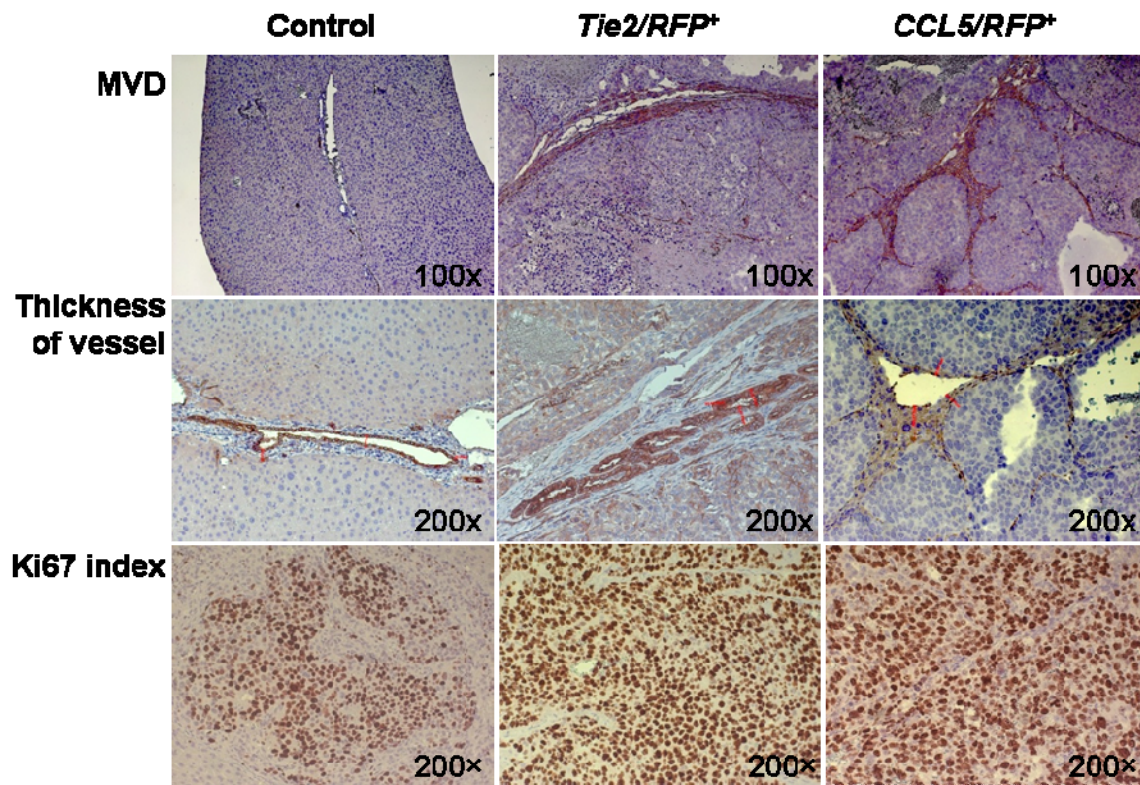


Figure 5.6. Exemplary microscopic images of anti-CD31 and anti-Ki67 staining of tumors in the control, *Tie2/RFP*⁺, and *CCL5/RFP*⁺ groups

To evaluate the effect of C57BL/6 MSC administration on tumor cell proliferation, *Ki67* indexes were calculated⁹⁴. Tumors of mice following injections of *Tie2/RFP*⁺ and *CCL5/RFP*⁺ MSCs demonstrated both a 1.44-fold increase in proliferating *Ki67*⁺ cells as compared to control tumors (0.68 [0.52-0.86] *Ki67*⁺ cells / total cells vs. 0.98[0.89-0.98] in the *Tie2/RFP*⁺ MSC group, and 0.98[0.98-0.99] in the *CCL5/RFP*⁺ MSC group, Table 5.2). Exemplary images of *Ki67*⁺ staining in the control group and following *Tie2/RFP*⁺ and *CCL5/RFP*⁺ MSCs injection are shown in Figure 5.6 last row.

5.1.2.3. MSCs promote cancerous ascites

No metastases in distant tissues were detected in this study either with or without MSC treatment. Wound tumors and bowel invasion were found in both control and MSC groups (Table 5.3). All animals in the *Tie2/RFP*⁺ MSC treatment group presented with significantly more cancerous ascites compared to the non-MSC control group (3/3 in *Tie2/RFP*⁺ group vs. 2/10 in control group, **p*<0.05). There was no statistical significance between the *CCL5/RFP*⁺

MSC group and the control group regarding ascites formation.

Table 5.3. Different patterns of cancer cell spread between reporter-gene eMSC and control group

Cancer cell spread	Control n=10	Tie2/RFP n=3	P value	CCL5/RFP n=3	P value
Wound	4(40%)	3(100%)	0.161	1(33.3%)	0.937
Bowel	3(30%)	1(33.3%)	1	1(33.3%)	1
Ascites	2(20%)	3(100%)	0.049*	2(66.7%)	0.287

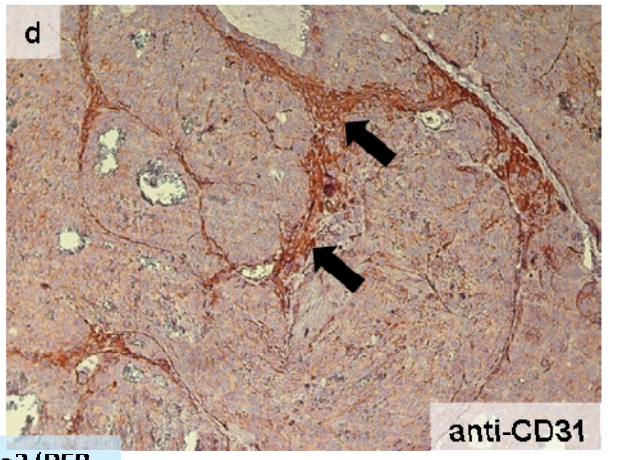
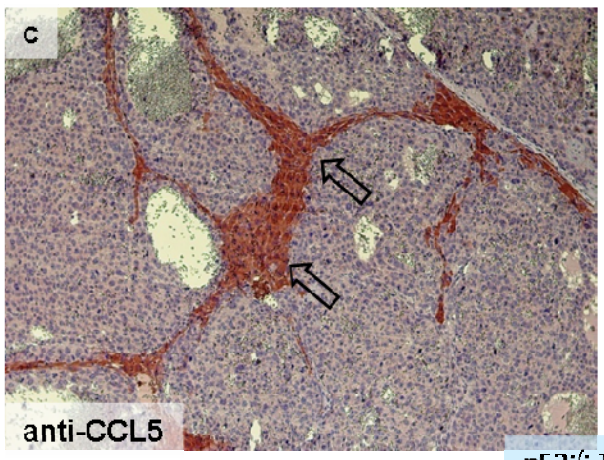
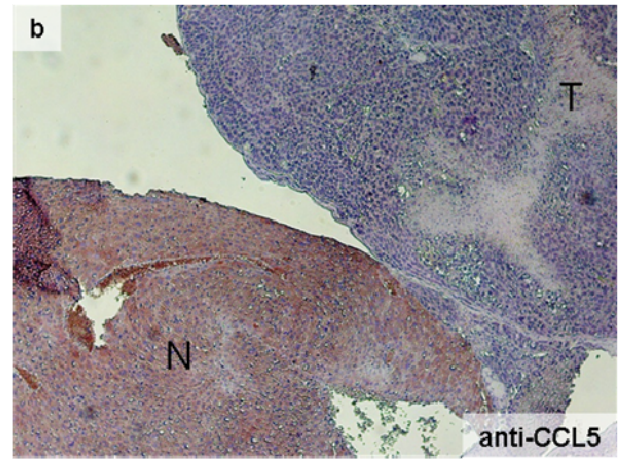
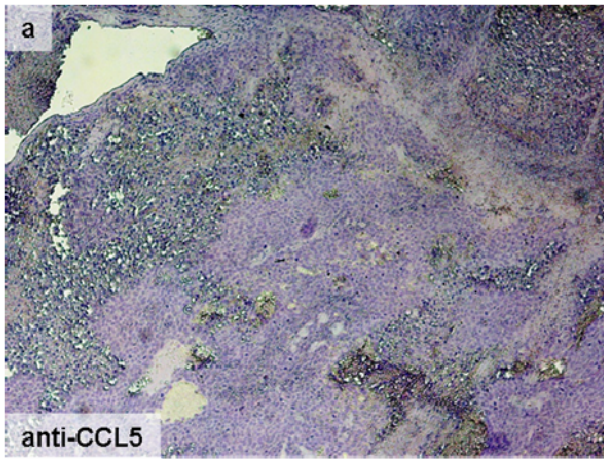
P: eMSC injected groups compare with control group, with Mann-Whitney U test.

5.2. Stroma- or angiogenesis-related signals and receptor gene expression in MSCs recruited to the tumor site

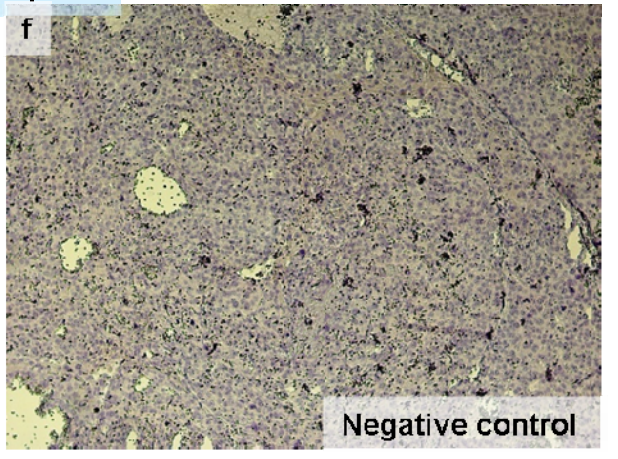
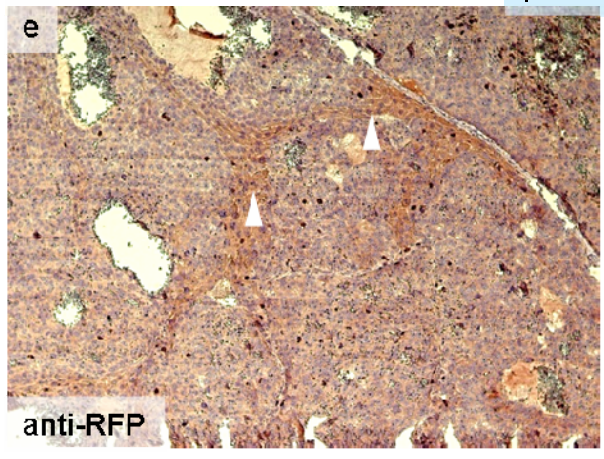
5.2.1. Systemically injected MSCs can activate Tie2- or CCL5- promoter driven reporter genes (RFP) following their recruitment to the HCC microenvironment

Tumors from the control group and the *Tie2/RFP*⁺ or *CCL5/RFP*⁺ MSCs treated groups were examined for RFP expression by immunohistochemistry. Staining showed strong RFP⁺ signals in tumors that were treated with MSCs expressing RFP either under control of the Tie2 promoter / enhancer or the CCL5 promoter.

Tumor samples were examined for RFP, murine CCL5, and CD31 expression by serial section immunohistochemistry. CCL5⁺ signals were only detectable in animals, which had received MSCs (Figure 5.7 c, g) as compared to the control group without any CCL5 expression either in normal liver tissue or in the tumor tissue (Figure 5.7 a, b). In tumors of both *Tie2/RFP*⁺ and *CCL5/RFP*⁺ MSC injected mice, RFP expression (Figure 5.7 e, i) was detected in close proximity to CCL5⁺ (Figure 5.7 c, g) and CD31⁺ signals (Figure 5.7 d, h) indicating that MSCs recruited to the tumor site were integrated into the tumor microenvironment in particular tumor stroma and angiogenesis. Following recruitment to the tumor microenvironment MSCs expressed the reporter gene RFP by activation of angiogenesis- or stroma- related promoters/enhancers such as Tie2 and CCL5.



p53^{-/-} Tie2/RFP



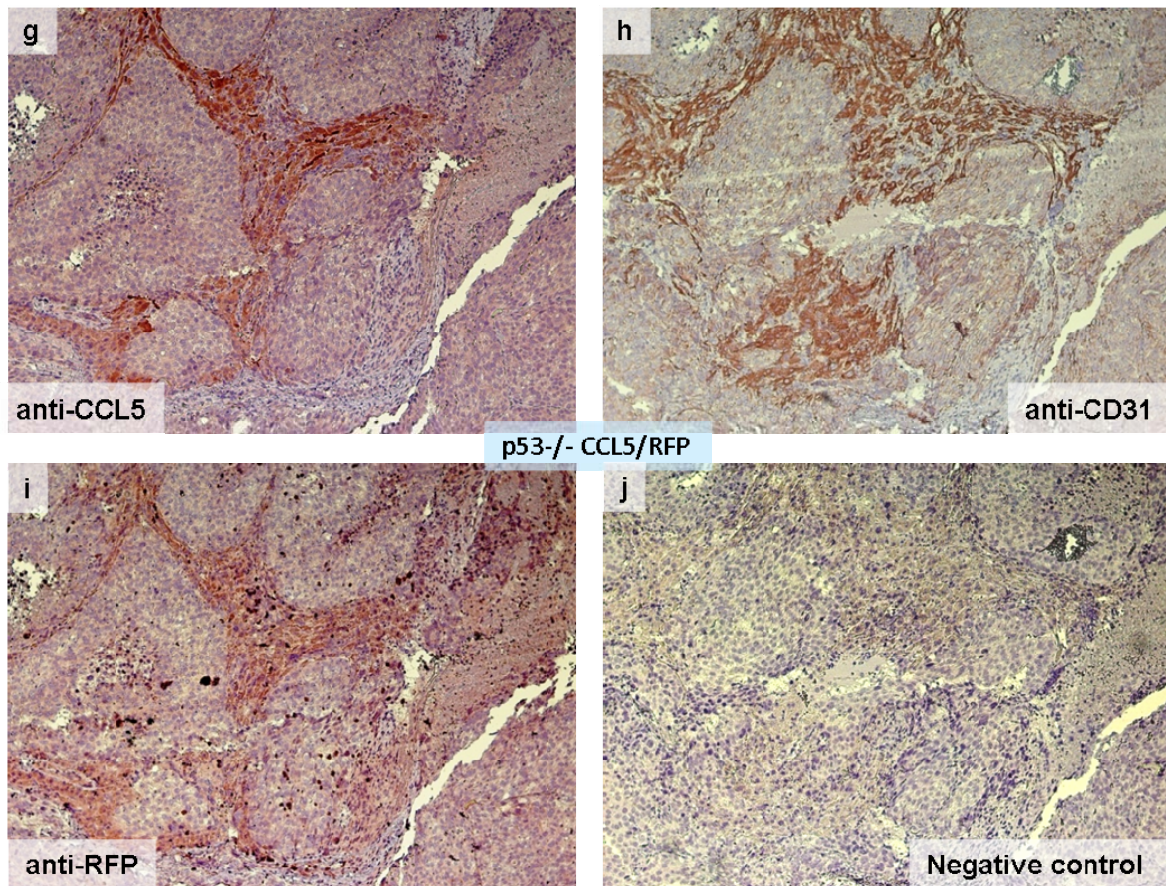


Figure 5.7. Expression of CCL5, CD31 and RFP in HCC xenografts. a, b) No positive signal for CCL5 was seen in either normal tissue or tumor tissue of the control group; c, d, e) In the *Tie2/RFP*⁺ MSC group, the serial section immunohistochemical stainings demonstrate positive signals of CCL5, CD31 and RFP in close proximity; f) Negative control; g, h, i) In the *CCL5/RFP*⁺ MSC group, the serial section immunohistochemical stainings also demonstrate positive signals of CCL5, CD31 and RFP in close proximity; j) Negative control.

5.2.2. Expression of CCL5 receptors in the tumor stroma

As shown above, exogenously applied MSCs are actively recruited to HCC tumors and express in the context of tumor stroma and tumor angiogenesis the transfected reporter gene as well as stroma- or angiogenesis-related markers such as CCL5 and CD31. However, the mechanism of how they home to the tumor site has to be further exploited. Both *Tie2/RFP*⁺ and *CCL5/RFP*⁺ MSCs expressed the chemokine CCL5, two of the common receptors of CCL5 – CCR5 and CCR1 - were further investigated. Serial section immunohistochemistry of tumor tissues was performed using anti-CCR5 and anti-CCR1 antibodies. The immunohistochemical results showed that either in the *Tie2/RFP* MSC group or in the

CCL5/RFP MSC group, CCR5 positive signals were in close proximity to CCL5 positive signals in the tumor (Figure 5.8).

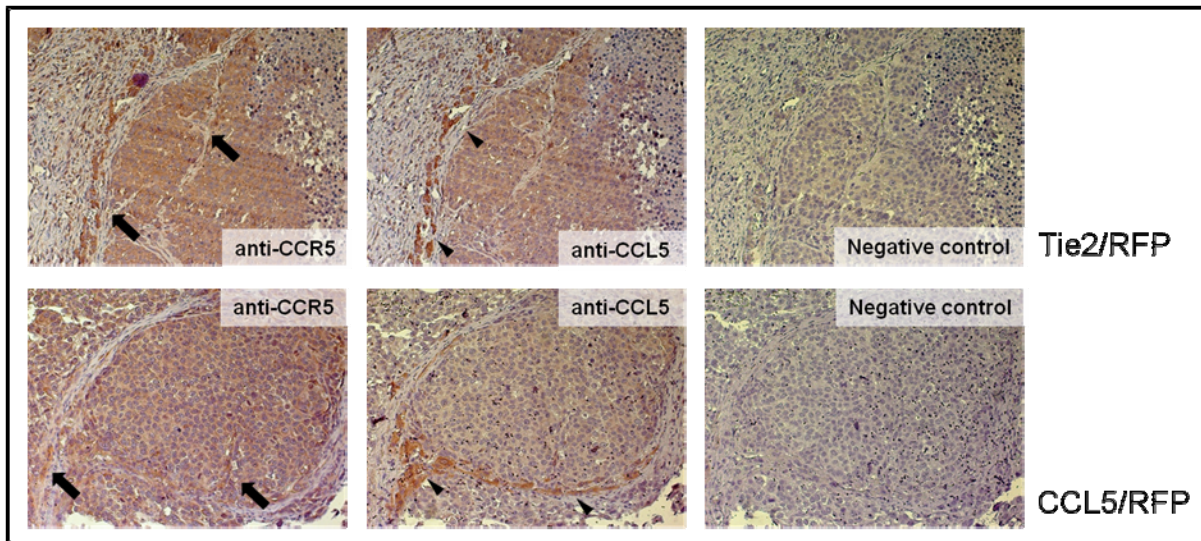


Figure 5.8. Immunohistochemical staining using anti-CCL5 and anti-CCR5 antibodies in *Tie2/RFP*⁺ and *CCL5/RFP*⁺ MSCs injected tumor tissues. CCR5 positive signals (arrows) were in close proximity to CCL5 positive signals (arrowheads) in serial sections of both tumor tissues either from the *Tie2/RFP*⁺ or the *CCL5/RFP*⁺ MSC group.

In serial section immunohistochemical staining of *Tie2/RFP* MSC injected tumor samples, CCR1 positive signals were close to CCL5 positive signals (Figure 5.9). Based on the serial staining results, the ligand and receptor interactions between CCL5 and CCR5 or CCR1 may play a key role in the MSCs recruitment.

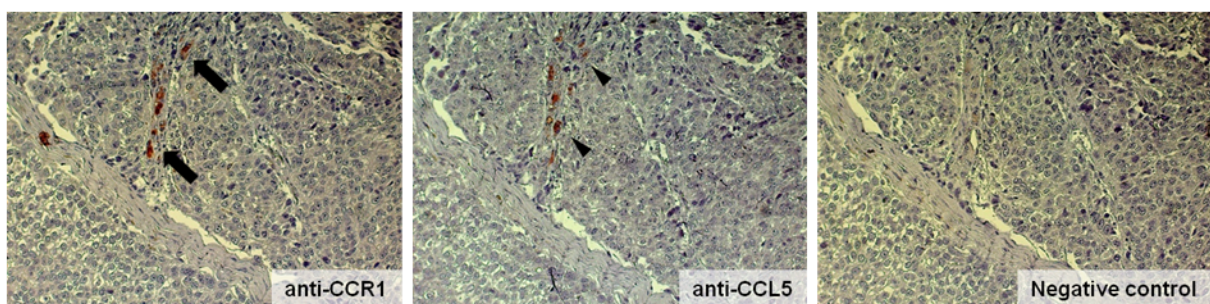


Figure 5.9. Immunohistochemistry staining of anti-CCL5 and anti-CCR1 antibodies in *Tie2/RFP* MSCs injected mice tumor tissues. CCR1 positive signals (arrows) were close to CCL5 positive signals (arrowheads) in the *Tie2/RFP* MSC groups.

5.3. *In vitro* data showed that CCL5 is secreted by MSCs

In order to mimic the interaction between hepatocellular carcinoma cells and mesenchymal stem cells, co-culture experiments were conducted followed by ELISA to evaluate the chemokine CCL5 expression levels *in vitro*. According to the *in vivo* data, the tumor microenvironment may attract MSCs through chemokine-receptor interactions like CCL5-CCR5 or CCL5-CCR1. The stimulating effects of CCL5 expression were supposed to appear *in vitro* in co-cultures using Huh7 cells and C57BL/6 MSCs. However, the ELISA results showed that the CCL5 expression level was only related to seeded amount of MSCs (from 1×10^5 to 0.67×10^5) and the incubation time (from 48 hours to 72 hours) (Figure 5.10). There was no synergetic effect of stimulating CCL5 expression by co-culturing Huh7 cells with MSCs *in vitro*.

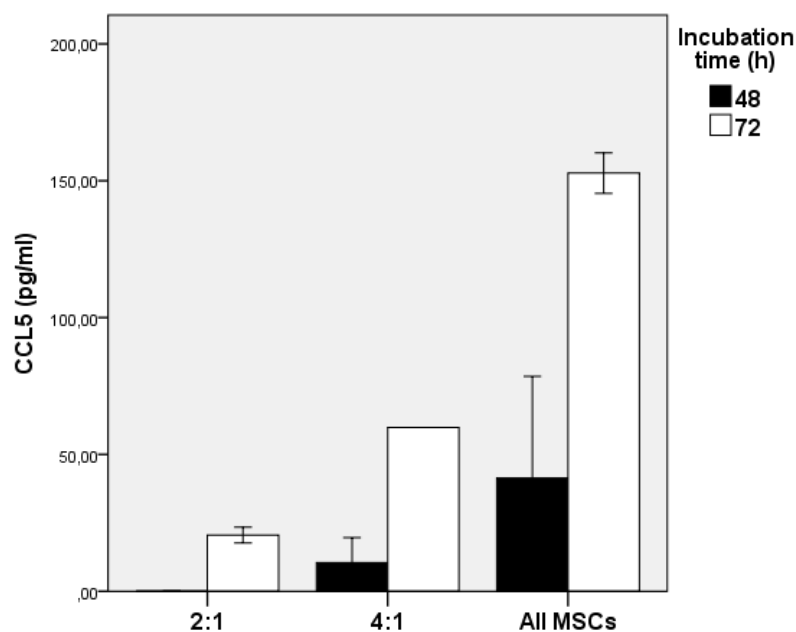


Figure 5.10. CCL5 expression level of co-culture of Huh7 cells and MSCs *in vitro*. The ELISA results showed that the CCL5 expression level was elevated depending on the seeded number of MSCs (from 1×10^5 to 0.67×10^5) and the incubation time (from 48 hours to 72 hours).

5.4. Tie2, CCL5, CCR5 expression in human samples

The RNA expression of Tie2, CCL5, and CCR5 in human hepatocellular carcinoma tissue and surrounding normal liver tissue was analyzed by qRT-PCR. There was no significant difference of expression of all three genes between cancer tissue and concomitant normal

tissue (Figure 5.11, $p^{\text{Tie2}}=0.22$, $p^{\text{CCL5}}=0.52$, $p^{\text{CCR5}}=0.33$).

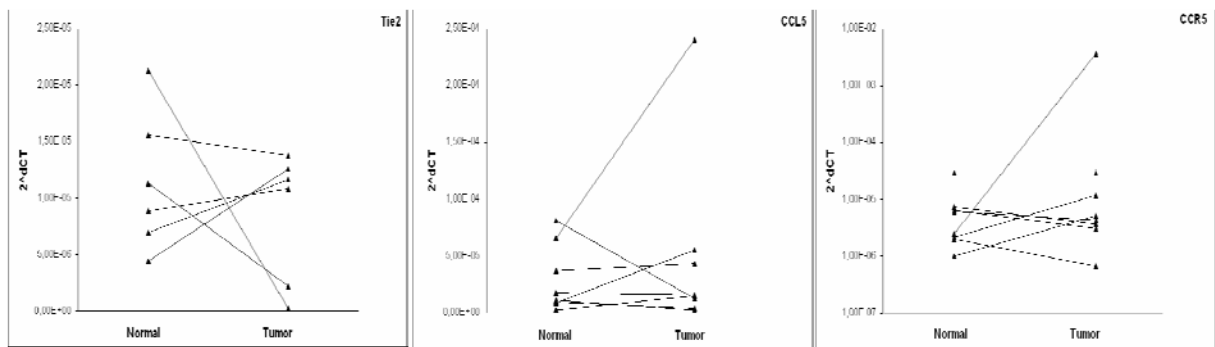


Figure 5.11. RNA expression of Tie2, CCL5 and CCR5 compared between cancer and concomitant normal liver tissues. There were no significant differences of expression of all three genes between cancer tissue and concomitant normal tissue (all $p>0.05$).

Three of the patients examined had liver cirrhosis (Table 5.4). To exclude the influence of cirrhosis on carcinogenesis, the Tie2, CCL5 and CCR5 expression levels were re-analyzed and compared with total healthy liver tissue (no cirrhosis).

Table 5.4. Patients' clinical data for qRT-PCR result analysis

no.	gender	main diag.	other diag.		HBV	HCV	HIV	medication	chemo
35	f	HCC			-	-	-	/	/
52	m	HCC, Segment V	strumectomy, Inguinal hernia	HTN	-	-	-	Bisoprolol, Duradiuret, Jod	/
63	m	HCC	Hyperthyroidism		-	-	-	/	/
76	m	HCC	cirrhosis by hemochromatosis, oesophageal varicose veins I°, COPD		-	-	-	Metformin	/
83	m	HCC	obstructive sleep apnea syndrome, strumectomy, vagotomy, akinetic parkinson syndrom, peripheral arterial occlusive disease(pAVK)	obesity, diabetes mellitus, HTN, hyperuricemia	-	-	-	Lasix, ASS, Allopurinol, Thyroxin, Madopar	/
103	m	HCC	sigmoid diverticulum	HTN	-	-	-	Nifedipin, Antazida, Esomeprozol	/
155	m	HCC	cirrhosis Child A	obesity, diabetes mellitus, HTN	-	-	-	Bisoprolol	/
279	m	HCC	cirrhosis Child A, mitral insufficiency, hemi-colectomy by carcinoma in situ, arterial hypertension	diabetes mellitus	-	-	-	Concor, Norvasc, Diovan, Amaryl, Legacon, Thioctacid, Vit B1	/

However, there was again no significant difference between cancer and normal tissues in CCL5 and CCR5 gene expression (Figure 5.12). Tie2 expression was elevated in normal liver tissue compared to tumor tissue (* $p^{\text{Tie2}}=0.01$).

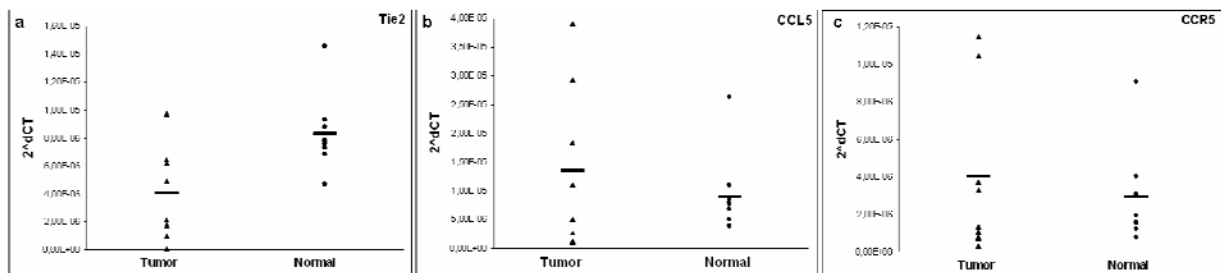


Figure 5.12. RNA expression of Tie2, CCL5 and CCR5 compared between cancer and total healthy liver tissues. a) Tie2 expression was elevated in normal liver tissue compared to tumor tissue (* $p^{\text{Tie2}}=0.01$). b) There was no significant difference between cancer and normal tissues in CCL5 and CCR5 genes ($p^{\text{CCL5}}=0.41$, $p^{\text{CCR5}}=0.52$).

5.5. Suicide gene engineered MSCs inhibit tumor growth

To assess the efficacy of engineered bone marrow derived MSCs as a vehicle for targeted gene therapy of hepatocellular carcinoma, the C57BL/6 murine mesenchymal stem cells were stably transfected with *HSV-Tk* suicide gene-based therapeutic constructs. Two suicide gene expressing MSC lines were produced: C57BL/6 *Tie2/HSV-Tk*⁺ and C57BL/6 *CCL5/HSV-Tk*⁺. In these cell lines targeted expression of the suicide gene was achieved by setting the *HSV-Tk* gene under the control of the tumor specific promoter/enhancer Tie2 or the promoter CCL5.

C57BL/6 *Tie2/HSV-TK*⁺ and C57BL/6 *CCL5/HSV-Tk*⁺ MSCs were injected at a concentration of 0.5×10^6 per week intravenously into mice carrying orthotopically growing HCC xenografts. MSC injections were then followed by three days of intraperitoneal ganciclovir (GCV) injections at an interval of three days after MSC inoculation (Figure 4.7).

5.5.1. Tumor volume decreased after injection of suicide gene engineered MSCs

Total liver volume was examined after sacrifice five weeks after tumor cell injection. Induction of the suicide gene expression by C57BL/6 *Tie2*- or *CCL5/HSV-Tk*⁺ MSCs was followed by intraperitoneal GCV injections. Treatment with C57BL/6 *CCL5/HSV-TK*⁺ MSC and GCV led to a statistically significant reduction in the median volume of tumor bearing

livers by 66.0% relative to tumor loaded livers of the control group which did not receive MSC injections (5.3 [1.5-7.5] cm³ vs. 1.8 [1.0-6.2] cm³; *p=0.027; Table 5.5). Injections of C57BL/6 *Tie2/HSV-Tk*⁺ MSC and GCV did not lead to a significant difference in total liver volume when compared to livers without MSC injections (5.3 [1.5-7.5] cm³ vs. 3.1 [2.9-6.8] cm³; p=0.165; Table 5.5).

Table 5.5. Effect of suicide gene engineered MSCs on tumor growth, angiogenesis and proliferation

	Control	<i>Tie2/HSV-Tk</i> ⁺	<i>CCL5/HSV-Tk</i> ⁺
Total liver volume (cm ³)	5.3 [1.5-7.5]	3.1 [2.9-6.8]	1.8 [1.0-6.2]*
MVD	9.17 [7.67-12.00]	10.33 [4.00-16.33]	11.33 [6.33-16.00]
<i>Ki67</i> index	0.68 [0.52-0.86]	0.57 [0.40-0.90]	0.67 [0.38-0.73]

Note: all data is shown as median [range] values. MVD, CD31+ vessels / 100× magnification field. As compared with control group, *p<0.05.

When comparing total liver volume after *CCL5/HSV-Tk*⁺ MSC treatment to tumor bearing livers after *CCL5/RFP*⁺ MSC injections, the reduction of total liver volume was 76.9% (7.8 [6.8-9.2] cm³ vs. 1.8 [1.0-6.2] cm³; *p=0.012; Table 5.6, Figure 5.13 a). However, *Tie2/HSV-Tk*⁺ MSC treatment showed no significant reduction of total liver volume as compared to *Tie2/RFP*⁺ MSC injections (8.0 [5.7-9.8] cm³ vs. 3.1 [2.9-6.8] cm³; p=0.071; Table 5.6, Figure 5.13 b)

Table 5.6. Total liver volume and *Ki67* index in all 5 groups

	Control	<i>Tie2/RFP</i> ⁺	<i>Tie2/HSV-Tk</i> ⁺	<i>CCL5/RFP</i> ⁺	<i>CCL5/HSV-Tk</i> ⁺
Total liver volume (cm ³)	5.3 [1.5-7.5]	8.00 [5.70-9.80]	3.1 [2.9-6.8]	7.80 [6.80-9.20]	1.8 [1.0-6.2]*
<i>Ki67</i> index	0.68 [0.52-0.86]	0.98 [0.89-0.98]	0.57 [0.40-0.90]	0.98 [0.98-0.99]	0.67 [0.38-0.73]*

Note: all data is shown as median [range] values. *p<0.05, both demonstrate *CCL5/HSV-Tk*⁺ group compared with *CCL5/RFP*⁺ group.

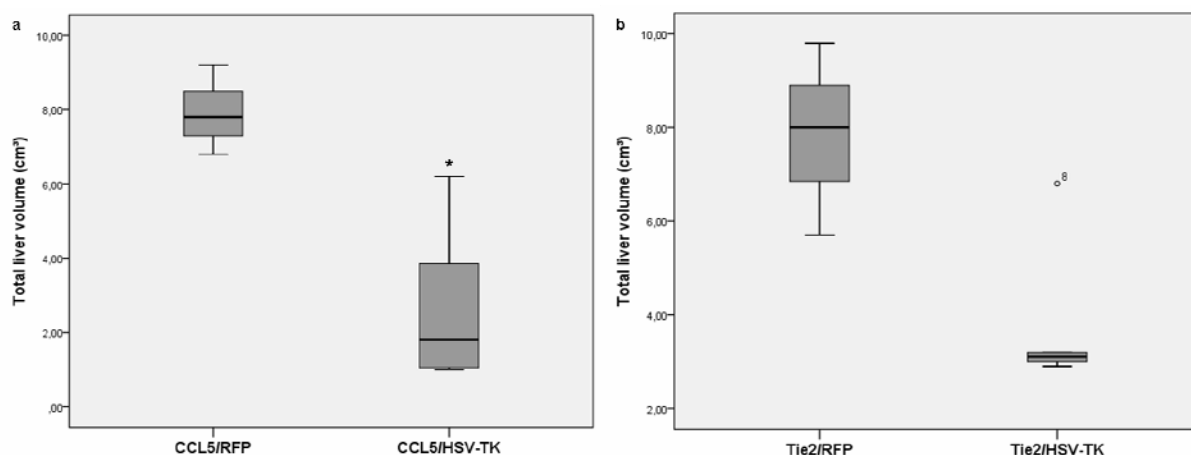


Figure 5.13. *CCL5/HSV-Tk*⁺ and *Tie2/HSV-Tk*⁺ MSCs inhibited tumor growth.

a) Compared to the *CCL5/RFP*⁺ group the total liver volume significantly decreased in the *CCL5/HSV-Tk*⁺ group (* $p < 0.05$); b) Compared to the *Tie2/RFP*⁺ group the *Tie2/HSV-Tk*⁺ group showed a tendency of decreased total liver volume without statistical significance ($p > 0.05$), °8 was missing value. There was also no statistically significant difference in total liver volume comparing treatment with *Tie2/HSV-TK*⁺ vs. *CCL5/HSV-Tk*⁺ transfected MSCs (Table 5.6, $p = 0.127$)

5.5.2. Effect on microvessel density

Microvessel density did not differ significantly between the groups of *HSV-TK*⁺ MSC treatment and the control groups without MSC administration (9.17 [7.67-12.00] CD31⁺ vessels / 100× magnification field in the control group vs. 10.33 [4.00-16.33] in the *Tie2/HSV-TK*⁺ group ($p = 0.833$) and 11.33 [6.33-16.00] in the *CCL5/HSV-TK*⁺ group ($p = 0.328$), *Tie2/HSV-TK*⁺ group vs. *CCL5/HSV-TK*⁺ group ($p = 0.943$); Table 5.5).

5.5.3. Effect on tumor proliferation

The median percentage of *Ki67*⁺ proliferating cells within tumors of *HSV-Tk*⁺ MSC injected animals did not significantly differ from that of the control group (0.68 [0.52-0.86] *Ki67*⁺ cells/total cells in the control group vs. 0.57 [0.40-0.90] in the *Tie2/HSV-Tk*⁺ group ($p = 0.931$) and 0.67 [0.38-0.73] in the *CCL5/HSV-Tk*⁺ group ($p = 0.329$); Table 5.5). However, *CCL5/HSV-Tk*⁺ MSC treatment led to a significantly reduced *Ki67* indexes as compared to

CCL5/RFP⁺ MSC administration (0.98 [0.98-0.99] in the *CCL5/RFP*⁺ MSC group vs. 0.67 [0.38-0.73] in the *CCL5/HSV-Tk*⁺ group (*p=0.036); Table 5.6, Figure 5.14 a, b). No statistical significance regarding *Ki67* index was found between *Tie2/RFP*⁺ and *Tie2/HSV-Tk*⁺ groups (0.98 [0.89-0.98] in *Tie2/RFP*⁺ group vs. 0.57 [0.40-0.90] in the *Tie2/HSV-Tk*⁺ group (p=0.071); Table 5.6, Figure 5.14 c, d).

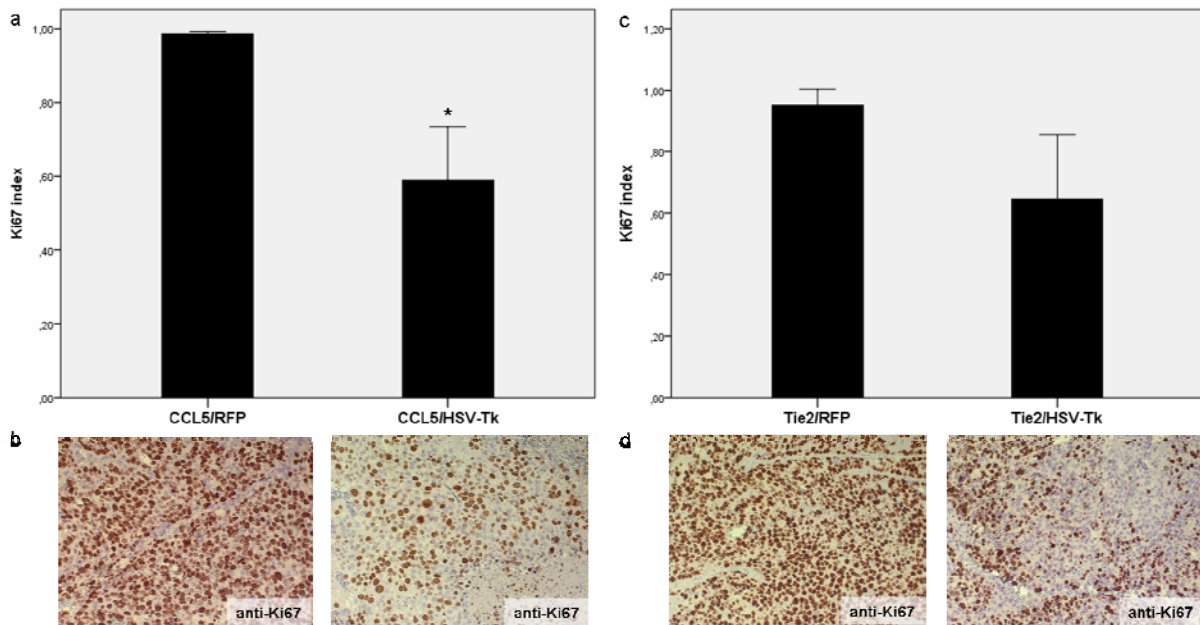


Figure 5.14. Comparison of *Ki67* after injection of different promoter engineered MSCs.

a) *CCL5/HSV-Tk*⁺ MSC treatment led to significantly reduced *Ki67* indexes as compared to *CCL5/RFP*⁺ MSC administration (*p=0.036); b) Exemplary anti-*Ki67* staining of each *CCL5* promoter group is shown; c) No statistical significance has been found between *Tie2/RFP*⁺ and *Tie2/HSV-Tk*⁺ groups (p=0.071), the tendency in a decrease of *Ki67* could be demonstrated; d) Exemplary anti-*Ki67* staining of each *Tie2* promoter group is shown.

VI. DISCUSSION

6.1. Therapy of HCC

Hepatocellular carcinoma is a major health problem with increasing incidence. With the continued development of surgical technologies, radical resection of tumor lesions and liver transplantation have become the standard curative therapies for this cancer. However, a majority of patients can not undergo resection because of advanced tumor stage. For these patients limitations in the availability of liver donors lead to therapy delay and consequently tumor progression. To improve prognosis, and potentially reduce the tumor stage, PEI, RFA, and TACE, are applied as bridging therapies. A series of prospective and retrospective studies have shown that there is no significant difference, or better outcome, on tumor progression when comparing these bridging therapies with radical resection⁹⁵⁻⁹⁸. Regardless of the mechanism applied by these individual various bridging therapies to suppress tumor growth, whether with physical effects such as cryoablation or radiofrequency ablation, chemical effects such as alcohol injection, or by combining the physical and chemical effects used in chemoembolization, significant damage to normal tissues occur in concert with the “suppression” of tumor growth. To better protect normal tissue and at the same time to selectively kill cancer cells and cancer associated stromal cells we evaluated the use of genetically engineered MSCs for selectively targeting of tumor stroma and angiogenesis as therapy of HCCs. As seen with other tumor entities, HCC is capable of building a tumor stroma comprised of cellular components that help to support tumor progression^{39, 99, 100}. HCC tumor stroma also includes an extensive tumor vasculature suggesting strong activation of proangiogenic signaling pathways¹⁰¹. These characteristics of HCC represent potential targets for therapeutic intervention. The potential targeting of this biological phenotype to inhibit HCC tumor growth is the central aim of this thesis.

MSCs are seen as potential candidates for cell-based cancer therapy based on several properties of the cells: 1) they have a natural tropism for recruitment to solid tumor sites; 2) they are reasonably simple to isolate; 3) they can be greatly expanded *in vitro*; 4) they retain the potential to differentiate under exogenous stimuli; 5) they lack immunogenicity; 6) they can be easily transduced by genetic vectors *in vitro*; and 7) they can be delivered systemically or locally¹⁰².

6.2.SPIO-labeled MSCs home to the tumor site from the peripheral circulation

Transient transfection of MSCs with iron particles (SPIO) allowed us to quantify the recruitment of MSCs into the tumor of HCC bearing mice using MRI as imaging technology. SPIO-labeled MSCs appeared as hypointense (dark) in the MRI due to significant shortening of the T2 and T2* relaxation times because of the incorporation of iron oxide nanoparticles in endosomes. We hypothesized that the recruitment of these MSCs^{iron} could be observed under MRI scanning. The MSCs^{iron} were injected into the tail vein. Three days later, after their recruitment to the tumor site, scanning of the T2 and T2* relaxation time by MRI was performed and showed a clear signal decay in the liver of MSC^{iron} injected mice. The recruitment of MSCs^{iron} was subsequently confirmed in paraffin-embedded sections using Prussian Blue staining. This approach will be developed in future studies for the direct quantification of MSC distribution in tumors and non-tumor tissues. Importantly, the magnetically labeling of stem cells does not appear to alter cell metabolism, function, proliferation, viability, or differentiation capacity, and has not been associated with short- or long-term toxicity issues¹⁰³⁻¹⁰⁵. Interestingly, only a few iron-positive cells were seen in the lung three days after injection. MSCs have been previously shown to be arrested in the lung early after peripheral application. This is thought to result from the large irregular size of the MSCs that result from their culture *in vitro*. The results here suggest that MSCs injected through tail vein enter the peripheral circulation and stay transiently within the pulmonary microcirculation. The cells eventually leave the lung and are distributed by the peripheral circulation, and finally, are selectively attracted by the chemokine / cytokine signals that derive from the tumor environment. They can be found in the tumor site by day 3-4 after injection. As discussed the use of MSCs^{iron} is being developed for the quantification and distribution of adoptively transferred MSCs. For future investigations, the T2 sequence signal of the MRI will be recorded before MSC^{iron} injection. This should allow a measurement in the context of titration of cell numbers relative to MRI signals allowing the generation of a standard curve. Following injection of the cells the regional liver signals can be quantified. Thus, the comparable signal decay can be used to evaluate the percentage of cells which arrive at the destination. In summary, labeling of MSCs with SPIO and the use of MR imaging provides a non-invasive method for tracking and quantifying the fate of transplanted cells *in vivo*.

6.3. Adoptively transferred MSCs promote tumor growth, angiogenesis, proliferation, and ascites formation

In comparison to untreated controls, the control MSC were found to significantly promote tumor growth (Table 5.1, Figure 5.3). Qiao and Kidd reported that MSCs could inhibit hepatocellular carcinoma and pancreatic cancer growth^{28, 38}. In these studies, the MSCs were co-injected with tumor cells *in vivo*. The apparent conflicting results may be explained by the different experimental approach: in our animal model MSCs were injected in already well established tumor systems. Our group has also confirmed these general results in other cancer models, including pancreatic cancer^{30, 31}. In these settings control MSCs were found to strongly promote tumor growth. It has been proposed that endogenous MSCs are actively recruited to tumors under physiologic conditions, where they assist with tissue repair, and in so doing, provide a microenvironment supporting tumor growth.

Both tumor weight and volume alterations were evaluated on the basis of total liver weight and volume. The orthotopic hepatocellular carcinoma model was established by intra-parenchymal injection of the human HCC cell line Huh7. The model generally induces one tumor lesion at the puncture site, but also leads to intra-hepatic metastatic lesions. There is generally a lack of metastases in distant tissues with or without MSC injection. Weight curves of the mice showed no significant difference in total body weight among the control and MSC treated groups (Figure 5.4). Total liver weight or volume was increased in mice receiving injections of reporter gene engineered MSCs as compared to mice receiving no MSCs at all due to larger tumors.

Macroscopically, the exogenously added MSCs strongly promoted tumor growth. Microscopically, MSCs also exacerbated bile secretion, invasion, and mitosis of the tumors. Engineered MSCs were found to induce numerous hemorrhages within the tumor area.

CD31 is an epithelial vascular cell surface marker. IHC performed using an anti-CD31 antibody was conducted to evaluate the effect of MSCs on tumor angiogenesis. Both micro-vascular density (MVD) and thickness of vessels were elevated in the MSC injected groups as compared to the control group. Angiogenesis is a key step in tumor progression: on the one hand, MSCs were found to promote angiogenesis in liver cancer; on the other hand, effective targeting of this process could limit tumor growth. MSCs are thought to differentiate into endothelial cells or pericytes, and thus participate in tumor angiogenesis^{4, 106}. MVD demonstrated an increased vessel number in MSC treated tumors. An increased thickness of

these vessels is demonstrated by a broader perivascular staining in these groups.

IHC with Ki67 antibody was used to investigate cancer cell proliferation. The Ki67 index reflects the general proliferation rate of tumor. Here we confirmed that MSCs promote tumor proliferation compared to the control group (Table 5.2, Figure 5.6).

6.4.Expression of reporter genes in the context of tumor stroma and angiogenesis

Cell fate is largely determined by the orchestration of specific gene expression programs. The capacity of a progenitor cell to differentiate into other cellular lineages is controlled by the activity of transcription factors that are capable of reprogramming gene networks. In eukaryotic cells promoters in concert with enhancers drive tissue specific expression through their interaction with specific transcription factors and mediators. MSCs have multilineage differentiation capacity. After recruitment to tumor stroma they start to undergo differentiation into stroma related cells and initiate the secretion of stroma related signals (e.g. CCL5)^{42, 107}. In the context of the studies outlined here the CCL5 promoter can drive expression of genes when MSCs interact with the tumor microenvironment. When used to drive expression of reporter genes (e.g., RFP, GFP, Gluc) or the suicide genes (e.g., HSV-Tk, iCasp9) the CCL5 promoter effectively induce their expression within the tumor stroma. A similar approach was used to drive expression of transgenes in the context of tumor hypoxia and angiogenesis. Here the MSCs differentiate into endothelial related cells and induce expression of angiogenesis related signals including Tie2. Consequently, the Tie2 promoter / enhancer was employed to drive the expression of transgenes in the context of tumor angiogenesis.

The homing and activation of MSCs within a tumor environment were verified using engineered MSCs to express the reporter gene RFP under the control of either the Tie2 promoter / enhancer or the CCL5 promoter. Tie2 is a cell surface receptor that binds to and is activated by the angiopoietins (Ang1, Ang2, Ang3, and Ang4). Studies have shown that MSCs can act as precursors for carcinoma associated fibroblasts, endothelial cells, or pericytes^{108, 109}. CCL5 (Chemokine (C-C motif) ligand 5), also known as RANTES (Regulated upon Activation, Normal T-cell Expressed, and Secreted), is a chemokine which is induced in tumor stroma and is chemotactic for T cells, eosinophils, basophils, and other cells. Following their integration into tumor stroma, MSCs exert effects at least partly through their secretion of factors including CCL5⁴². In our studies RFP expression was placed under the

control of a Tie2 or CCL5 promoter, supporting conditional activation of the transgene in the context of either angiogenesis or tumor stroma. Serial section staining with anti-RFP indicated that RFP signals were found proximal to the CCL5 and CD31 signals, strongly suggesting MSC association to tumor stroma or angiogenesis.

6.5. Chemokines and their receptors play a predominant role in MSCs' recruitment

The mechanism underlying the recruitment of MSCs to the tumor site remains an open question. A number of groups have demonstrated that growth factors and chemokines are released from cancer cells. These factors can promote the migration of MSCs from bone marrow towards the tumor site. Such as vascular endothelial cell growth factors (VEGFs), transforming growth factors (TGFs), fibroblast growth factors (FGFs), epidermal growth factors (EGFs), stromal cell-derived growth factor-1 α (SDF-1 α)/CXCL12, platelet derived growth factors (PDGFs), IL-1 β , IL-8/CXCL8, monocyte chemoattractant protein-1 (CCL2), and CCL5, which are released from the tumor environment are possible candidates in the mobilization and chemotaxis of progenitor cells towards target tissues^{17, 42, 110-115}. Additionally, inhibition of the tumor associated inflammatory response by an anti-inflammatory agent, which down-regulates NF- κ B, VEGF, IL-6, CCL3, and CCL25, resulted in the inhibition of MSC recruitment³⁸. Most recently, Quante and associates illustrated that the recruitment of MSCs to the tumor was dependent on TGF- β - and SDF-1 α ¹¹⁶. CCR1 and CCR5 are two common receptors for CCL5. The IHC results here showed that CCR1 and CCR5 positive signals were located proximal to the CCL5 signals (Figure 5.8, 5.9) supporting the potential role of these ligand receptor interactions in the targeting of MSCs to tumor stroma.

6.6. Stroma and angiogenesis gene expression in human HCC and normal samples

Quantitative RT-PCR assays were used to study the differential expression of Tie2, CCL5, and CCR5 genes in human HCC samples and adjacent normal liver tissues. However, there was no significant difference found in the mRNA levels of the three genes between tumor tissue and adjacent normal liver samples (Figure 5.11). Based on the clinical data of the patients, most of them suffered from liver cirrhosis (Table 5.4). The apparent bias in gene expression may be caused by the background of a chronic disease in these samples. To help addressing this qRT-PCR was conducted in patient liver tumor samples and compared to healthy liver samples. Here again we observed no difference in CCL5 or CCR5 expression

relative to endogenous controls (Figure 5.12 b, c). However, there was a significant increase in the expression of Tie2 in the healthy tissue group (*p=0.01, Figure 5.12 a) as compared to the tumor group. HCC is generally regarded as a hypervascular tumor, the angiogenesis related gene Tie2 should be highly expressed in tumor tissue. However, as Zhao and Zhang reported^{117, 118}, there was no significantly different expression of Tie2 between HCC and non-cancerous liver tissue. The differential expression of Tie2, CCL5, and CCR5 in tumor and normal tissues suggests that it is important to integrate the general expression of inflammatory cytokines and the level of tumor differentiation when planning future experiments^{119, 120}.

6.7.Suicide gene engineered MSCs followed by GCV application inhibit tumor growth

For therapeutic application MSCs were engineered to express the herpes simplex virus – thymidine kinase (HSV-Tk) under the control of the Tie2 promoter / enhancer or the CCL5 promoter. The cells were injected into the peripheral circulation and three days later, the animals were treated with the prodrug ganciclovir (GCV). The mechanism of HSV-Tk suicide gene killing has been well characterized. The HSV-Tk gene is derived from the Herpes simplex virus. It is an enzyme that phosphorylates the prodrug ganciclovir to the active form GCV-triphosphate (GCV-TP), which subsequently inhibits cellular DNA polymerases and acts as a chain terminator in DNA synthesis, thereby selectively killing dividing cells¹⁰⁷. The major mechanism responsible for GCV-TP transfer into neighboring cells is their transfer through gap junctions that are established between neighbouring cells. In this way, the tumor cells which are not transduced with the suicide gene, also become sensitive to prodrugs and are eliminated along with the suicide gene-transfected MSCs referred to as the “bystander effect”. One advantage of using HSV-Tk as a suicide gene in MSC is that it demonstrates not only bystander cytotoxic effect on tumor cells, but eliminates even those MSCs that have not been activated within the tumor environment¹²¹ since a small level of promoter activity is still seen in MSCs at other locations leading to cells that become sensitive to GCV treatment. This effectively limits potential MSC driven side effects. In addition to its use as a therapeutic gene, HSV-Tk has also been developed as a marker for non-invasive imaging. HSV-Tk-specific tracers, like [¹⁸F]FHBG and [¹²⁴I]FIAU can be detected by PET imaging in HSV-Tk expressing MSCs²⁵. However, the HSV-Tk and GCV setting does have drawbacks. For example, GCV only kills proliferating cells and does not kill postmitotic cells¹²². Some other suicide genes are currently under investigation including iCasp9¹²³.

It remains an open question when it is most suitable to inject GCV after application of MSCs. Here we chose a three-day interval between MSC injection and GCV treatment. First, after MSC injection in the tail vein, they had to traffic through the body and potentially to leave the lung before eventually reaching the tumor site. Second, the MSCs need time to undergo differentiation and activation of the transgenes. The bystander effect that underlies the use of Tk-GCV here requires time to be “communicated” to the surrounding cells. Amano et al showed that HSV-Tk transfected MSCs required at least three days before GCV induced cell death occurred *in vitro*²⁶. For these reasons, the MSCs were given three days to home to the tumor environment, proliferate, and set up tight junctions with bystander tumor cells.

VII. PERSPECTIVES

From a clinical perspective, MSC based gene therapy appears to be more feasible for clinical application than many other cell therapy approaches currently under study. This is based on the observation that MSCs are easy to obtain from adult subjects, for example, they can be isolated from patient's bone marrow, adipose tissue, umbilical cord blood, placental tissue, amniotic fluid, peripheral circulation, and even tumor tissue¹²⁴⁻¹²⁹. After isolation, they can be expanded *in vitro* and are relatively easy to transfect with transgenes. In a future clinical trial, each patient could be treated with autologous MSCs. This obviates potential immunologic incompatibilities. Intravenous injection of MSCs has the advantage that repeated injections over an extended period are clinically feasible.

Practically, this approach could likely be partnered with existing strategies. For example, in hepatocellular carcinoma, TACE is generally applied as a bridging therapy to control tumor growth. If performed in concert with MSC injection, an enhanced therapeutic effect may be seen. However, recent studies have shown that adoptively applied MSCs can protect tumor cells from chemotoxicity¹³⁰. The effect was transient and suggests that while the two therapies can not be co-applied, a therapeutic schedule that limits potential negative effects of MSCs has to be developed. The application of engineered MSCs represents an important new approach for the treatment of solid tumors.

VIII. SUMMARY

- MSCs home to the tumor site from the peripheral circulation, and when transfected with SPIO, their recruitment to the tumor site can be followed and evaluate by MRI scanning
- Engineering MSCs express the reporter gene RFP by activation of the tissue-specific promoters CCL5 or Tie2 in the context of tumor stroma and angiogenesis
- MSCs promote tumor growth, angiogenesis, and proliferation as they differentiate into tumor stromal cells and angiogenic endothelial cells
- MSCs may potentially be recruited to the tumor site through ligand-receptor interaction between CCL5, CCR5, and CCR1
- There is no differential expression of Tie2, CCL5, and CCR5 between normal and tumor tissues of HCC patients and healthy normal hepatic tissue
- Suicide gene engineered MSCs under the control of tissue-specific promoters targeting tumor stroma or angiogenesis followed with GCV injection can inhibit experimental HCC tumor growth in mice

IX. ZUSAMMENFASSUNG

Einleitung

Mesenchymale Stammzellen (MSCs) spielen eine entscheidende Rolle in der Tumorbiologie. Unter anderem werden MSCs nach Rekrutierung in einen wachsenden Tumor in das Tumorgefäßsystem eingebaut. In präklinischen Untersuchungen konnte beispielsweise für das Mammakarzinom gezeigt werden, daß in Richtung Tumorstroma rekrutierte MSCs selbst durch Sekretion des Cytokins RANTES (CCL5) Tumorwachstum und Metastasierung unterstützen. In eigenen Vorarbeiten konnte nachgewiesen werden, daß exogen zugeführte MSCs substantiell in Tumoren wie Pankreaskarzinomen homen. Daher sind MSCs potentielle Transportvehikel für therapeutisch wirksame Gene im Kontext eines wachsenden Tumors, insofern sie für hoch selektive, gewebspezifische Expression entwickelt werden. In Vorarbeiten haben wir immortalisierte MSCs (imMSCs) stabil mit dem Herpes simplex virus (HSV) - Thymidinkinase (tk) Gen unter der Kontrolle des Tie2 Promoter/Enhancer transfiziert, der hoch selektiv im Rahmen der Angiogeneese beim Pankreaskarzinom zur Genexpression führt. Die Tk-Expression führt zur Phosphorylierung des Prodrugs Ganciclovir (GCV), welches dann zum Zelltod der transfizierten Zelle und angrenzender Zellen (andere Endothel- oder Tumorzellen) über den sog. Bystandereffekt führt.

Ziel war es nun, den biologischen Mechanismus der stammzell-basierten, primär gegen die Angiogeneese gerichteten Therapie auf eine das Tumorstroma adressierende Therapie auszuweiten und beim humanen hepatozellulären Karzinom zu evaluieren. Dazu wurden MSCs mit der Herpes Simplex (HSV) Thymidinkinase (Tk) unter der Kontrolle des CCL5- / Tie2-Promoters zur gewebspezifischen Genexpression stabil transfiziert. Zur Lokalisation der MSCs in Assoziation zum Therapieeffekt werden diagnostische Tie2/CCL5-RFP enthaltende MSCs eingesetzt.

Methodik

MSCs wurden aus dem Knochenmark von C57BL/6 p53 knock-out Mäusen isoliert, charakterisiert und kultiviert. Diese wurden mittels Elektroporation jeweils mit HSV-Tk oder Red Fluorescent Protein (RFP) unter der Kontrolle des CCL5- und Tie2-Promoters stabil transfiziert. Für die *in vivo* Versuche wurde ein orthotopes Mausmodell verwendet, wobei humane Huh7 HCC-Tumorzellen in die Leber von immuninkompetenten Nacktmäusen (Balb/c nu/nu) injiziert wurden. Die RFP und HSV-Tk transfizierten Stammzellen sowie die

nativen MSCs wurden über 3 Wochen einmal wöchentlich intravenös über die Schwanzvene injiziert. Die HSV-Tk Therapiegruppe erhielt in jedem Zyklus an den Tagen 5-7 nach Stammzellgabe Ganciclovir durch intraperitoneale Verabreichung. Nach 36 Tagen wurden die Tiere getötet und neben Erfassung des makroskopisch sichtbaren Tumorbefalls, histologische und immunhistochemische Untersuchungen verschiedener Gewebe vorgenommen.

Ergebnisse

In der Mikroskopie konnten RFP-Signale in den Tumorgewebeproben der entsprechenden Stammzellgruppen, nicht jedoch in der Kontrollgruppe, detektiert werden. Im orthotopen HCC-Modell konnte gezeigt werden, dass die CCL5/HSV-Tk transfizierten Stammzellen in Verbindung mit Ganciclovir zu einer signifikanten Tumormassenreduktion um 66% gegenüber der unbehandelten Gruppe führten ($p < 0.05$). Der Effekt auf das Tumorwachstum war deutlicher nach Gabe von CCL5/HSV-Tk MSCs im Vergleich zu Tie2/HSV-Tk MSCs. Ferner konnte gezeigt werden, dass die systemische Gabe von nativen MSCs oder diagnostischen RFP-MSCs das Tumorwachstum fördert.

Schlussfolgerung

Die erhobenen Daten weisen darauf hin, dass MSCs und die Aktivierung des CCL5- / Tie2-Promoters für das Wachstum und das Metastasierungspotential des hepatozellulären Karzinoms eine Rolle spielen. Die RFP Genexpression im Tumorgewebe nach Gabe von diagnostischen Tie2/CCL5-RFP enthaltende MSCs zeigt aktives Homing der exogen zugeführten MSCs ins Tumorgewebe. Des Weiteren zeigte sich eine Reduktion des Primärtumorgewichts und der Metastasierungsrate nach Gabe von therapeutischen HSV-Tk-MSCs unter Ganciclovir, wohingegen sich native MSCs oder RFP-MSCs am Tumorwachstum beteiligen. Eine auf das Tumorstroma oder Angiogenese zielende MSCs basierte CCL5-/Tie2-HSV-Tk-Suizidtherapie stellt damit eine erfolgversprechende Therapiestrategie beim hepatozellulären Karzinom dar, wobei weitere experimentelle Untersuchungen zur Optimierung dieser Behandlungsstrategie und zur nicht-invasiven Erfassung des Therapieerfolgs (*in vivo* imaging) bis zur Entwicklung einer klinischen Studie erforderlich sind.

X. ABBREVIATION

5-FC, 5-fluorocytosine

5-FU, fluorouracil

C57BL/6, C57 black 6 mouse

CCL5, chemokine (C-C motif) ligand 5

RANTES, regulated upon activation normal T cell expressed presumed secreted

CCR1, 5, C-C chemokine receptor type 1,5

CD, cytosine deaminase

CD, cluster of differentiation, CD14, CD19, CD34, CD45, CD73, CD 90, CD105

CMV, cytomegalovirus

CX3CL1, RGDFKN

DMEM, Dulbecco's modified eagle medium

DMSO, dimethyl sulfoxide

ELISA, enzyme-linked immunosorbent assay

Fe, ferrum

GCV, ganciclovir

GFP, green fluorescent protein

HCC, hepatocellular carcinoma

HE, hematoxylin and eosin

HLA-DR, human leukocyte antigens-DR (major histocompatibility complex, MHC class II)

HSV-Tk, herpes simplex virus-thymidine kinase

hTERT, human telomerase reverse transcriptase

IFN- β , beta-Interferon

IL, interleukin, IL-1 β , IL-2, IL-8, IL-12, IL-17, IL-22

iNOS, inducible nitric oxide synthase

i.v., intravenous

MHC-I, major histocompatibility complex class I

MRI, magnetic resonance imaging

MSC, mesenchymal stem cell

eMSC, engineering mesenchymal stem cell

hBM-MSC, human bone marrow-derived mesenchymal stem cell
hAT-MSC, human adipose tissue-derived mesenchymal stem cell
mMSC, mouse bone marrow-derived mesenchymal stem cell
rMSC, rat bone marrow-derived mesenchymal stem cell
MVD, microvascular density
NF- κ B, nuclear factor kappa-light-chain-enhancer of activated B cells
NK4, antagonist of hepatocyte growth factor (HGF)
PDL, population doubling level
PEDF, pigment epithelium-derived factor
PEI, percutaneous ethanol injection
RFA, radio frequency ablation
RFP, red fluorescent protein
ROR- γ , RAR-related orphan receptor-gamma
s.c., subcutaneous
SPIO, supermagnetic iron oxide
TACE, transcatheter arterial chemoembolization
T-cell, T lymphocytes
Tie2, angiopoietin receptor 2
TGF β , transforming growth factor beta
TNF- α , tumor necrosis factor-alpha
TRAIL, tumor necrosis factor-related apoptosis-inducing ligand
VEGFR-1, vascular endothelial growth factor receptor-1
VPCs, vector-producing cells

XI. REFERENCES

1. Dominici M, Le Blanc K, Mueller I, Slaper-Cortenbach I, Marini F, Krause D, Deans R, Keating A, Prockop D, Horwitz E: Minimal criteria for defining multipotent mesenchymal stromal cells. The International Society for Cellular Therapy position statement, *Cytotherapy* 2006, 8:315-317
2. Pittenger MF, Mackay AM, Beck SC, Jaiswal RK, Douglas R, Mosca JD, Moorman MA, Simonetti DW, Craig S, Marshak DR: Multilineage potential of adult human mesenchymal stem cells, *Science* 1999, 284:143-147
3. Huss R, Heil M, Moosmann S, Ziegelhoeffer T, Sagebiel S, Seliger C, Kinston S, Gottgens B: Improved arteriogenesis with simultaneous skeletal muscle repair in ischemic tissue by SCL(+) multipotent adult progenitor cell clones from peripheral blood, *J Vasc Res* 2004, 41:422-431
4. Silva GV, Litovsky S, Assad JA, Sousa AL, Martin BJ, Vela D, Coulter SC, Lin J, Ober J, Vaughn WK, Branco RV, Oliveira EM, He R, Geng YJ, Willerson JT, Perin EC: Mesenchymal stem cells differentiate into an endothelial phenotype, enhance vascular density, and improve heart function in a canine chronic ischemia model, *Circulation* 2005, 111:150-156
5. Dvorak HF: Tumors: wounds that do not heal. Similarities between tumor stroma generation and wound healing, *N Engl J Med* 1986, 315:1650-1659
6. Kucerova L, Altanerova V, Matuskova M, Tyciakova S, Altaner C: Adipose tissue-derived human mesenchymal stem cells mediated prodrug cancer gene therapy, *Cancer Res* 2007, 67:6304-6313
7. Kidd S, Spaeth E, Klopp A, Andreeff M, Hall B, Marini FC: The (in) auspicious role of mesenchymal stromal cells in cancer: be it friend or foe, *Cytotherapy* 2008, 10:657-667
8. Coussens LM, Werb Z: Inflammation and cancer, *Nature* 2002, 420:860-867
9. Ren G, Zhang L, Zhao X, Xu G, Zhang Y, Roberts AI, Zhao RC, Shi Y: Mesenchymal stem cell-mediated immunosuppression occurs via concerted action of chemokines and nitric oxide, *Cell Stem Cell* 2008, 2:141-150
10. Ramasamy R, Tong CK, Seow HF, Vidyadaran S, Dazzi F: The immunosuppressive effects of human bone marrow-derived mesenchymal stem cells target T cell proliferation but not its effector function, *Cell Immunol* 2008, 251:131-136
11. Plumas J, Chaperot L, Richard MJ, Molens JP, Bensa JC, Favrot MC: Mesenchymal stem cells induce apoptosis of activated T cells, *Leukemia* 2005, 19:1597-1604
12. Li H, Guo Z, Jiang X, Zhu H, Li X, Mao N: Mesenchymal stem cells alter migratory property of T and dendritic cells to delay the development of murine lethal acute graft-versus-host disease, *Stem Cells* 2008, 26:2531-2541
13. Wei J, Blum S, Unger M, Jarmy G, Lamparter M, Geishausser A, Vlastos GA, Chan G, Fischer KD, Rattat D, Debatin KM, Hatzopoulos AK, Beltinger C: Embryonic endothelial progenitor cells armed with a suicide gene target hypoxic lung metastases after intravenous delivery, *Cancer Cell* 2004, 5:477-488
14. Studeny M, Marini FC, Champlin RE, Zompetta C, Fidler IJ, Andreeff M: Bone marrow-derived mesenchymal stem cells as vehicles for interferon-beta delivery into tumors, *Cancer Res* 2002, 62:3603-3608
15. Studeny M, Marini FC, Dembinski JL, Zompetta C, Cabreira-Hansen M, Bekele BN, Champlin RE, Andreeff M: Mesenchymal stem cells: potential precursors for tumor stroma and targeted-delivery vehicles for anticancer agents, *J Natl Cancer Inst* 2004, 96:1593-1603
16. Loebinger MR, Eddaoudi A, Davies D, Janes SM: Mesenchymal stem cell delivery of TRAIL can eliminate metastatic cancer, *Cancer Res* 2009, 69:4134-4142
17. Nakamizo A, Marini F, Amano T, Khan A, Studeny M, Gumin J, Chen J, Hentschel S,

- Vecil G, Dembinski J, Andreeff M, Lang FF: Human bone marrow-derived mesenchymal stem cells in the treatment of gliomas, *Cancer Res* 2005, 65:3307-3318
18. Hakkarainen T, Sarkioja M, Lehenkari P, Miettinen S, Ylikomi T, Suuronen R, Desmond RA, Kanerva A, Hemminki A: Human mesenchymal stem cells lack tumor tropism but enhance the antitumor activity of oncolytic adenoviruses in orthotopic lung and breast tumors, *Hum Gene Ther* 2007, 18:627-641
 19. Grisendi G, Bussolari R, Cafarelli L, Petak I, Rasini V, Veronesi E, De Santis G, Spano C, Tagliazzucchi M, Barti-Juhász H, Scarabelli L, Bambi F, Frassoldati A, Rossi G, Casali C, Morandi U, Horwitz EM, Paolucci P, Conte P, Dominici M: Adipose-derived mesenchymal stem cells as stable source of tumor necrosis factor-related apoptosis-inducing ligand delivery for cancer therapy, *Cancer Res* 2010, 70:3718-3729
 20. Eliopoulos N, Francois M, Boivin MN, Martineau D, Galipeau J: Neo-organoid of marrow mesenchymal stromal cells secreting interleukin-12 for breast cancer therapy, *Cancer Res* 2008, 68:4810-4818
 21. Xin H, Sun R, Kanehira M, Takahata T, Itoh J, Mizuguchi H, Saijo Y: Intratracheal delivery of CX3CL1-expressing mesenchymal stem cells to multiple lung tumors, *Mol Med* 2009, 15:321-327
 22. Gu C, Li S, Tokuyama T, Yokota N, Namba H: Therapeutic effect of genetically engineered mesenchymal stem cells in rat experimental leptomeningeal glioma model, *Cancer Lett* 2010, 291:256-262
 23. Hu M, Yang JL, Teng H, Jia YQ, Wang R, Zhang XW, Wu Y, Luo Y, Chen XC, Zhang R, Tian L, Zhao X, Wei YQ: Anti-angiogenesis therapy based on the bone marrow-derived stromal cells genetically engineered to express sFlt-1 in mouse tumor model, *BMC Cancer* 2008, 8:306
 24. Uchibori R, Okada T, Ito T, Urabe M, Mizukami H, Kume A, Ozawa K: Retroviral vector-producing mesenchymal stem cells for targeted suicide cancer gene therapy, *J Gene Med* 2009, 11:373-381
 25. Miletic H, Fischer Y, Litwak S, Giroglou T, Waerzeggers Y, Winkeler A, Li H, Himmelreich U, Lange C, Stenzel W, Deckert M, Neumann H, Jacobs AH, von Laer D: Bystander killing of malignant glioma by bone marrow-derived tumor-infiltrating progenitor cells expressing a suicide gene, *Mol Ther* 2007, 15:1373-1381
 26. Amano S, Li S, Gu C, Gao Y, Koizumi S, Yamamoto S, Terakawa S, Namba H: Use of genetically engineered bone marrow-derived mesenchymal stem cells for glioma gene therapy, *Int J Oncol* 2009, 35:1265-1270
 27. Xiang J, Tang J, Song C, Yang Z, Hirst DG, Zheng QJ, Li G: Mesenchymal stem cells as a gene therapy carrier for treatment of fibrosarcoma, *Cytotherapy* 2009, 11:516-526
 28. Qiao L, Xu Z, Zhao T, Zhao Z, Shi M, Zhao RC, Ye L, Zhang X: Suppression of tumorigenesis by human mesenchymal stem cells in a hepatoma model, *Cell Res* 2008, 18:500-507
 29. Qiao L, Zhao TJ, Wang FZ, Shan CL, Ye LH, Zhang XD: NF-kappaB downregulation may be involved the depression of tumor cell proliferation mediated by human mesenchymal stem cells, *Acta Pharmacol Sin* 2008, 29:333-340
 30. Conrad C, Husemann Y, Niess H, von Luetlichau I, Huss R, Bauer C, Jauch KW, Klein CA, Bruns C, Nelson PJ: Linking transgene expression of engineered mesenchymal stem cells and angiopoietin-1-induced differentiation to target cancer angiogenesis, *Ann Surg* 2011, 253:566-571

31. Zischek C, Niess H, Ischenko I, Conrad C, Huss R, Jauch KW, Nelson PJ, Bruns C: Targeting tumor stroma using engineered mesenchymal stem cells reduces the growth of pancreatic carcinoma, *Ann Surg* 2009, 250:747-753
32. Niess H, Bao Q, Conrad C, Zischek C, Notohamiprodjo M, Schwab F, Schwarz B, Huss R, Jauch KW, Nelson PJ, Bruns CJ: Selective targeting of genetically engineered mesenchymal stem cells to tumor stroma microenvironments using tissue-specific suicide gene expression suppresses growth of hepatocellular carcinoma, *Ann Surg* 2011, 254:767-775
33. Li GC, Ye QH, Xue YH, Sun HJ, Zhou HJ, Ren N, Jia HL, Shi J, Wu JC, Dai C, Dong QZ, Qin LX: Human mesenchymal stem cells inhibit metastasis of a hepatocellular carcinoma model using the MHCC97-H cell line, *Cancer Sci* 2010, 101:2546-2553
34. Li L, Tian H, Yue W, Zhu F, Li S, Li W: Human mesenchymal stem cells play a dual role on tumor cell growth in vitro and in vivo, *J Cell Physiol* 2010,
35. Qiao L, Xu ZL, Zhao TJ, Ye LH, Zhang XD: Dkk-1 secreted by mesenchymal stem cells inhibits growth of breast cancer cells via depression of Wnt signalling, *Cancer Lett* 2008, 269:67-77
36. You MH, Kim WJ, Shim W, Lee SR, Lee G, Choi S, Kim DY, Kim YM, Kim H, Han SU: Cytosine deaminase-producing human mesenchymal stem cells mediate an antitumor effect in a mouse xenograft model, *J Gastroenterol Hepatol* 2009, 24:1393-1400
37. Wang SS, Asfaha S, Okumura T, Betz KS, Muthupalani S, Rogers AB, Tu S, Takaishi S, Jin G, Yang X, Wu DC, Fox JG, Wang TC: Fibroblastic colony-forming unit bone marrow cells delay progression to gastric dysplasia in a helicobacter model of gastric tumorigenesis, *Stem Cells* 2009, 27:2301-2311
38. Kidd S, Caldwell L, Dietrich M, Samudio I, Spaeth EL, Watson K, Shi Y, Abbruzzese J, Konopleva M, Andreeff M, Marini FC: Mesenchymal stromal cells alone or expressing interferon-beta suppress pancreatic tumors in vivo, an effect countered by anti-inflammatory treatment, *Cytotherapy* 2010, 12:615-625
39. Shinagawa K, Kitadai Y, Tanaka M, Sumida T, Kodama M, Higashi Y, Tanaka S, Yasui W, Chayama K: Mesenchymal stem cells enhance growth and metastasis of colon cancer, *Int J Cancer* 2010, 127:2323-2333
40. Chen XC, Wang R, Zhao X, Wei YQ, Hu M, Wang YS, Zhang XW, Zhang R, Zhang L, Yao B, Wang L, Jia YQ, Zeng TT, Yang JL, Tian L, Kan B, Lin XJ, Lei S, Deng HX, Wen YJ, Mao YQ, Li J: Prophylaxis against carcinogenesis in three kinds of unestablished tumor models via IL12-gene-engineered MSCs, *Carcinogenesis* 2006, 27:2434-2441
41. Wolf D, Rumpold H, Koeck R, Gunsilius E: Re: Mesenchymal stem cells: potential precursors for tumor stroma and targeted-delivery vehicles for anticancer agents, *J Natl Cancer Inst* 2005, 97:540-541; author reply 541-542
42. Karnoub AE, Dash AB, Vo AP, Sullivan A, Brooks MW, Bell GW, Richardson AL, Polyak K, Tubo R, Weinberg RA: Mesenchymal stem cells within tumour stroma promote breast cancer metastasis, *Nature* 2007, 449:557-563
43. Cousin B, Ravet E, Poglio S, De Toni F, Bertuzzi M, Lulka H, Touil I, Andre M, Grolleau JL, Peron JM, Chavoïn JP, Bourin P, Penicaud L, Casteilla L, Buscail L, Cordelier P: Adult stromal cells derived from human adipose tissue provoke pancreatic cancer cell death both in vitro and in vivo, *PLoS One* 2009, 4:e6278
44. Llovet JM, Burroughs A, Bruix J: Hepatocellular carcinoma, *Lancet* 2003, 362:1907-1917
45. Parkin DM, Bray F, Ferlay J, Pisani P: Global cancer statistics, 2002, *CA Cancer J Clin* 2005, 55:74-108

46. Llovet JM, Fuster J, Bruix J: The Barcelona approach: diagnosis, staging, and treatment of hepatocellular carcinoma, *Liver Transpl* 2004, 10:S115-120
47. Llovet JM, Bruix J: Systematic review of randomized trials for unresectable hepatocellular carcinoma: Chemoembolization improves survival, *Hepatology* 2003, 37:429-442
48. Grazi GL, Ercolani G, Pierangeli F, Del Gaudio M, Cescon M, Cavallari A, Mazziotti A: Improved results of liver resection for hepatocellular carcinoma on cirrhosis give the procedure added value, *Ann Surg* 2001, 234:71-78
49. Bruix J, Llovet JM: Prognostic prediction and treatment strategy in hepatocellular carcinoma, *Hepatology* 2002, 35:519-524
50. Mazzaferro V, Regalia E, Doci R, Andreola S, Pulvirenti A, Bozzetti F, Montalto F, Ammatuna M, Morabito A, Gennari L: Liver transplantation for the treatment of small hepatocellular carcinomas in patients with cirrhosis, *N Engl J Med* 1996, 334:693-699
51. Llovet JM, Fuster J, Bruix J: Intention-to-treat analysis of surgical treatment for early hepatocellular carcinoma: resection versus transplantation, *Hepatology* 1999, 30:1434-1440
52. Bismuth H, Majno PE, Adam R: Liver transplantation for hepatocellular carcinoma, *Semin Liver Dis* 1999, 19:311-322
53. Jonas S, Bechstein WO, Steinmuller T, Herrmann M, Radke C, Berg T, Settmacher U, Neuhaus P: Vascular invasion and histopathologic grading determine outcome after liver transplantation for hepatocellular carcinoma in cirrhosis, *Hepatology* 2001, 33:1080-1086
54. Yao FY, Ferrell L, Bass NM, Watson JJ, Bacchetti P, Venook A, Ascher NL, Roberts JP: Liver transplantation for hepatocellular carcinoma: expansion of the tumor size limits does not adversely impact survival, *Hepatology* 2001, 33:1394-1403
55. Kawai S, Okamura J, Ogawa M, Ohashi Y, Tani M, Inoue J, Kawarada Y, Kusano M, Kubo Y, Kuroda C, et al.: Prospective and randomized clinical trial for the treatment of hepatocellular carcinoma--a comparison of lipiodol-transcatheter arterial embolization with and without adriamycin (first cooperative study). The Cooperative Study Group for Liver Cancer Treatment of Japan, *Cancer Chemother Pharmacol* 1992, 31 Suppl:S1-6
56. Kawai S, Tani M, Okamura J, Ogawa M, Ohashi Y, Monden M, Hayashi S, Inoue J, Kawarada Y, Kusano M, et al.: Prospective and randomized clinical trial for the treatment of hepatocellular carcinoma--a comparison between L-TAE with farmorubicin and L-TAE with adriamycin: preliminary results (second cooperative study). Cooperative Study Group for Liver Cancer Treatment of Japan, *Cancer Chemother Pharmacol* 1994, 33 Suppl:S97-102
57. Bruix J, Llovet JM, Castells A, Montana X, Bru C, Ayuso MC, Vilana R, Rodes J: Transarterial embolization versus symptomatic treatment in patients with advanced hepatocellular carcinoma: results of a randomized, controlled trial in a single institution, *Hepatology* 1998, 27:1578-1583
58. Pelletier G, Ducreux M, Gay F, Luboinski M, Hagege H, Dao T, Van Steenberg W, Buffet C, Rougier P, Adler M, Pignon JP, Roche A: Treatment of unresectable hepatocellular carcinoma with lipiodol chemoembolization: a multicenter randomized trial. Groupe CHC, *J Hepatol* 1998, 29:129-134
59. Lo CM, Ngan H, Tso WK, Liu CL, Lam CM, Poon RT, Fan ST, Wong J: Randomized controlled trial of transarterial lipiodol chemoembolization for unresectable hepatocellular carcinoma, *Hepatology* 2002, 35:1164-1171
60. Llovet JM, Real MI, Montana X, Planas R, Coll S, Aponte J, Ayuso C, Sala M, Muchart J, Sola R, Rodes J, Bruix J: Arterial embolisation or chemoembolisation

- versus symptomatic treatment in patients with unresectable hepatocellular carcinoma: a randomised controlled trial, *Lancet* 2002, 359:1734-1739
61. Okada S: Local ablation therapy for hepatocellular carcinoma, *Semin Liver Dis* 1999, 19:323-328
 62. Livraghi T, Giorgio A, Marin G, Salmi A, de Sio I, Bolondi L, Pompili M, Brunello F, Lazzaroni S, Torzilli G, et al.: Hepatocellular carcinoma and cirrhosis in 746 patients: long-term results of percutaneous ethanol injection, *Radiology* 1995, 197:101-108
 63. Lencioni R, Pinto F, Armillotta N, Bassi AM, Moretti M, Di Giulio M, Marchi S, Uliana M, Della Capanna S, Lencioni M, Bartolozzi C: Long-term results of percutaneous ethanol injection therapy for hepatocellular carcinoma in cirrhosis: a European experience, *Eur Radiol* 1997, 7:514-519
 64. Lencioni R, Crocetti L: A critical appraisal of the literature on local ablative therapies for hepatocellular carcinoma, *Clin Liver Dis* 2005, 9:301-314, viii
 65. Rossi S, Di Stasi M, Buscarini E, Quaretti P, Garbagnati F, Squassante L, Paties CT, Silverman DE, Buscarini L: Percutaneous RF interstitial thermal ablation in the treatment of hepatic cancer, *AJR Am J Roentgenol* 1996, 167:759-768
 66. Buscarini L, Buscarini E, Di Stasi M, Vallisa D, Quaretti P, Rocca A: Percutaneous radiofrequency ablation of small hepatocellular carcinoma: long-term results, *Eur Radiol* 2001, 11:914-921
 67. Mulier S, Mulier P, Ni Y, Miao Y, Dupas B, Marchal G, De Wever I, Michel L: Complications of radiofrequency coagulation of liver tumours, *Br J Surg* 2002, 89:1206-1222
 68. Lai CL, Wu PC, Chan GC, Lok AS, Lin HJ: Doxorubicin versus no antitumor therapy in inoperable hepatocellular carcinoma. A prospective randomized trial, *Cancer* 1988, 62:479-483
 69. Yang TS, Lin YC, Chen JS, Wang HM, Wang CH: Phase II study of gemcitabine in patients with advanced hepatocellular carcinoma, *Cancer* 2000, 89:750-756
 70. Gish RG, Porta C, Lazar L, Ruff P, Feld R, Croitoru A, Feun L, Jeziorski K, Leighton J, Gallo J, Kennealey GT: Phase III randomized controlled trial comparing the survival of patients with unresectable hepatocellular carcinoma treated with nolatrexed or doxorubicin, *J Clin Oncol* 2007, 25:3069-3075
 71. Ahmed F, Steele JC, Herbert JM, Steven NM, Bicknell R: Tumor stroma as a target in cancer, *Curr Cancer Drug Targets* 2008, 8:447-453
 72. Farrow B, Albo D, Berger DH: The role of the tumor microenvironment in the progression of pancreatic cancer, *J Surg Res* 2008, 149:319-328
 73. Korc M: Pancreatic cancer-associated stroma production, *Am J Surg* 2007, 194:S84-86
 74. Fritz V, Jorgensen C: Mesenchymal stem cells: an emerging tool for cancer targeting and therapy, *Curr Stem Cell Res Ther* 2008, 3:32-42
 75. Hall B, Andreeff M, Marini F: The participation of mesenchymal stem cells in tumor stroma formation and their application as targeted-gene delivery vehicles, *Handb Exp Pharmacol* 2007, 263-283
 76. Kiaris H, Trimis G, Papavassiliou AG: Regulation of tumor-stromal fibroblast interactions: implications in anticancer therapy, *Curr Med Chem* 2008, 15:3062-3067
 77. Anders HJ, Frink M, Linde Y, Banas B, Wornle M, Cohen CD, Vielhauer V, Nelson PJ, Grone HJ, Schlondorff D: CC chemokine ligand 5/RANTES chemokine antagonists aggravate glomerulonephritis despite reduction of glomerular leukocyte infiltration, *J Immunol* 2003, 170:5658-5666
 78. Yang JD, Nakamura I, Roberts LR: The tumor microenvironment in hepatocellular

- carcinoma: current status and therapeutic targets, *Semin Cancer Biol* 2011, 21:35-43
79. Azenshtein E, Luboshits G, Shina S, Neumark E, Shahbazian D, Weil M, Wigler N, Keydar I, Ben-Baruch A: The CC chemokine RANTES in breast carcinoma progression: regulation of expression and potential mechanisms of promalignant activity, *Cancer Res* 2002, 62:1093-1102
 80. Fischer M, Juremalm M, Olsson N, Backlin C, Sundstrom C, Nilsson K, Enblad G, Nilsson G: Expression of CCL5/RANTES by Hodgkin and Reed-Sternberg cells and its possible role in the recruitment of mast cells into lymphomatous tissue, *Int J Cancer* 2003, 107:197-201
 81. Soria G, Ben-Baruch A: The inflammatory chemokines CCL2 and CCL5 in breast cancer, *Cancer Lett* 2008, 267:271-285
 82. Folkman J: Tumor angiogenesis: therapeutic implications, *N Engl J Med* 1971, 285:1182-1186
 83. Kerbel RS: Tumor angiogenesis, *N Engl J Med* 2008, 358:2039-2049
 84. Nakabayashi H, Taketa K, Miyano K, Yamane T, Sato J: Growth of human hepatoma cells lines with differentiated functions in chemically defined medium, *Cancer Res* 1982, 42:3858-3863
 85. Von Lutichau I, Notohamiprodjo M, Wechselberger A, Peters C, Henger A, Seliger C, Djafarzadeh R, Huss R, Nelson PJ: Human adult CD34- progenitor cells functionally express the chemokine receptors CCR1, CCR4, CCR7, CXCR5, and CCR10 but not CXCR4, *Stem Cells Dev* 2005, 14:329-336
 86. Conrad C, Gottgens B, Kinston S, Ellwart J, Huss R: GATA transcription in a small rhodamine 123(low)CD34(+) subpopulation of a peripheral blood-derived CD34(-)CD105(+) mesenchymal cell line, *Exp Hematol* 2002, 30:887-895
 87. Conrad C, Zeindl-Eberhart E, Moosmann S, Nelson PJ, Bruns CJ, Huss R: Alkaline phosphatase, glutathione-S-transferase-P, and cofilin-1 distinguish multipotent mesenchymal stromal cell lines derived from the bone marrow versus peripheral blood, *Stem Cells Dev* 2008, 17:23-27
 88. Rohrer M, Bauer H, Mintorovitch J, Requardt M, Weinmann HJ: Comparison of magnetic properties of MRI contrast media solutions at different magnetic field strengths, *Invest Radiol* 2005, 40:715-724
 89. Himmelreich U, Hoehn M: Stem cell labeling for magnetic resonance imaging, *Minim Invasive Ther Allied Technol* 2008, 17:132-142
 90. Nolte M, Werner M, Nasarek A, Bektas H, von Wasielewski R, Klempnauer J, Georgii A: Expression of proliferation associated antigens and detection of numerical chromosome aberrations in primary human liver tumours: relevance to tumour characteristics and prognosis, *J Clin Pathol* 1998, 51:47-51
 91. Detwiler KY, Fernando NT, Segal NH, Ryeom SW, D'Amore PA, Yoon SS: Analysis of hypoxia-related gene expression in sarcomas and effect of hypoxia on RNA interference of vascular endothelial cell growth factor A, *Cancer research* 2005, 65:5881-5889
 92. Weidner N, Semple JP, Welch WR, Folkman J: Tumor angiogenesis and metastasis--correlation in invasive breast carcinoma, *N Engl J Med* 1991, 324:1-8
 93. Weidner N: Current pathologic methods for measuring intratumoral microvessel density within breast carcinoma and other solid tumors, *Breast Cancer Res Treat* 1995, 36:169-180
 94. Gramantieri L, Trere D, Chieco P, Lacchini M, Giovannini C, Piscaglia F, Cavallari A, Bolondi L: In human hepatocellular carcinoma in cirrhosis proliferating cell nuclear antigen (PCNA) is involved in cell proliferation and cooperates with P21 in DNA repair, *J Hepatol* 2003, 39:997-1003

95. Curley SA, Izzo F, Delrio P, Ellis LM, Granchi J, Vallone P, Fiore F, Pignata S, Daniele B, Cremona F: Radiofrequency ablation of unresectable primary and metastatic hepatic malignancies: results in 123 patients, *Ann Surg* 1999, 230:1-8
96. Zhong C, Guo RP, Li JQ, Shi M, Wei W, Chen MS, Zhang YQ: A randomized controlled trial of hepatectomy with adjuvant transcatheter arterial chemoembolization versus hepatectomy alone for Stage III A hepatocellular carcinoma, *J Cancer Res Clin Oncol* 2009, 135:1437-1445
97. Chapman WC, Majella Doyle MB, Stuart JE, Vachharajani N, Crippin JS, Anderson CD, Lowell JA, Shenoy S, Darcy MD, Brown DB: Outcomes of neoadjuvant transarterial chemoembolization to downstage hepatocellular carcinoma before liver transplantation, *Ann Surg* 2008, 248:617-625
98. Daniele B, De Sio I, Izzo F, Capuano G, Andreana A, Mazzanti R, Aiello A, Vallone P, Fiore F, Gaeta GB, Perrone F, Pignata S, Gallo C: Hepatic resection and percutaneous ethanol injection as treatments of small hepatocellular carcinoma: a Cancer of the Liver Italian Program (CLIP 08) retrospective case-control study, *J Clin Gastroenterol* 2003, 36:63-67
99. De Wever O, Mareel M: Role of tissue stroma in cancer cell invasion, *J Pathol* 2003, 200:429-447
100. Bhowmick NA, Neilson EG, Moses HL: Stromal fibroblasts in cancer initiation and progression, *Nature* 2004, 432:332-337
101. Llovet JM, Ricci S, Mazzaferro V, Hilgard P, Gane E, Blanc JF, de Oliveira AC, Santoro A, Raoul JL, Forner A, Schwartz M, Porta C, Zeuzem S, Bolondi L, Greten TF, Galle PR, Seitz JF, Borbath I, Haussinger D, Giannaris T, Shan M, Moscovici M, Voliotis D, Bruix J: Sorafenib in advanced hepatocellular carcinoma, *N Engl J Med* 2008, 359:378-390
102. Pereboeva L, Komarova S, Mikheeva G, Krasnykh V, Curiel DT: Approaches to utilize mesenchymal progenitor cells as cellular vehicles, *Stem Cells* 2003, 21:389-404
103. Arbab AS, Yocum GT, Kalish H, Jordan EK, Anderson SA, Khakoo AY, Read EJ, Frank JA: Efficient magnetic cell labeling with protamine sulfate complexed to ferumoxides for cellular MRI, *Blood* 2004, 104:1217-1223
104. Arbab AS, Yocum GT, Rad AM, Khakoo AY, Fellowes V, Read EJ, Frank JA: Labeling of cells with ferumoxides-protamine sulfate complexes does not inhibit function or differentiation capacity of hematopoietic or mesenchymal stem cells, *NMR Biomed* 2005, 18:553-559
105. Arbab AS, Yocum GT, Wilson LB, Parwana A, Jordan EK, Kalish H, Frank JA: Comparison of transfection agents in forming complexes with ferumoxides, cell labeling efficiency, and cellular viability, *Mol Imaging* 2004, 3:24-32
106. Bianco P, Riminucci M, Gronthos S, Robey PG: Bone marrow stromal stem cells: nature, biology, and potential applications, *Stem Cells* 2001, 19:180-192
107. Fillat C, Carrio M, Cascante A, Sangro B: Suicide gene therapy mediated by the Herpes Simplex virus thymidine kinase gene/Ganciclovir system: fifteen years of application, *Curr Gene Ther* 2003, 3:13-26
108. Spaeth EL, Dembinski JL, Sasser AK, Watson K, Klopp A, Hall B, Andreeff M, Marini F: Mesenchymal stem cell transition to tumor-associated fibroblasts contributes to fibrovascular network expansion and tumor progression, *PLoS One* 2009, 4:e4992
109. Bexell D, Gunnarsson S, Tormin A, Darabi A, Gisselsson D, Roybon L, Scheduling S, Bengzon J: Bone marrow multipotent mesenchymal stroma cells act as pericyte-like migratory vehicles in experimental gliomas, *Mol Ther* 2009, 17:183-190
110. Tille JC, Pepper MS: Mesenchymal cells potentiate vascular endothelial growth

- factor-induced angiogenesis in vitro, *Exp Cell Res* 2002, 280:179-191
111. Wang L, Li Y, Chen X, Chen J, Gautam SC, Xu Y, Chopp M: MCP-1, MIP-1, IL-8 and ischemic cerebral tissue enhance human bone marrow stromal cell migration in interface culture, *Hematology* 2002, 7:113-117
 112. Wang L, Li Y, Chen J, Gautam SC, Zhang Z, Lu M, Chopp M: Ischemic cerebral tissue and MCP-1 enhance rat bone marrow stromal cell migration in interface culture, *Exp Hematol* 2002, 30:831-836
 113. Yu J, Ustach C, Kim HR: Platelet-derived growth factor signaling and human cancer, *J Biochem Mol Biol* 2003, 36:49-59
 114. Hellstrom M, Kalen M, Lindahl P, Abramsson A, Betsholtz C: Role of PDGF-B and PDGFR-beta in recruitment of vascular smooth muscle cells and pericytes during embryonic blood vessel formation in the mouse, *Development* 1999, 126:3047-3055
 115. Andrades JA, Han B, Becerra J, Sorgente N, Hall FL, Nimni ME: A recombinant human TGF-beta1 fusion protein with collagen-binding domain promotes migration, growth, and differentiation of bone marrow mesenchymal cells, *Exp Cell Res* 1999, 250:485-498
 116. Quante M, Tu SP, Tomita H, Gonda T, Wang SS, Takashi S, Baik GH, Shibata W, Diprete B, Betz KS, Friedman R, Varro A, Tycko B, Wang TC: Bone marrow-derived myofibroblasts contribute to the mesenchymal stem cell niche and promote tumor growth, *Cancer Cell* 2011, 19:257-272
 117. Zhao ZC, Zheng SS, Wan YL, Jia CK, Xie HY: The molecular mechanism underlying angiogenesis in hepatocellular carcinoma: the imbalance activation of signaling pathways, *Hepatobiliary Pancreat Dis Int* 2003, 2:529-536
 118. Zhang ZL, Liu ZS, Sun Q: Expression of angiopoietins, Tie2 and vascular endothelial growth factor in angiogenesis and progression of hepatocellular carcinoma, *World J Gastroenterol* 2006, 12:4241-4245
 119. Sugimachi K, Tanaka S, Taguchi K, Aishima S, Shimada M, Tsuneyoshi M: Angiopoietin switching regulates angiogenesis and progression of human hepatocellular carcinoma, *J Clin Pathol* 2003, 56:854-860
 120. Chew V, Chen J, Lee D, Loh E, Lee J, Lim KH, Weber A, Slankamenac K, Poon RT, Yang H, Ooi LL, Toh HC, Heikenwalder M, Ng IO, Nardin A, Abastado JP: Chemokine-driven lymphocyte infiltration: an early intratumoural event determining long-term survival in resectable hepatocellular carcinoma, *Gut* 2011,
 121. Matuskova M, Hlubinova K, Pastorakova A, Hunakova L, Altanerova V, Altaner C, Kucerova L: HSV-tk expressing mesenchymal stem cells exert bystander effect on human glioblastoma cells, *Cancer Lett* 2010, 290:58-67
 122. Miletic H, Fischer YH, Giroglou T, Rueger MA, Winkeler A, Li H, Himmelreich U, Stenzel W, Jacobs AH, von Laer D: Normal brain cells contribute to the bystander effect in suicide gene therapy of malignant glioma, *Clin Cancer Res* 2007, 13:6761-6768
 123. Di Stasi A, Tey SK, Dotti G, Fujita Y, Kennedy-Nasser A, Martinez C, Straathof K, Liu E, Durett AG, Grilley B, Liu H, Cruz CR, Savoldo B, Gee AP, Schindler J, Krance RA, Heslop HE, Spencer DM, Rooney CM, Brenner MK: Inducible apoptosis as a safety switch for adoptive cell therapy, *N Engl J Med* 2011, 365:1673-1683
 124. Zhang X, Nakaoka T, Nishishita T, Watanabe N, Igura K, Shinomiya K, Takahashi TA, Yamashita N: Efficient adeno-associated virus-mediated gene expression in human placenta-derived mesenchymal cells, *Microbiol Immunol* 2003, 47:109-116
 125. Tsai MS, Lee JL, Chang YJ, Hwang SM: Isolation of human multipotent

- mesenchymal stem cells from second-trimester amniotic fluid using a novel two-stage culture protocol, *Hum Reprod* 2004, 19:1450-1456
126. Bieback K, Kluter H: Mesenchymal stromal cells from umbilical cord blood, *Curr Stem Cell Res Ther* 2007, 2:310-323
 127. Zuk PA, Zhu M, Ashjian P, De Ugarte DA, Huang JI, Mizuno H, Alfonso ZC, Fraser JK, Benhaim P, Hedrick MH: Human adipose tissue is a source of multipotent stem cells, *Mol Biol Cell* 2002, 13:4279-4295
 128. Le Blanc K, Pittenger M: Mesenchymal stem cells: progress toward promise, *Cytotherapy* 2005, 7:36-45
 129. Cao H, Xu W, Qian H, Zhu W, Yan Y, Zhou H, Zhang X, Xu X, Li J, Chen Z: Mesenchymal stem cell-like cells derived from human gastric cancer tissues, *Cancer Lett* 2009, 274:61-71
 130. Greco SJ, Patel SA, Bryan M, Pliner LF, Banerjee D, Rameshwar P: AMD3100-mediated production of interleukin-1 from mesenchymal stem cells is key to chemosensitivity of breast cancer cells, *Am J Cancer Res* 2011, 1:701-715

XII. CURRICULUM VITAE

Personal data

Family Name Bao
First Name Qi
Gender Male
Date of birth 29.11.1983
Place of birth Zhejiang, China
Nationality Chinese
Parents Bao, Lixing
Shen, Xinjuan
Address Pfingstrosenstr. 62/2-154, 81377 Munich, Germany
Phone +49-176-62361928
+86-13588159520
E-mail baoqi.zju@gmail.com

Academic education

09/1997 – 07/2002 Hangzhou High School, Zhejiang, China

10/2002 – 06/2007 Zhejiang University, School of Medicine
2007 awarded Bachelor's degree

09/2007 – 06/2009 Zhejiang University, School of Medicine
2009 awarded Master's degree

03/2008 – 05/2008 Clerkship in David Geffen School of Medicine at
UCLA, USA

09/2009 – present Dr. hum biol. Doktorand in Chirurgische Klinik und
Poliklinik, LMU München - Klinikum Großhadern

National and international conferences and educational meetings

1. 14. Chirurgische Forschungstage

23. – 25. September 2010, Rostock, Germany

Presentation, “Targeting tumor stroma and angiogenesis using genetically engineered mesenchymal stem cells results in reduced tumor growth in hepatocellular carcinoma”

2. 128. Kongress der Deutschen Gesellschaft für Chirurgie & 13. Jahreskongress der Deutschen Gesellschaft für Allgemein und Viszeralchirurgie

3. – 6. May 2011, Munich, Germany

H. Nieß, **Q. Bao**, C. Conrad, B. Schwarz, K-W. Jauch, P. Nelson, C.J. Bruns. “Targeting tumor stroma and angiogenesis using suicide-gene carrying mesenchymal stem cells results in reduced tumor growth in hepatocellular carcinoma”

3. 88. Jahrestagung Vereinigung der Bayerischen Chirurgen e.V. – 100 jähriges Jubiläum des VBC

20. – 23. July 2011, Munich Germany

H. Nieß, **Q. Bao**, K.-W. Jauch, P. J. Nelson, C. Bruns. “CCL5 and Tie2 mediated tissue-specific suicide-gene expression of mesenchymal stem cells in tumor microenvironments inhibits growth of hepatocellular carcinoma”

4. Doktorandenkolloquium & Dienstagskolloquium in Surgery Department

06. October 2010, Munich, Germany

Presentation, “Targeting tumor stroma and angiogenesis using genetically engineered mesenchymal stem cells results in reduced tumor growth in hepatocellular carcinoma”

5. Journal Club oder Methodenseminar in Surgery Department

30. April 2010, Munich, Germany

Presentaion, Journal Club “J Natl Cancer Inst 2010; 102: 340-351”

6. Ärztliche Fortbildung in Bayern in Zusammenarbeit mit der Bayerischen Landesärztekammer – Akademie für ärztliche Fortbildung – Post-ASCO-GI-Meeting 2011

13. April 2011, Munich, Germany

7. 3. Doktorarbeitstag Medizin

14. May 2011, Munich, Germany

Poster presentation, “Selective targeting of genetically engineered mesenchymal stem cells to tumor stroma microenvironments using tissue-specific suicide-gene expression suppresses growth of hepatocellular carcinoma”

8. CSC-LMU program auditing seminar

23. - 24. May 2011, Munich, Germany

Presentation, “Mesenchymal stem cell-based targeting tumor stroma and angiogenesis gene therapy”

9. 15. Chirurgische Forschungstage

22. – 24. September 2011, Dresden, Germany

Poster Presentation, “GPI-anchored tissue inhibitor of matrix metalloproteinase-1 (TIMP-1) influences pancreatic cancer growth”, Won the Poster Prize

10. 30. Deutscher Krebskongress 2012

22. – 25. February 2012, Berlin, Germany

Poster Presentation, “GPI-anchored tissue inhibitor of matrix metalloproteinase-1 (TIMP-1) inhibits tumor growth in fibrosarcoma and pancreatic cancer”

11. 129. Kongress der Deutschen Gesellschaft für Chirurgie

24. – 27. April 2012, Berlin, Germany

Presentation, “Exogenously applied TIMP-1-GPI inhibits fibrosarcoma growth and renders side-population cells killing”

Publications:

1. **Bao Q**, Chen L. Thrombotic mesenteric ischemia due to aortic dissection. *J Vasc Surg.* 2010 Dec; 52(6):1674.
2. **Qi Bao**, Yue Zhao, Andrea Renner, Hanno Niess, Hendrik Seeliger, Karl-Walter Jauch, Christiane J. Bruns. Cancer Stem Cells in Pancreatic Cancer. *Cancers* 2010, 2, 1629-1641.
3. **Bao Q**, Zhao Y, Niess H, Conrad C, Schwarz B, Jauch KW, Huss R, Nelson PJ, Bruns CJ. Mesenchymal Stem Cell-Based Tumor-Targeted Gene Therapy in Gastrointestinal Cancer. *Stem Cells Dev.* 2012 Jun 26. PMID:22530882.
4. Niess H, **Bao Q**, Conrad C, Zischek C, Notohamiprodjo M, Schwab F, Schwarz

- B, Huss R, Jauch KW, Nelson PJ, Bruns CJ. Selective targeting of genetically engineered mesenchymal stem cells to tumor stroma microenvironments using tissue-specific suicide gene expression suppresses growth of hepatocellular carcinoma. *Ann Surg.* 2011;254(5):767-75.
5. Zhao Y, **Bao Q**, Renner A, Camaj P, Eichhorn M, Ischenko I, Angele M, Kleespies A, Jauch KW, Bruns C. Cancer stem cells and angiogenesis. *Int J Dev Biol.* 2011; 55(4-5):477-82. (Co-first authorship)
 6. Zhao L, Zhao Y, **Bao Q**, Niess H, Jauch KW, Bruns CJ. Clinical Implication of Targeting of Cancer Stem Cells. *Eur Surg Res.* 2012 Jul 11;49(1):8-15. [Epub ahead of print]
 7. Li Chen, **Qi Bao**, Xingfei Yu, Ning Dai. The situation of acupuncture in China. *Minimal Invasive Chirurgie* 2007, 16(1): 14-15.
 8. Li Chen, **Qi Bao**, GW Yang, Ning Dai. Endoskopische Chirurgie in China. *Minimal Invasive Chirurgie.* 2006. 15(2):119-121.
 9. Yixiong Zheng, Luqing Zhang, **Qi Bao**. Reconstruction of the stomach with smooth muscle cell seeded constructs in rat model. *Key Engineering Materials* Vols. 2011. Feb. 467-469
 10. Gong DJ, Miao CF, **Bao Q**, Jiang M, Zhang LF, Tong XT, Chen L. Risk factors for operative morbidity and mortality in gastric cancer patients undergoing total gastrectomy. *World J Gastroenterol.* 2008 Nov 14;14(42):6560-3.

XIII. ACKNOWLEDGEMENTS

Foremost, I would like to express my sincere gratitude to my advisor -- Prof. Dr. med. Christiane J. Bruns for the continuous support of my doctoral study and research, for her patience, motivation, enthusiasm, and immense knowledge. Her guidance helped me in all the time of research and writing of this thesis. I could not have imagined having a better advisor and mentor for my doctoral study.

My sincere thanks also goes to Prof. Dr. med. Dr. h.c. mult. Karl-Walter Jauch for totally supporting me the doctor-title issue and for offering the chance for Berry and me as a guide in visiting China trip.

I would like to express my deeply gratitude to Prof. Dr. rer. Nat. Peter J. Nelson. With his enthusiasm, his inspiration, and his great efforts to explain things clearly and simply, he helped to make molecular cell biology fun and helpful for me. Throughout my study design, data analysis, paper and thesis-writing, doctor-title issue, pre-examination, he provided encouragement, sound advice, good teaching, big support and lots of good ideas. I would have been lost without him.

I would like to thank the other member of my thesis committee – Prof. Dr. med. Dr. h.c. mult. Ralf Huss. Thanks for taking care of my pre-examination and thesis during his illness. Wish he get well soon and always has healthy days ahead.

In particular, I am sincerely grateful to Dr. med. Hanno Niess. Without his great guidance and help, I won't be able to finish my whole doctoral program and thesis. I would like to thank him for his continuously support on my research project and life in Munich.

I would like to thank all my lab members, Yue Zhao, Bettina Schwarz, Andrea Renner, Xiaoliang Wang, Ruth Mair, Dr.med. Stefano Primo, Nina Seel, Dr. rer. Nat. Peter Camaj, Dr.med. Hendrik Seeliger, Dr. med. Ivan Ischenko for their help on my work, including suggestion, discussion and technique assistance.

I would like to thank Anke Mojaat, Alex, Sylke Rohrer, Monika Hofstetter, Dr. Roghieh Djafarzadeh from Prof. Nelson's group. I would like to thank them for the help they gave as the cooperation on the project and paper.

I would like to thank Chinese Scholarship Council to provide the economic support

since 2009. I would like to thank Mr. Matthias Hadesbeck and Ms. Munique Esnof from the International Office, LMU to give the orientation course and living assistance. I would like to thank Prof. Dr. Alexander Baetmann, LMU and Mr. Jiqiang Dai from Chinese Consulate Munich for the help on my overseas issues.

Most importantly, I wish to thank my parents -- Lixing Bao and Xinjuan Shen. They bore me, raised me, supported me, taught me, and loved me. Finally, I would like to thank my wife – Jie Pan. To her I dedicate this thesis.